

FACHBEREICH MATHEMATIK UND INFORMATIK
FREIE UNIVERSITÄT BERLIN

BACHELORARBEIT

ZUM ERWERB DES AKADEMISCHEN GRADES
BACHELOR OF SCIENCE

Computational Modelling of Midazolam Clearance:
Effect of Inhibitors and Inducers

Computermodellierung des Midazolam-Abbaus:
Effekt von Inhibitoren und Induktoren

vorgelegt von:

Name: **Yannick Duport**

Matrikelnummer: **5095008**

Email: **yannick.duport@fu-berlin.de**

angefertigt in der Arbeitsgruppe Systems Medicine of the Liver
am Institut für Theoretische Biologie, HU Berlin
Berlin, August 2020

Betreuer: **Dr. Matthias König**

1. Prüfer: **Dr. Matthias König**

2. Prüfer: **Prof. Dr. Tim Conrad**



Selbstständigkeitserklärung

Name: DUPORT	
Vorname: YANNICK	
geb.am: 18.11.1986	(Nur Block- oder Maschinenschrift verwenden.)
Matr.Nr.: 5095008	

Ich erkläre gegenüber der Freien Universität Berlin, dass ich die vorliegende Bachelorarbeit selbstständig und ohne Benutzung anderer als der angegebenen Quellen und Hilfsmittel angefertigt habe.

Die vorliegende Arbeit ist frei von Plagiaten. Alle Ausführungen, die wörtlich oder inhaltlich aus anderen Schriften entnommen sind, habe ich als solche kenntlich gemacht.

Diese Arbeit wurde in gleicher oder ähnlicher Form noch bei keiner anderen Universität als Prüfungsleistung eingereicht.

Datum: 24.08.20

Unterschrift: U. Duport

Contents

1	Introduction	4
1.1	Pharmacokinetics	4
1.2	Midazolam	5
1.2.1	Metabolism of midazolam	5
1.2.2	First-pass effect	5
1.2.3	Midazolam as a CYP3A4 probe	7
1.2.4	Inhibitors and inducers of CYP3A	7
1.3	Physiological-based pharmacokinetic models (PBPK)	8
1.4	Question, scope and hypotheses	9
2	Methods	10
2.1	Calculation of pharmacokinetic parameters	10
2.2	Curation of pharmacokinetics data	12
2.2.1	PK-DB - pharmacokinetics database	12
2.2.2	Curation of pharmacokinetic studies	12
2.2.3	Meta-analysis	12
2.3	Physiological-based pharmacokinetics models (PBPK)	13
2.3.1	Model representation and simulation	13
2.3.2	Parameter fitting (model optimization)	13
2.4	Uncertainty analysis	14
2.5	Sensitivity analysis	14
2.6	Parameter scans	14
3	Results	16
3.1	Midazolam pharmacokinetics data	16
3.1.1	Meta-analysis	18
3.2	Midazolam model	24
3.2.1	Physiological-based pharmacokinetics model	24
3.2.2	Model parameterization	26
3.2.3	Parameter fitting	26
3.2.4	Model performance	29
3.2.5	Sensitivity analysis	34
3.3	Effect of inhibitors and inducers	34
3.3.1	CYP3A4 induction and inhibition	34
3.3.2	Scan of CYP3A4 activity	40
3.4	Summary	42
4	Discussion	43
5	Outlook	47
6	Acknowledgements	48
Appendices		56
A	Figures and Tables	57
A.1	Midazolam studies overview	57
A.2	Meta-analysis	58
A.3	Midazolam simulation experiments	60
A.4	Model validation	83
A.5	CYP3A4 scans	86

Abstract

English

Midazolam is one of the most effective and safe medicines used for anesthesia and procedural sedation, as well as treating trouble sleeping and severe agitation. Midazolam is metabolised in the liver as well as in the small intestine to cytochrome P450 3A4 (CYP3A4). Many factors can alter the pharmacokinetics of midazolam due to inhibition or induction of hepatic and/or intestinal metabolism, resulting in either (i) adverse effects due to increased plasma midazolam concentrations in case of inhibition of metabolism or (ii) ineffectiveness as a consequence of too low concentrations if metabolism is induced. Within this thesis the clearance and pharmacokinetics of midazolam were studied, using a computational modeling approach. A large data base of midazolam pharmacokinetics data was established and utilized to develop a physiological-based pharmacokinetics model of midazolam. The model was applied to study the following questions: (i) What are the effects of CYP3A4 inhibition and induction on midazolam pharmacokinetics? (ii) What are the differences of intestinal and hepatic CYP3A4 inhibition and induction on midazolam pharmacokinetics?

German

Midazolam ist eines der wirksamsten und sichersten Medikamente zur Anästhesie und Sedierung bei Eingriffen, sowie zur Behandlung von Schlafstörungen und schwerer Unruhe. Midazolam wird sowohl in der Leber als auch im Dünndarm von Cytochrom P450 3A4 (CYP3A4) metabolisiert. Viele Faktoren können die Pharmakokinetik von Midazolam durch Hemmung oder Induktion des Leber- und/oder Darmstoffwechsels verändern, was entweder (i) zu unerwünschten Wirkungen durch erhöhte Midazolam Plasmakonzentrationen bei Hemmung des Stoffwechsels oder (ii) bei Induktion des Stoffwechsels zu Unwirksamkeit als Folge zu niedriger Konzentrationen im Blut führt. Im Rahmen dieser Arbeit wurde der Metabolismus und Pharmakokinetik von Midazolam mit Hilfe eines rechnergestützten Modellierungsansatzes untersucht. Es wurde eine umfangreiche Datenbank mit Daten über die Pharmakokinetik von Midazolam etabliert, welche zur Entwicklung eines physiologisch-basierten pharmakokinetischen Modells von Midazolam verwendet wurde. Mit Hilfe des Modells wurden die folgenden Fragestellungen untersucht: (i) Welche Auswirkungen haben Hemmung und Induktion von CYP3A4 auf die Pharmakokinetik von Midazolam? (ii) Was sind die Unterschiede der intestinalen und hepatischen CYP3A4-Hemmung bzw. -Induktion auf die Pharmakokinetik von Midazolam?

1 Introduction

Within this work a computational modelling approach was used to study midazolam as a probe drug for cytochrome P450 activity and the effects of inhibitors and inducers on midazolam metabolism and pharmacokinetics *in silico*. A physiological-based pharmacokinetic (PBPK) model of midazolam was developed and applied to elucidate how such modifiers can effect the intestinal and hepatic midazolam metabolism, the first-pass effect of midazolam, and the pharmacokinetics of midazolam and its metabolites. In the following we will give a short introduction to the field of pharmacokinetics (Sec. 1.1), to midazolam and its metabolism (Sec. 1.2), and computational modelling using PBPK models (Sec. 1.3). Finally, the hypotheses and questions of this thesis are introduced (Sec. 1.4).

1.1 Pharmacokinetics

The field of pharmacokinetics studies the processes a drug undergoes after application to the human body. To do so, the concentration of an administered drug is measured over time at a site of exposure (e.g. blood, plasma, saliva, or breath). From this concentration-time curves information about absorption, distribution, metabolism and elimination (ADME) of the drug and its metabolites can be derived. Most pharmacokinetic time curves are measured in blood/plasma, saliva or urine which are easily accessible to sampling [1].

The ADME processes are the main processes responsible for the pharmacokinetics of a substance. Absorption is the transfer of a drug from the site of administration to the site of measurement. The main administration routes of midazolam are intravenous administration (i.e. via injection in the venous blood) and oral administration (via tablets or solution). An important quantity is the fraction of administered drug, which reaches the systemic circulation, the so-called bioavailability. In case of intravenous administration the bioavailability of a substance is 100%, i.e., the complete dose appears in the plasma. However, if the same substance is administered orally and measured in the venous blood, only a fraction of the dose appears at the site of measurement, for instance due to metabolic conversions [1].

Distribution is the process by which drugs and metabolites are distributed in the body. The rate of distribution of a drug depends on many factors such as blood-flow, binding to tissues or proteins in the blood, and the ability of drugs to cross membranes. An important quantity is the volume of distribution (V_d), a parameter relating the concentration of a drug in the plasma to the total amount of the drug in the body. A highly lipophilic drug can easily pass through membranes and therefore has a large volume of distribution. Drugs heavily bound to plasma proteins on the other hand, will have a much smaller V_d and can be very close to plasma volume [2].

While absorption and distribution determine the time until a drug starts acting, duration of the action is determined by metabolism and elimination of the drug. Metabolism is the metabolic conversion of a drug into different chemical compounds. The main site of metabolism is the liver, but for many drugs also metabolism at other sites such as the kidney or intestines can play a role. The drug and its metabolites can be removed from the body via the process of elimination often via the kidneys in the urine [1]. An important pharmacokinetic

parameter in this context is clearance, describing the efficiency of irreversible elimination of a drug from the systemic circulation [2].

1.2 Midazolam

Midazolam is one of the most effective and safe medicines used for anesthesia and procedural sedation, as well as treating trouble sleeping and severe agitation [3]. It is one of the drugs on the World Health Organization's List of Essential Medicines, listing the minimum medicine needs for a basic health-care system [4].

Midazolam was first synthesized by Fryer and Walser in 1976 and belongs to the class of benzodiazepines [5]. It contains an imidazole ring that is responsible for some of its chemical properties. It is relatively basic which allows the preparation of water soluble salts, from which solutions for intravenous application can be prepared [6].

Like other benzodiazepines, midazolam causes anxiolytic, sedative, hypnotic, anticonvulsant, muscle-relaxant and anterograde amnesic effects. However, compared to other benzodiazepines it has a more rapid onset and shorter duration [7]. The pharmacological effects of midazolam are due to its interaction with gamma-aminobutyric acid (GABA) receptors. Midazolam has a binding site on the ionotropic GABA_A receptors, different from the one of GABA, and enhances the receptors inhibitory potential by increasing the chloride current into the cell [8].

1.2.1 Metabolism of midazolam

After administration, midazolam is metabolized very rapidly. This happens by hydroxylation of midazolam to its main metabolite 1-hydroxymidazolam. An alternative route is the conversion of midazolam to 4-hydroxymidazolam and the subsequent conversion of these metabolites to 1,4-hydroxymidazolam, but both metabolites only play a minor role in the elimination of midazolam. All three metabolites are rapidly conjugated by glucuronic acid and subsequently excreted via the urine [9].

The cytochromes are a superfamily of haemproteins that are involved in oxidative biotransformation of xeno- and endobiotics. The cytochrome P450 (CYP) 3A subfamily consists of multiple isoforms, 3A3, 3A4, 3A5 and 3A7, and is responsible for the majority of drug metabolism in human liver and intestine. Hydroxylation of midazolam is catalyzed by the CYP3A isoforms 3A4 and, to some extent, 3A5 [10]. CYP3A4 is the most abundant CYP expressed in human liver and intestine (30-40% of CYP content) [11], is involved in the metabolism of approximately half of the drugs available [12] and is the main isoform participating in midazolam metabolism [13]. CYP3A5 has a similar substrate specificity to 3A4 and is often described as a part of midazolam metabolism. However, expression levels and activity of intestinal- and hepatic CYP3A5 differ greatly between individuals and recent studies have shown that its importance in midazolam metabolism is limited [14, 15].

1.2.2 First-pass effect

The first pass effect describes the effect that for certain drugs only a fraction of the orally administered dose appears in the systemic blood circulation, compared to intravenous administration. The first-pass effect is due to metabolism before

the substance can reach the venous blood. For most drugs the liver is the main site of elimination and solely responsible for the first-pass effect. But in case of CYP3A4 substrates, such as midazolam, intestinal CYP3A4 plays a major role in addition to hepatic CYP3A4 [16]. Hepatic and intestinal CYP3A4 cDNAs are identical, and multiple studies failed to detect any differences in their metabolism. This suggests that hepatic and intestinal CYP3A4 are the same protein, and therefore, observations about the catalytic activity of hepatic CYP3A4 should be directly applicable to intestinal CYP3A4 [17].

Before entering the systemic blood circulation, orally administered midazolam first has to pass the intestinal wall. While being absorbed by the intestinal enterocytes, midazolam is metabolized by CYP3A4, which removes around 45% of the orally administered dose. The remaining drug then passes the liver, where another 45% of the remaining 55% is removed. Ultimately only a small fraction of the administered midazolam will reach the systemic circulation resulting in an oral bioavailability of only $30\% \pm 10\%$ [16, 18] (Fig.1).

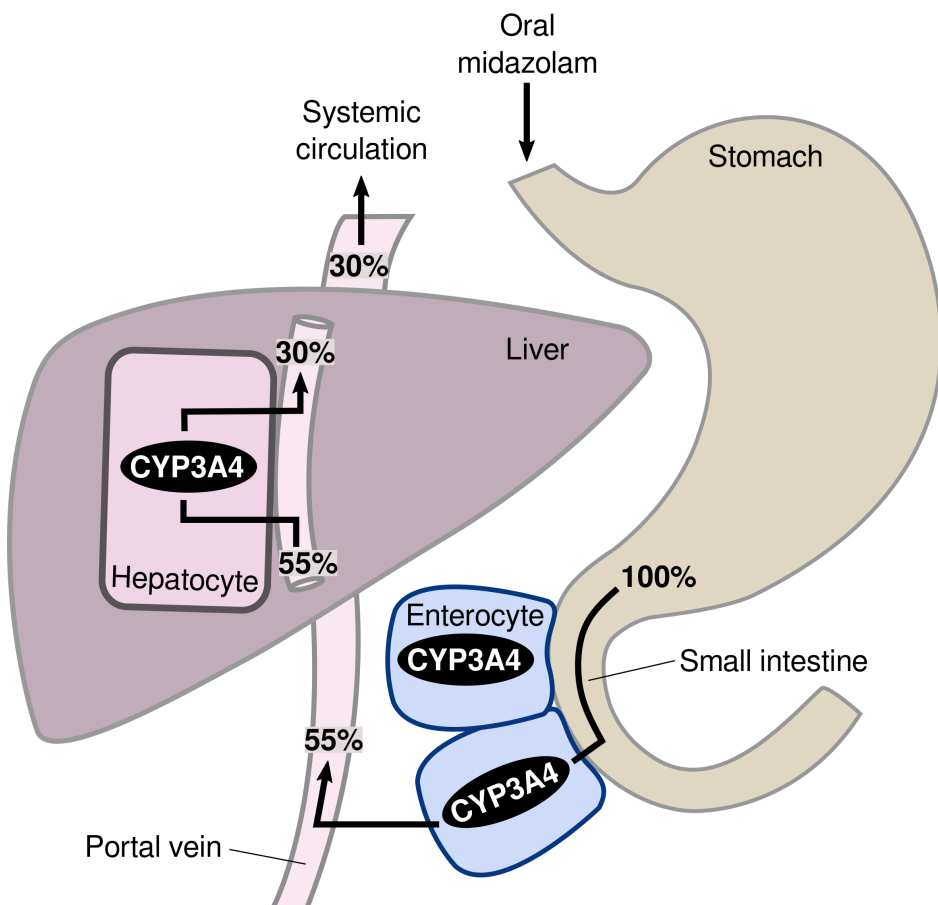


Figure 1: First-pass metabolism. Orally administered midazolam being absorbed by the enterocytes in the small intestine and subsequently metabolized by CYP3A4 in the small intestine and the liver before it reaches the systemic blood circulation. The percentage shows the remaining unmetabolized drug after passing through the enterocytes and hepatocytes, respectively.

1.2.3 Midazolam as a CYP3A4 probe

With the central role of CYP3A4 in the metabolism of many drugs besides midazolam (e.g. alfentanil, erythromycin, ketoconazol, triazolam [19]), it is of importance to have methods to assess the individual CYP3A4 phenotype, i.e., CYP3A4 activity. Such information could allow for personalized drug-therapies based on the individual CYP3A4 phenotype of a patient [20]. The preferred way of phenotyping CYP3A4 activity is with the help of a probe drug. Hereby, a test substrate is applied, which is selective for the cytochrome which should be tested. The blood is sampled repeatedly after application and from the pharmacokinetic information the clearance of the substrate can be calculated, which describes the cytochrome's activity [21]. Midazolam is recognized as one of the preferred in-vivo probes for CYP3A4 activity, since it has many characteristics of an ideal phenotyping probe: (i) it's mostly metabolized by CYP3A4; (ii) it has a short half-life, so that pharmacokinetic parameters can be measured rapidly; (iii) it can be administered both orally and intravenously, and therefore both hepatic and intestinal CYP3A4 activity can be determined [22]. The rate at which midazolam and other CYP3A4-substrates are being eliminated from the body differs greatly between individuals. This inter-individual variability can partly be explained by differences in CYP3A4 activity [23]. One reason for the variability are differences in CYP3A activity between different CYP3A variants. For example, different expression levels of CYP3A5, caused by single nucleotide polymorphisms in the CYP3A5 gene, can influence CYP3A activity [22]. Other factors affecting CYP3A4 activity are sex [22], age [24] or bodyweight [24] as well as nutrition, e.g., consumption of grapefruit juice [25]. Another major source of variation is drug-drug interaction which can have inhibitory or inducing effects on CYP3A activity [10, 23].

1.2.4 Inhibitors and inducers of CYP3A

Of special importance for an accurate CYP3A phenotyping is to gain a better understanding of the effects of inhibitors and inducers on CYP3A metabolism in the liver and intestines.

CYP3A4 induction is caused by an increase of protein amount. Enzyme induction results in a faster metabolism and clearance of CYP3A4 drugs such as midazolam. Individuals exposed to such an inducer develop an increased tolerance towards drugs metabolized by CYP3A4, i.e., a higher dose is required to achieve the same therapeutic effect [27]. In case of midazolam higher doses are required to induce sedation and its duration will be weakened [28]. A prominent example of an CYP3A4 inducer is rifampin, an antibiotic mostly used in the treatment of tuberculosis. Rifampin increases the activity of CYP3A4 in the liver as well as small intestine. As a consequence the total exposure of midazolam to the body (i.e. the area under the curve $AUC_{0-\infty}$) is significantly reduced. The effect of rifampin on midazolam pharmacokinetics especially affects orally administered midazolam, due to the increased first-pass metabolism [28].

In contrast to inducers, CYP3A4 inhibitors cause a slower biotransformation of its substrates. Inhibitors of CYP3A4 increase plasma concentrations and elimination half-life of midazolam, leading to prolonged effects [28]. Various types of CYP3A4 inhibition exist. One mechanism is via competitive inhibition in which a substrate competes with the drug for the same binding site. Another common

Table 1: Overview of clinical relevant CYP3A4 inhibitors and inducers. A subset (in **bold**) was chosen for further investigation. (*Source: Petri, H. 2020 [26]*)

CYP3A4 Inhibitors		CYP3A4 Inducers
Amiodaron	Idelalisib	Apalutamid
Aprepitant	Imatinib	Bosentan
Atazanavir-Ritonavir	Isavuconazole	Carbamazepin
Ciprofloxacin	Itraconazole	Dabrafenib
Clarithromycin	Ketoconazole	Efavirenz
Cobicistat	Lopinavir-Ritonavir	Enzalutamid
Clotrimazole	Nelfinavir	Eslicarbazepinacetat
Crizotinib	Nilotinib	St John's wort
Darunavir-Ritonavir	Posaconazole	Mitotan
Diltiazem	Ribociclib	Modafinil
Dronedaron	Ritonavir	Nevirapin
Erythromycin	Troleandomycin	Oxcarbazepin
Fluconazole	Verapamil	Phenobarbital
Fluvoxamin	Voriconazole	Phenytoin
Grapefruit		Primidon
		Rifampicin
		Topiramat

type is the so-called mechanism-based, or suicide, inhibition. In mechanism-based inhibition a substrate analogue binds to the active site and forms a covalent bond with the enzyme. In contrast to competitive inhibition, this irreversibly inhibits the enzyme. The effect can only be reversed by synthesis of new CYP3A4 [27].

Substances which inhibit the CYP3A4 enzyme system mechanism-based, can be found in some citrus fruits, the most studied are grapefruits. There are over 85 drugs that are known or predicted to interact with grapefruit juice. 43 of these drugs have the potential to cause serious effects like myelotoxicity, nephrotoxicity or respiratory depression. Since grapefruit juice primarily inhibits intestinal CYP3A, all affected drugs have in common that they are administered orally and have a low oral bioavailability. If the first-pass metabolism is significantly reduced by inhibition of intestinal CYP3A, it causes a high risk of overdose [29].

1.3 Physiological-based pharmacokinetic models (PBPK)

Within this work a computational model of midazolam pharmacokinetics was used to gain insights into the effects of inhibitors and inducers on midazolam metabolism and its pharmacokinetics. More specifically, a physiological-based (PBPK) pharmacokinetic model of midazolam metabolism was developed.

A PBPK model is a mathematical model, which allows to predict the pharmacokinetics of an administered substance, based on absorption, distribution, metabolism and elimination (ADME). Such models consist of multiple compartments, representing different organs or tissues in the body. Compartments are connected by flow rates that stand for blood circulating in the body. ADME processes such as transport- or metabolic reactions are included into the respective tissue compartments, e.g., the metabolic conversion of midazolam to 1-hydroxymidazolam in the liver compartment. PBPK models can predict the

pharmacokinetics of modeled drugs and metabolites [30].

PBPK models can be built using a 'bottom-up' approach. This means that all information in the model is based on well-known physiological and pharmacological mechanisms and data from previous *in-vivo* or *in-vitro* studies. Such a model could even be used to predict the kinetics of a new substance. Another approach would be more of a 'middle-way', where most of the model's reactions and parameters also come from previous knowledge, but then being fitted to create a desired output, like a concentration-time profile from a clinical study [31].

In this work a middle-approach was selected with tissue volumes and blood flows from prior knowledge, whereas the kinetic parameters of the metabolism were fitted using time course data.

1.4 Question, scope and hypotheses

Within this thesis the effect of inhibitors and inducers on midazolam metabolism was studied by the means of computational modeling. Specifically, a physiological-based pharmacokinetic model (PBPK) of midazolam was developed and applied to study the following question:

- What are the effects of intestinal and hepatic CYP3A4 inhibition and induction on midazolam pharmacokinetics?

Our main hypothesis was:

The clinically observed effect of many modifiers of midazolam pharmacokinetics can be explained by a simple model of intestinal and hepatic inhibition/activation of CYP3A4.

Our main objective was:

To elucidate and quantify factors affecting midazolam pharmacokinetics using a modelling approach, thereby improving the use of midazolam as CYP3A4 probe.

2 Methods

Within this work the effects of inhibitors and inducers on midazolam metabolism were studied by the means of a physiological-based pharmacokinetic model. The model was built in a data-driven approach using pharmacokinetics time courses and data curated from published clinical studies. Pharmacokinetic parameters were calculated from the predicted model time courses and compared to reported values.

The main methods applied were: calculation of pharmacokinetic parameters from time course data (Sec. 2.1), curation of pharmacokinetic data for model building (Sec. 2.2), development of a physiological-based pharmacokinetic model (Sec. 2.3), parameter fitting of model parameters (Sec. 2.3.2), uncertainty analysis (Sec. 2.4) and sensitivity analysis of model predictions (Sec. 2.5).

2.1 Calculation of pharmacokinetic parameters

The pharmacokinetics of a drug can be characterized by deriving parameters from the concentration-time curve. C_{max} and t_{max} describe the maximum concentration measured and the respective time at which the maximum is observed. The area under the curve (AUC) describes the area under the concentration time course and is a measure of the exposure of the body to the drug. The fractional elimination rate (k_{el}) represents the fraction of drug being eliminated per unit time. Further, the half-life (t_{half}), describes the time it takes to halve the drug concentration. Clearance (Cl) describes the fraction of blood that is being cleared per unit time. The volume of distribution (V_d) represents the artificial volume in which a substance distributes. An overview over the pharmacokinetic parameters used in this work and an illustration can be found in Tab. 2 and Fig. 2.

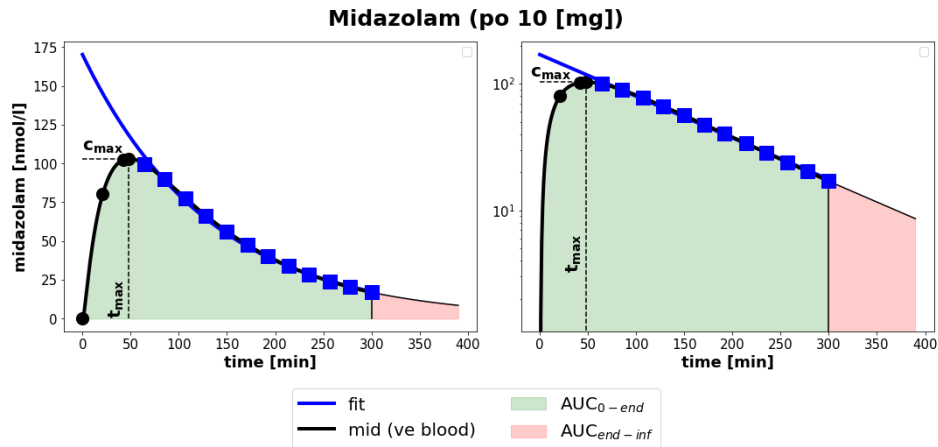


Figure 2: Illustration of pharmacokinetic parameters. Depicted are the midazolam concentration-time curve (black), predicted by the model, and the regression-line (blue), fitted over all time points after C_{max} (blue squares). Its slope describes the fractional elimination rate (k_{el}). The colored areas depict the AUC up to the last time point (green) and the AUC extrapolated to infinity (red).

Pharmacokinetic parameters of midazolam and 1-hydroxymidazolam were calculated by non-compartmental methods. To determine the elimination rate (k_{el})

Table 2: An overview over all, for this work, relevant pharmacokinetic parameters (PK), including a short description and their units.

PK	Description	Unit
AUC_{0-t}	Area under the curve, up to the last measured timepoint. Describes the exposure to the drug.	$\frac{g \cdot hr}{l}$
$AUC_{0-\infty}$	Area under the curve, extrapolated to infinity. Describes the estimated total exposure to the drug.	$\frac{g \cdot hr}{l}$
<i>Bioavailability</i>	The fraction of the total administered drug reaching systemic circulation.	%
Clearance	The fraction of blood that is cleared (via metabolism and elimination) per unit time.	$\frac{l}{hr}$
C_{max}	Describes the maximum concentration measured	$\frac{g}{l}$
k_{el}	Fractional elimination rate - The fraction of drug in the body that is eliminated per unit time	$\frac{1}{hr}$
t_{half}	The time it takes to remove half of the drug concentration	hr
t_{max}	The time at which C_{max} occurs.	hr
V_d	Apparent volume of distribution that explains the measured drug-concentration. Apparent because it doesn't explain where the drug goes, but only that it goes somewhere.	l

a linear-regression line (Eq. 2.1) was fitted over the log-timecourse after C_{max} . The negative slope of that regression line was then defined as k_{el} .

$$C = C_0 \cdot e^{-k_{el} \cdot t} \quad (2.1)$$

The half-life (t_{half}) was derived from the linear-regression line by setting up the linear-regression at t_{half}

$$\begin{aligned} 0.5 \cdot C_0 &= C_0 \cdot e^{-k_{el} \cdot t_{half}} \\ \Leftrightarrow 0.5 &= e^{-k_{el} \cdot t_{half}} \end{aligned} \quad (2.2)$$

and solving for t_{half} .

$$t_{half} = \frac{\ln(2)}{k_{el}} \quad (2.3)$$

To calculate the area under the curve up to the last time point (AUC_{0-t}) the trapezoidal rule was used.

$$AUC_{0-t} = \sum_{i=0}^{N-1} (t_{i+1} - t_i) \frac{(C_i + C_{i+1})}{2} \quad (2.4)$$

The total area under the curve ($AUC_{0-\infty}$) was calculated as $AUC_{0-\infty} = AUC_{0-t} + AUC_{t-\infty}$, with $AUC_{t-\infty}$ being the area extrapolated to infinity, which is equal

to the definite integral of the linear regression between the last measured time point (t_{last}) and infinity.

$$AUC_{t-\infty} = \int_{t_{last}}^{\infty} C_{last} \cdot e^{-k_{el} \cdot t} \cdot dt = \frac{C_{last}}{k_{el}} \quad (2.5)$$

From k_{el} and $AUC_{0-\infty}$ midazolam's volume of distribution (V_d)

$$V_d = \frac{Dose}{AUC_{0-\infty} \cdot k_{el}} \quad (2.6)$$

and subsequently, its clearance (Cl) can be calculated.

$$Cl = k_{el} \cdot V_d \quad (2.7)$$

2.2 Curation of pharmacokinetics data

2.2.1 PK-DB - pharmacokinetics database

PK-DB (<https://pk-db.com>) is an open database for pharmacokinetic data from clinical studies. It provides information on (i) patient cohorts and participating subjects (e.g. age, sex, smoking status); (ii) study design (e.g. administered substances, administration route, dosing); (iii) experimentally measured concentration-time-courses; and (iv) pharmacokinetic parameters (e.g area under the curve, clearance, bioavailability) [32].

PK-DB was used as curation platform and database for the midazolam pharmacokinetics studies curated in this work.

2.2.2 Curation of pharmacokinetic studies

An initial literature research was performed selecting clinical studies in Humans: (i) in which midazolam was applied orally and intravenously; (ii) in which inducers and/or inhibitors were applied in addition to midazolam. Subsequent literature searches extended the corpus of pharmacokinetic studies. In the curation process information on patient characteristics, study design and pharmacokinetic data was extracted from these studies, and encoded in a standardized file format based on JSON for automatic database upload.

To digitize time-course data 'Plot Digitizer' (<http://plotdigitizer.sourceforge.net>) was used, a software to extract data points from figures. These data points and the pharmacokinetic parameters from the studies were first entered into excel tables, and then referenced in the JSON file. Finally, all the information was uploaded to PK-DB. After automatic validation a second curator checked each study after to minimize curation errors.

2.2.3 Meta-analysis

For most pharmacokinetic parameters ($AUC_{0-\infty}$, clearance, t_{half} , V_d , oral bioavailability, oral C_{max} , oral t_{max}) a meta-analysis of the curated data was performed, thereby integrating results from multiple studies. This allowed identifying outliers and curation errors in the data (which were corrected subsequently). To perform the meta-analysis the set of all curated midazolam studies was queried from PK-DB. The analysis only included healthy subjects, since hepatic or renal

disease can change pharmacokinetics of midazolam significantly. For parameters and doses, that were given as values relative to subjects bodyweights, absolute values were calculated using the reported bodyweights. Querying was performed using the PK-DB REST API and the python pkdb.analysis [33] tools which allowed simple querying of the PK-DB database.

2.3 Physiological-based pharmacokinetics models (PBPK)

From the gathered data we built a PBPK model to predict midazolam and 1-hydroxymidazolam concentrations in the blood after either oral (po) or intravenous (iv) administration. The resulting concentration-time curves were used to calculate pharmacokinetic parameters as described in Sec. 2.1. The model was then fitted onto the curated time courses (Sec. 2.3.2).

2.3.1 Model representation and simulation

The PBPK models are ordinary differential equation (ODE) models and can be numerically solved with respective ODE solvers. From a given starting condition the time courses of all state variables (concentrations of midazolam and 1-hydroxymidazolam) in all tissues can be simulated. All models were encoded in the Systems Biology Markup Language (SBML) [34, 35], the de facto standard to describe and exchange models in systems biology.

The models were generated using sbmlutils [36], python-based tools for the work with SBML, and simulated using sbmlsim [37] with libroadrunner [38] as high-performance simulator. Tissue models of midazolam metabolism in the liver, intestines and the kidneys were developed as part of this work and coupled to an existing whole-body model. The tissue models were encoded in SBML core with model coupling of tissues to the whole-body models using SBML hierarchical model composition (comp) [39]. For model simulation the hierarchical model was flattened resulting in a single SBML model.

2.3.2 Parameter fitting (model optimization)

The goal of the model optimization was to adjust the model's parameters so that the resulting time course predictions of midazolam and 1-hydroxymidazolam match the time course data from the curated studies. The problem can be formulated as an optimization problem which minimizes the residuals between the simulation and data curves.

The optimization problem was solved using SciPy's least_squares method [40] which solves non-linear, bounded-variable least-squares problems. As the objective function a simple L2-Norm was used consisting of the sum of weighted residuals,

$$cost = 0.5 * \sum (w_k * w_{i,k} * res_{i,k})^2 \quad (2.8)$$

$res_{i,k}$ is the residual of time point i in time course k , i.e., the distance between model prediction and data. $w_{i,k}$ is the weighting of the respective data point i in timecourse k based on the error of the data point. w_k is the weighting factor of time course k .

The weighting of the time courses by w_k was necessary because (i) reported concentrations of midazolam are larger than those of 1-hydroxymidazolam (approx. by factor 10) and (ii) concentrations of different studies are very different for instance if the dosing is different. To solve these issues and make the contribution to the cost of time courses comparable the residuals were normalized by the average reported concentration of a time course. Further, residuals were weighted with $w_{i,k}$ based on their respective error (SD). The smaller the error was, the greater they were weighted. This allowed to include uncertainty information about the experimental data in the parameter fitting.

For each parameter included in the optimization problem an upper and lower bound was defined. 1000 sets of initial parameter guesses, sampled from a log-uniform distribution within the defined bounds, were used to perform a multi-start least squares fit.

2.4 Uncertainty analysis

To quantify the uncertainty of model predictions depending on parameters a simple uncertainty analysis was performed for all model simulations. Each model parameter was changed individually by $\pm 50\%$ and the model was simulated. From the sets of resulting time course predictions the standard deviation (SD), and minimum and maximum values at each time point were calculated. These uncertainty areas were displayed as shaded areas. In an analogue manner the uncertainty of pharmacokinetic parameters was derived. Here for the set of timecourses the corresponding sets of pharmacokinetic parameters (as described in Sec. 2.1) and the standard deviation (SD) were calculated.

Parameters corresponding to physical constants (such as molecular weights) and dosing (such as oral or intravenous dose) were not varied in the uncertainty analysis.

2.5 Sensitivity analysis

The effect of individual parameter changes on the model outcome was analysed using sensitivity analysis. Individual model parameters p_i were changed by 10% from their reference value ($p_{i,0} \rightarrow p_{i,\Delta}$). The sensitivity was then calculated by normalizing the change in the pharmacokinetic parameter from baseline with the parameter change. The sensitivity $S(q_k, p_i)$ of the pharmacokinetic parameter q_k with respect to model parameter p_i is given as

$$S(q_k, p_i) = \frac{q_k(p_{i,0}) - q_k(p_{i,\Delta})}{p_{i,0} - p_{i,\Delta}} \quad (2.9)$$

Parameters corresponding to physical constants (such as molecular weights) and dosing (such as oral or intravenous dose) were not varied in the sensitivity analysis.

2.6 Parameter scans

Parameter scans were performed to evaluate the effect of changing CYP3A4 activity in the liver and/or intestines. Variation in v_{max} values, corresponding to intestinal and hepatic CYP3A4, was performed by changing the respective v_{max}

by a factor f systematically from 10e-2 to 10e1. For every v_{max} factor the model was simulated and the pharmacokinetics calculated on the predicted midazolam time courses. Uncertainty analysis for the 1D scans was performed as described in Sec. 2.4. For the 2D-Scan of the intestinal and hepatic v_{max} factors no uncertainty analysis was performed.

3 Results

Within this work the effects of inhibitors and inducers on midazolam metabolism were studied using a computational approach. The main results of this work are presented in this section, consisting of (i) establishing a pharmacokinetics data base for midazolam (Sec. 3.1), (ii) development of a physiological-based pharmacokinetic model of midazolam (Sec. 3.2), and (iii) application of the model to study the effect of inhibitors and inducers (Sec. 3.3).

3.1 Midazolam pharmacokinetics data

Within this work a large data base of pharmacokinetics data from clinical studies has been established. In total 43 clinical studies were systematically digitized and curated. An overview of the studies including application route, administered inducers and inhibitors and study objective is given in Tab. 3. The curation included all information relevant for subsequent simulation of the studies, consisting of group, individual, intervention, output and time course information. The focus was on publications studying the effect of inducers and inhibitors on hepatic as well as intestinal CYP3A4 in healthy subjects, as well as studies comparing oral and intravenous application of midazolam (thereby providing information on bioavailability and first-pass effect).

Overall, 298 time courses and 4542 pharmacokinetic measurements were curated (2932 from studies, 1610 derived from time courses). Information on the curated group and individual characteristic are provided in 8.

The complete data set is made accessible as FAIR (findable, accessible, interoperable, reusable) data [41] in a standardized open accessible database (<https://pk-db.com>).

Table 3: Overview of all 43 curated studies. Study - Study name as represented in PK-DB (first-author, year of publication), PK-DB identifier, and Pubmed identifier; N - Total number of study participants; Route - Administration routes of midazolam (iv = intravenous; im = intramuscular; oral); Co-administered substances - All, for this work relevant, co-administered substances (+) = inducers; (-) = inhibitors; no label = substance has no significant effect on midazolam kinetics.

Study	N	Route	Co-administered Substances	Study Objective
Allonen1981 [42] PKDB00181 6117393	6	iv oral		Study the effects of dose and administration route on midazolam kinetics [42]
Backman1996 [28] PKDB00227 8549036	10	oral	rifampin (+)	Study the effects of rifampin on midazolam kinetics [28]
Backman1998 [43] PKDB00228 9591931	9	oral	rifampin (+) Itraconazole (-)	Study the effect of itraconazole and rifampin on midazolam kinetics [43]
Bornemann1985 [44] PKDB00251 2932334	12	oral		Study the relationship between dose and midazolam kinetics [44]
Chaobal2005 [45] PKDB00326 16321619	10	iv oral	rifampin (+) Grapefruit juice (-) Troleandomycin (-)	Study alfentanil as a CYP3A probe drug [45]
Chung2006 [22] PKDB00243 16580903	19	oral	rifampin (+) Ketoconazole (-)	Compare simvastatin as a possible CYP3A probe with the validated probe midazolam [22]
Darwish2008 [46] PKDB00328 18076219	77	iv oral	Armodafinil (+)	Study effects of armodafinil on CYP1A2, 3A4 and 2C19 activity [46]

Dyk2019 [47] PKDB00308 31611799	30	oral	rifampin (+) Clarithromycin (-)	Validate whether reduced sampling intervals can assess inter-individual variation and effects of inhibitors and inducers on CYP3A activity [47]
Eap2004 [48] PKDB00327 15114429	21	oral	rifampin (+) Ketoconazole (-)	Investigate if a low oral midazolam dose (75 ug) can be used to measure in-vivo CYP3A activity [48]
Ecckhoudt1998 [49] PKDB00247 9686884	9	iv	rifampin (+)	Study describes a HPLC assay for midazolam and its metabolite 1-hydroxymidazolam [49]
Ecckhoudt2001 [50] PKDB00322 11471773	8	iv	rifampin (+)	Investigate possible correlation between midazolam and 6-beta-OH cortisol as CYP3A probe drugs [50]
Erp2011 [51] PKDB00249 20512335	8	oral	Grapefruit juice (-)	Determine effect of grapefruit juice on sunitinib kinetics. Midazolam was used to assess intestinal CYP3A4 activity [51]
Farkas2007 [52] PKDB00209 17322140	13	iv oral	Grapefruit juice (-) Pomegranate juice	Study the effects of pomegranate juice on midazolam kinetics (Grapefruit juice as comparison) [52]
Gorski2003 [53] PKDB00205 12966371	52	iv oral	rifampin (+)	Investigate the relationship between age and sex, and rifampin induced CYP3A induction [53]
Greenblatt1986 [54] PKDB00179 2935051	14	iv oral	Cimetidine Ranitidine	Study the effects of co-administered cimetidine or ranitidine on midazolam kinetics [54]
Greenblatt2003 [55] PKDB00254 1289122	25	oral	Grapefruit juice (-)	Study the recovery rate of CYP3A after inhibition with grapefruit juice [55]
Greenblatt2004 [56] PKDB00298 15145968	8	iv		Study the pharmacokinetics of midazolam after different infusion times (1 min, 1 hour, 3 hours) [56]
Heizmann1983 [57] PKDB00178 6138080	6	iv oral		Study midazolam kinetics after oral and intravenous administration [57]
Kanto1985 [58] PKDB00250 3161005	207	im iv oral		Literature review of midazolam pharmacology and pharmacokinetics [58]
Kawaguchi-Suzuki2017 [59] PKDB00252 27503364	12	oral	Grapefruit juice (-)	Study the effects of grapefruit juice low in furanocoumarins on CYP3A activity [59]
Kharasch1997 [60] PKDB00245 9232132	9	iv	rifampin (+) Troleandomycin (-)	Evaluate the role of CYP3A4 in alfentanil metabolism. Midazolam was used to validate CYP3A4 activity [60]
Kharasch2004 [23] PKDB00211 15536460	10	iv oral	rifampin (+) Grapefruit juice (-) Troleandomycin (-)	Further investigate alfentanil as a CYP3A probe drug [23]
Klotz1982 [61] PKDB00203 7083724	6	iv oral		Study the effects of administration time (morning vs. evening) on midazolam kinetics [61]
Kupferschmidt1995 [25] PKDB00207 7628179	8	iv oral	Grapefruit juice (-)	Study the effects of grapefruit juice on midazolam kinetics [25]
Lee2002 [62] PKDB00306 12496753	12	iv oral	Ketoconazole (-)	Study the effects of semisimultaneous midazolam administration (po, iv), and the effect of ketoconazole on midazolam kinetics [62]
Link2008 [63] PKDB00248 18537963	8	iv oral	rifampin (+)	Evaluate whether saliva is suitable as a site of measurement for CYP3A phenotyping after midazolam administration [63]
Liu2017 [64] PKDB00305 28004396	15	oral	Ketoconazole (-)	Study the effects of different ketoconazole doses on midazolam kinetics [64]
Ma2009 [65] PKDB00325 19220276	13	iv		Show that subject posture has no effect on intravenous midazolam clearance [65]
Mandema1992 [66] PKDB00206 1611810	8	iv oral		Characterize the relationship between plasma concentration and CNS effects of midazolam and 1-hydroxymidazolam [66]

McCrea1999 [67] PKDB00321 10586386	12	oral	Ketoconazole (-) Erythromycin (low dose)	Evaluate simultaneous administration of erythromycin and oral midazolam to measure CYP3A activity [67]
Olkkola1993 [68] PKDB00246 8453848	12	iv oral	Erythromycin (-)	Study the effects of erythromycin on midazolam kinetics [68]
Olkkola1994 [69] PKDB00307 8181191	9	oral	Itraconazole (-) Ketoconazole (-)	Study the effects of ketoconazole and itraconazole on midazolam kinetics [69]
Pentikaeinen1989 [70] PKDB00269 2723115	14	iv oral		Study the effects of cirrhosis of the liver on midazolam kinetics [70]
Pentikis2007 [71] PKDB00244 17896891	27	iv oral	Rifaximin	Evaluate the potential of rifaximin as an inducer of intestinal or hepatic CYP3A, with midazolam as a CYP3A probe drug [71]
Rogers1999 [72] PKDB00208 10546919	16	oral	Grapefruit juice (-)	Study the effects of grapefruit juice on lovastatin kinetics, with midazolam as a positive control [72]
Shord2010 [73] 20233179 20233179	10	iv oral	Clotrimazole (-)	Study the effects of clotrimazole on midazolam kinetics [73]
Sjoevall1983 [74] PKDB00268 6628509	57	im iv oral		Investigate whether the rapid onset of midazolam can be explained by the rate and extend of its passage into cerebrospinal fluid [74]
Smith1981 [75] PKDB00199 6116606	6	iv oral		Study the kinetics of orally administered midazolam, in regard of its water solubility at low pH [75]
Thummel1996 [18] PKDB00202 8646820	20	iv oral		Assess the roles of intestinal and hepatic CYP3A in oral first-pass metabolism. Midazolam was used as a model compound [18]
Tsunoda1999 [76] PKDB00201 10579473	9	iv oral	Ketoconazole (-)	Determine the roles of intestinal and hepatic CYP3A in first-pass metabolism of midazolam with the use of ketoconazole [76]
Vanakoski1996 [77] PKDB00253 8858279	120	oral	Erythromycin (-) Grapefruit juice (-)	Study the potential of grapefruit juice to enhance effects of midazolam and triazolam [77]
Veronese2003 [78] PKDB00217 12953340	24	oral	Grapefruit juice (-)	Compare effects of different quantities of grapefruit juice on CYP3A4 activity, with midazolam as the CYP3A4 probe [78]
Yu2004 [15] PKDB00324 15289787	19	iv	rifampin (+) Itraconazole (-)	Study the effect of the CYP3A5 genotype on midazolam clearance [15]

The curated time course information was used for model building (overview provided in Tab. 6). The curated pharmacokinetic parameters were used for model validation (overview provided in Tab. 4/5).

3.1.1 Meta-analysis

Using the established data-based a meta-analysis was performed to integrate the data from the various sources and to improve data quality by detecting curation errors and outlier data. To account for the varying midazolam doses administered in the studies the dose-dependency of the pharmacokinetic parameters $AUC_{0-\infty}$, clearance, t_{half} , V_d , oral bioavailability, oral C_{max} and oral t_{max} were plotted against the administered dose of midazolam. For the analysis we first filtered for midazolam and 1-hydroxymidazolam outputs in blood/plasma and excluded all unhealthy subjects, which left us with 3403 outputs from 41 studies. Outliers were identified and corrected if they resulted from a curation mistake.

The following outliers were removed from all subsequent analysis: two C_{max} values after a dose of 40 mg oral midazolam in Heizmann1983 [57]; all reported parameters from Pentikis2007 [71], since some parameters were very different

Table 4: Overview of curated pharmacokinetics parameters (continued). For each study the table shows which pharmacokinetics parameters of midazolam (mid), 1-hydroxymidazolam (mid1oh) and 4-hydroxymidazolam (mid4oh) were reported. Whether a parameter was reported for individuals, groups and whether an error (SD or SE) was reported is shown as a triplet (in this order). Either, a parameter was reported for all individuals/groups (✓), only for some individuals/groups (⊖) or not reported at all (whitespace). The remaining pharmacokinetic parameters are listed in Tab. 5

pkdb	name	auc			clearance			cmax			kel		
		mid	mid1oh	mid4oh	mid	mid1oh	mid4oh	mid	mid1oh	mid4oh	mid	mid1oh	mid4oh
PKDB00181	Allonen1981	✓			✓✓✓			✓✓✓			✓		
PKDB00227	Backman1996	✓✓✓			✓			✓✓✓			✓		
PKDB00228	Backman1998	✓✓			✓			✓✓			✓		
PKDB00251	Bornemann1985	✓✓✓			✓✓✓			✓✓✓			✓✓		
PKDB00326	Chaoal2005												
PKDB00243	Chung2006	∅			∅∅			∅∅			∅∅		
PKDB00328	Darwishi2008	∅∅			∅∅			∅∅			∅∅		
PKDB00308	Dyk2019	✓			✓			✓			∅		
PKDB00327	Eap2004	✓✓			∅∅			∅∅			∅∅		
PKDB00247	Beckhoudt1998	∅			∅			∅			∅		
PKDB00322	Beckhoudt2001				∅∅			∅∅			∅∅		
PKDB00249	Erp2011	✓			✓✓			✓✓			✓✓		
PKDB00209	Farkas2007	✓✓			✓✓			✓✓			✓✓		
PKDB00205	Gorski2003	✓✓			✓✓			✓✓			∅∅∅		
PKDB00179	Greenblatt1986	∅∅∅			∅∅∅			∅∅∅			∅∅∅		
PKDB00254	Greenblatt2003	✓✓			✓✓			✓✓			∅		
PKDB00298	Greenblatt2004	✓			✓✓			✓			✓		
PKDB00178	Heizmann1983	✓✓∅			∅∅∅			✓			✓		
PKDB00250	Kanto1985	∅			∅∅			∅∅			∅∅		
PKDB00252	Kawaguchi-Suzuki2017	∅✓✓			✓✓			✓✓			✓✓		
PKDB00245	Kharasch1997				✓✓			✓✓			✓✓		
PKDB00211	Kharasch2004	✓✓			✓✓			✓✓			∅∅∅		
PKDB00203	Klotz1982	∅			∅∅			∅∅			∅∅∅		
PKDB00207	Kupferschmidt1995	✓✓			✓✓			✓✓			✓✓✓		
PKDB00306	Lee2002	∅∅∅			∅∅∅			∅∅∅			∅∅∅		
PKDB00248	Link2008	✓✓			∅∅			✓			∅∅		
PKDB00305	Liu2017	✓✓			✓			✓✓			✓✓		
PKDB00325	Ma2009	✓			✓			✓			✓		
PKDB00206	Mandema1992	✓			✓			✓✓✓			✓✓✓		
PKDB00321	McCreath1999	✓∅			∅∅			∅∅			∅∅		
PKDB00246	Olkkiola1993	∅∅			∅∅			∅∅			∅∅		
PKDB00307	Olkkiola1994	✓✓			✓			✓✓			✓✓		
PKDB00269	Penttiläinen1989	✓✓			✓✓			✓✓			✓✓		
PKDB00244	Penttiläinen2007	∅∅			∅∅			∅∅			∅∅		
PKDB00208	Rogers1999	✓✓			✓✓			✓✓			✓✓		
PKDB00323	Shord2010	✓✓			✓✓			✓✓			✓✓		
PKDB00268	Sjøeås1983	✓✓			✓✓			✓✓			✓✓		
PKDB00199	Smith1981	✓✓✓			✓✓✓			✓✓✓			✓✓✓		
PKDB00202	Thummel1996	∅			∅∅∅			∅∅∅			∅∅∅		
PKDB00201	Tsunoda1999	✓✓			✓✓			✓✓			✓✓		
PKDB00253	Vanakostki1996	∅			∅			∅			∅		
PKDB00217	Veronese2003	✓			✓			✓			✓		
PKDB00324	Yu2004	✓			✓			✓			✓		

Table 5: Overview of curated pharmacokinetics parameters (continued). For each study the table shows which pharmacokinetics parameters of midazolam (mid), 1-hydroxymidazolam (mid1oh) and 4-hydroxymidazolam (mid4oh) were reported. Whether a parameter was reported for individuals, groups and whether an error (SD or SE) was reported is shown as a triplet (in this order). Either a parameter was reported for all individuals/groups (✓), only for some individuals/groups (⊖) or not reported at all (whitespace). The remaining pharmacokinetic parameters are listed in Tab. 4

pkdb	name	thalf			tmax			vd		
		mid	mid1oh	mid4oh	mid	mid1oh	mid4oh	mid	mid1oh	mid4oh
PKDB00181	Allonen1981	✓✓✓			✓✓✓			✓✓✓		
PKDB00227	Backman1996	✓✓✓			✓✓			✓		
PKDB00228	Backman1998	✓✓			✓			✓		
PKDB00251	Bornemann1985	✓	✓		✓✓			✓		
PKDB00326	Chaoabai2005									
PKDB00243	Chung2006	⊖			⊖			⊖		
PKDB00328	Darwishi2008	⊖	⊖		⊖			⊖⊖		
PKDB00308	Dyk2019	✓			✓			⊖		
PKDB00327	Eap2004	✓✓			⊖⊖			⊖⊖		
PKDB00247	Eeckhout1998	⊖	⊖		⊖			⊖		
PKDB00322	Eeckhout2001									
PKDB00249	Erp2011									
PKDB00209	Farkas2007				✓			✓✓		
PKDB00205	Gorski2003	✓✓						✓✓		
PKDB00179	Greenblatt1986	⊖✓✓			⊖⊖⊖			⊖⊖⊖		
PKDB00254	Greenblatt2003	✓✓			⊖			⊖		
PKDB00298	Greenblatt2004	✓✓			✓			✓✓		
PKDB00178	Heizmann1983	✓✓⊖	✓		✓	✓		⊖		
PKDB00250	Kantol1985	⊖⊖			⊖⊖			⊖⊖		
PKDB00252	Kawaguchi-Suzuki2017	✓	✓		✓	✓		✓		
PKDB00245	Kharasch1997	✓✓								
PKDB00211	Kharasch2004	✓✓			✓✓			⊖✓✓		
PKDB00203	Klotz1982	⊖✓✓	✓		✓	✓		✓		
PKDB00207	Kupferschmidt1995	✓	✓		✓	✓		⊖✓✓		
PKDB00306	Lee2002	⊖✓✓			⊖			⊖✓✓		
PKDB00248	Liu2008	✓	⊖✓	✓	✓	⊖✓	✓	✓		
PKDB00305	Liu2017									
PKDB00325	Ma2009	✓			✓	✓✓✓	✓✓✓	✓		
PKDB00206	Mandema1992	✓✓✓			✓					
PKDB00321	McCrea1999									
PKDB00246	Oikkola1993	✓✓						⊖		
PKDB00307	Oikkola1994	✓✓						✓		
PKDB00269	Pentikainen1989	✓✓						✓		
PKDB00244	Pentikis2007	⊖⊖			⊖	⊖		⊖		
PKDB00208	Rogers1999	✓			✓✓					
PKDB00323	Shord2010	✓✓	✓		✓	✓		✓		
PKDB00268	Sjöeval1983	✓⊖			✓⊖			✓⊖		
PKDB00199	Smith1981	✓✓✓			✓✓✓			✓✓✓		
PKDB00202	Thummel1996	✓✓✓	⊖		⊖	⊖		✓✓✓		
PKDB00201	Tsunoda1989	✓✓			✓✓			✓✓		
PKDB00253	Vanakoski1996	⊖			⊖			⊖		
PKDB00217	Veronesi2003	✓								
PKDB00324	Yi2004	✓	✓		✓	✓		✓		

Table 6: Overview of all curated time courses. The table shows for each study whether time course data for midazolam (mid), 1-hydroxymidazolam (mid1oh) and 4-hydroxymidazolam was reported. The table further shows whether the time course data was reported for single individuals, groups, whether an error (SD or SE) was reported and the site of measurement (plasma/blood, urine and saliva). Either, time course data (or errors) was reported for all individuals/groups (✓), only for some individuals/groups (Ø) or not reported at all (whitespace).

pkdb	name	mid				mid1oh				mid4oh			
		individual	group	error	plasma	urine	saliva	individual	group	error	plasma	urine	saliva
PKDB00181	Allonen1981	✓	✓	✓									
PKDB00227	Backman1996	✓	✓	✓									
PKDB00228	Backman1998	✓	✓	✓				✓	✓	✓			
PKDB00251	Bornemann1985	✓	✓					✓	✓				
PKDB00326	Chaobal2005												
PKDB00243	Chung2006	Ø	Ø	✓									
PKDB00328	Darwishi2008	Ø	Ø	✓									
PKDB00308	Dyk2019	Ø		✓									
PKDB00327	Eap2004	Ø	Ø	✓				Ø	Ø	✓		Ø	Ø
PKDB00247	Eeckhoudt1998	Ø		✓		Ø				✓			
PKDB00322	Eeckhoudt2001												
PKDB00249	Erp2011												
PKDB00209	Farkas2007	✓		✓									
PKDB00205	Gorski2003	Ø	Ø	✓									
PKDB00179	Greenblatt1986	Ø		✓									
PKDB00254	Greenblatt2003	Ø	Ø	✓									
PKDB00298	Greenblatt2004	✓	✓	✓									
PKDB00178	Heizmann1983	✓		✓				✓		✓			
PKDB00250	Kanto1985	Ø	Ø	✓									
PKDB00252	Kawaguchi-Suzuki2017	✓	✓	✓				✓	✓	✓			
PKDB00245	Kharasch1997	Ø		✓		Ø				✓			
PKDB00211	Kharasch2004	✓	✓	✓									
PKDB00203	Klotz1982	Ø		✓									
PKDB00207	Kupferschmidt1995	✓	✓	✓				✓	✓	✓			
PKDB00306	Lee2002	Ø	✓	✓	✓								
PKDB00248	Link2008	✓	✓	✓		✓	Ø	✓	✓	✓		✓	
PKDB00305	Liu2017												
PKDB00325	Ma2009	✓	✓	✓									
PKDB00206	Mandema1992	✓	✓	✓				✓	✓	✓			
PKDB00321	McCrea1999	✓	✓	✓				✓	✓	✓			
PKDB00246	Olkkola1993	Ø	Ø	✓									
PKDB00307	Olkkola1994	✓	✓	✓									
PKDB00269	Pentikaeinen1989	✓	✓	✓									
PKDB00244	Pentikis2007	Ø		✓				Ø		✓			
PKDB00208	Rogers1999												
PKDB00323	Shord2010	✓	✓	✓				✓	✓	✓			
PKDB00268	Sjoevall1983	✓	✓	✓									
PKDB00199	Smith1981	✓	✓	✓									
PKDB00202	Thummel1996	Ø		✓		Ø				✓			
PKDB00201	Tsunoda1999	✓	✓	✓									
PKDB00253	Vanakoski1996	Ø		✓									
PKDB00217	Veronese2003	✓	✓	✓									
PKDB00324	Yu2004	✓	✓	✓				✓	✓	✓			

from all other studies, and a reported C_{max} value contradicted the corresponding reported time course.

The resulting meta-analysis of pharmacokinetics for midazolam after intravenous (iv) and oral (po) administration of midazolam is depicted in Fig. 3. To study the effect of inducers and inhibitors the data was classified in 5 groups: (i) Control (black) - only administration of midazolam; (ii) No interaction (gray) - pre-treatment with substances that have no influence on midazolam metabolism; (iii) Induction (blue) - CYP3A4 inducers; (iv) Systemic inhibition (red) - hepatic and intestinal CYP3A4 inhibitors; Intestinal inhibition (orange) - inhibitors only affecting intestinal CYP3A4 (intestinal inhibition). The corresponding meta-analyses of additional parameters and for 1-hydroxymidazolam are provided in the supplementary information (Sec. A.2).

While some parameters like oral bioavailability, t_{half} and t_{max} showed a large variability between studies, it was still possible to observe clear trends.

A clear correlation between midazolam dose and its $AUC_{0-\infty}$, as well as C_{max} could be observed. I.e., with increasing midazolam dose the area under the midazolam plasma concentration curve as well as the maximal concentration increase. In contrast, dosing had no influence on the remaining pharmacokinetic parameters. In addition, clearance of midazolam was increased when administered orally, compared to intravenous administration.

CYP3A4 inhibition and induction showed clear effects on the pharmacokinetic parameters.

Pre-treatment with rifampin, a CYP3A4 inducer, showed an up to 10-fold decrease of the $AUC_{0-\infty}$ and increase in midazolam clearance respectively. Interestingly, CYP3A4-activation affected these two parameters much stronger, when midazolam was administered orally. Consequently, C_{max} , t_{max} and t_{half} showed a decrease, while the V_d increased. The induction of CYP3A4 also effects the first pass metabolism, which shows in a lower oral bioavailability, with some studies reporting a drop down to almost zero.

CYP3A4-inhibitors, which inhibit hepatic and intestinal CYP3A4, used in the studies were erythromycin, itraconazole, ketoconazole and troleandomycin. Pre-treatment with one of these inhibitors lead to an increased $AUC_{0-\infty}$, t_{half} , *oral* C_{max} , *oral* t_{max} (except for Olkkola1993 [68], which reported a shorter t_{max}) and a bioavailability of almost 90%, whereas clearance and *oral* V_d was lowered). In contrast to treatment with CYP3A4-inducers, no difference between the administration routes of midazolam could be observed. Furthermore, no clear difference between the different inhibitors was visible.

As expected, CYP3A4-inhibitors, which only affect intestinal CYP3A4 (grapefruit juice and clotrimazole), only changed midazolam's kinetics when midazolam was given orally. Overall, the same trends as with hepatic and intestinal CYP3A4 inhibitors could be observed, but the effects were much weaker.

An important outcome of the meta-analysis was that most of the data from the various sources is consistent. Relatively large inter-study variability can be observed as seen by the large point clouds (note the logarithmic axes), as well as large intra-study variability as evident by the large error bars.

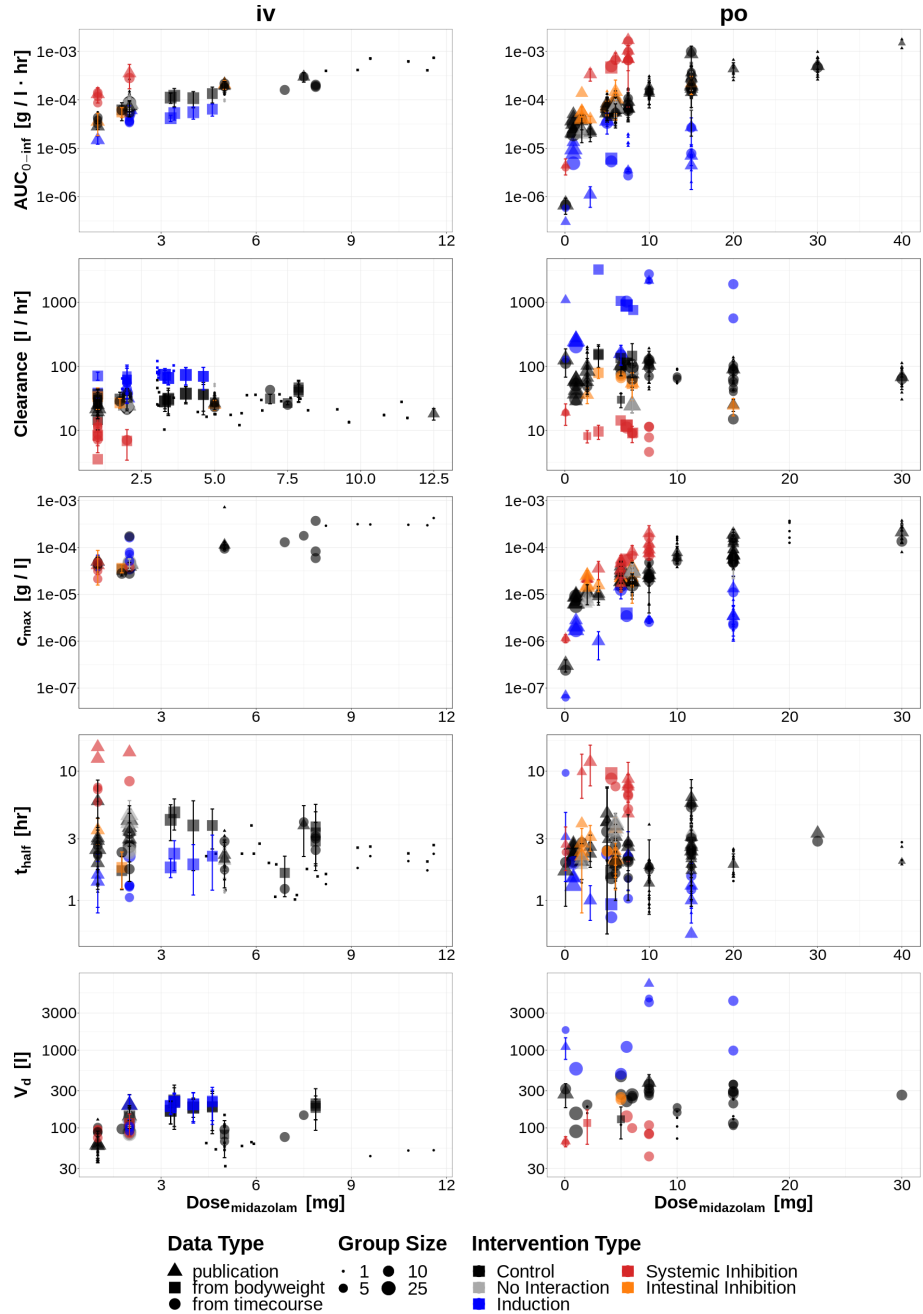


Figure 3: Meta-analysis of pharmacokinetic parameters ($AUC_{0-\infty}$, clearance, C_{max} , t_{half} , t_{max} and V_d) of midazolam in healthy subjects. Depicted are the respective parameters after intravenous (iv) and oral (po) midazolam administration either for controls, pre-treatment with substances that have no influence on midazolam metabolism (no interaction), CYP3A4 inducers (induction), hepatic and intestinal CYP3A4 inhibitors (systemic inhibition), and inhibitors only affecting intestinal CYP3A4 (intestinal inhibition). Data points were either taken directly from the publication (from publication), transformed in absolute values with the respective bodyweight if given relative to bodyweight (from bodyweight) or calculated from time courses (from timecourse). The corresponding meta-analysis of additional parameters and for 1-hydroxymidazolam is provided in the supplementary Sec. A.2. Data is mean (+- SD).

3.2 Midazolam model

3.2.1 Physiological-based pharmacokinetics model

For this thesis an existing framework of a whole-body PBPK model was adapted Fig. 4. The whole-body model contained all relevant compartments, blood-flow rates between compartments and reactions for absorption and distribution of an administered template drug. Within this work the model was extended and applied to midazolam. The first task was to create tissue models, representing the organs partaking in the metabolism of midazolam (small intestine, liver, kidney) (Fig. 5) (for an overview of midazolam metabolism see Sec. 1.2.1). Once created, the tissue models were coupled with the whole-body model, by replacing the existing compartments with the newly created tissue models. The model coupling was performed using hierarchical model composition.

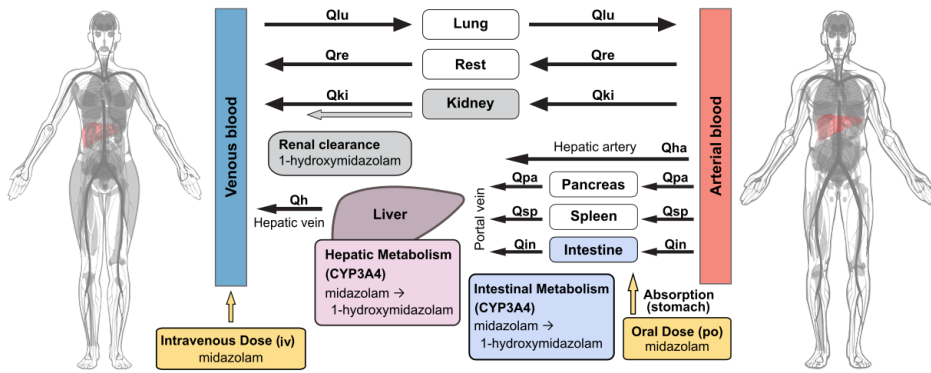


Figure 4: Illustration of the physiological-based whole-body model. It consists of the two blood-compartments, venous blood and arterial blood, and several tissue-compartments. All compartments are connected by the circulating blood. Blood travels from the venous blood, through the lung-compartment, to the arterial blood, and then, through the remaining compartments, back to the venous blood. The blood-flow rates are depicted by the values Q_{lu} , Q_{re} , etc. Midazolam can be administered either intravenously (iv) or orally (po). Once administered, midazolam is absorbed into the venous blood, passing intestine and liver first when administered orally, then distributed by the blood flow, subsequently metabolized by the intestine and liver, and ultimately its metabolite 1-hydroxymidazolam is excreted into the urine via the kidney.

For all three tissue models an external and internal compartment were created, representing the blood and the organ itself respectively. For the kidney a third compartment (urine) was defined. For the liver- and intestine model the following reactions were included: (i) transport of midazolam and 1-hydroxymidazolam in and out of the tissues and (ii) conversion of midazolam into 1-hydroxymidazolam catalyzed by the respective hepatic or intestinal CYP3A4 (named MIDOH in the model). For the kidney model only a single reaction was defined, representing the irreversible excretion of 1-hydroxyidazolam from blood into urine, via the renal elimination route.

The rate laws of all reactions in the liver and intestine were based on Michaelis-Menten kinetics. The transport reactions were defined as reversible (Eq. 3.2) and the metabolic reactions as irreversibly (Eq. 3.1),

$$v = V_{tissue} \cdot f \cdot v_{max,MIDOH} \cdot \frac{[S]}{[S] + K_m} \quad (3.1)$$

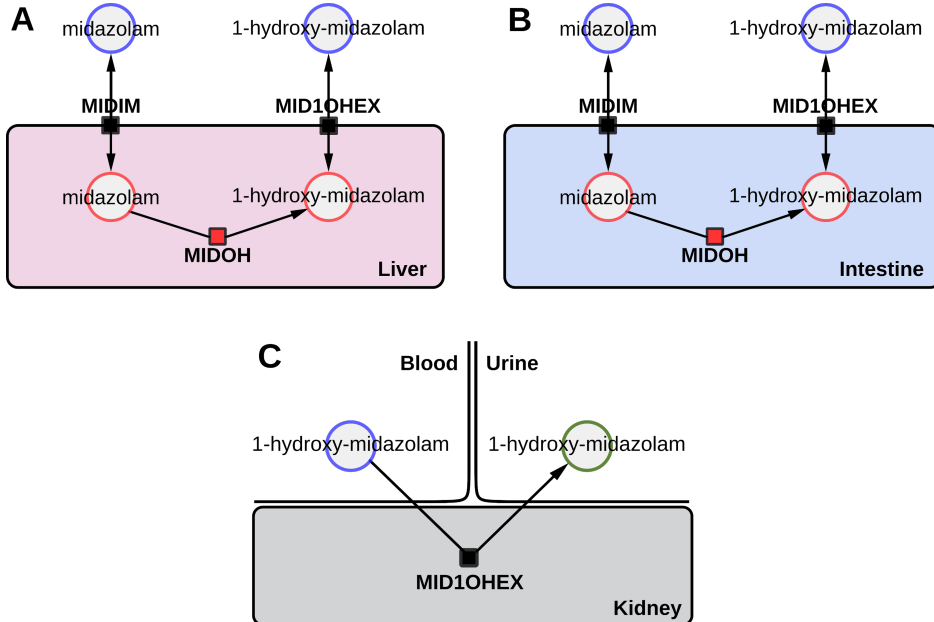


Figure 5: Illustration of the tissue models. (A/B) The structure of the liver and intestine models are identical, they only differ in their parameter values. Midazolam and 1-hydroxymidazolam can be transported in and out of the tissues by their respective transporters (MIDIM and MID1OHEX). Once inside the tissue, midazolam is converted to 1-hydroxymidazolam by the irreversible reaction MIDOH catalyzed by CYP3A4. (C) Kidney model in which the transport reaction MID1OHEX transports 1-hydroxymidazolam irreversibly from the arterial blood into the urine.

$$v = V_{tissue} \cdot \frac{v_{max}}{K_m} \cdot \frac{[S_i] - [S_o]}{1 + \frac{[S_i]}{K_m} + \frac{[S_o]}{K_m}} \quad (3.2)$$

with $[S]$ being the substance concentration (midazolam or 1-hydroxymidazolam), v_{max} the maximum reaction rate, towards which the function converges, and K_m the Michaelis-Menten constant, which determines the concentration at which the reaction rate is half of v_{max} . f is a scaling factor for MID1OH which can be used to scale v_{max} up or down to simulate CYP3A4 activation or inhibition, respectively. In the reversible transport reactions the difference between the substance concentration inside ($[S_i]$) and outside ($[S_o]$) of the compartment determines the direction of the reaction flux.

Based on experimental evidence that intestinal and hepatic CYP3A4 are identical isoforms (see 1.2.2 and [17]), the model assumption was made that intestinal and hepatic MID1OH reactions have the identical K_m parameter (modeled as a single parameter in the model).

For the 1-hydroxymidazolam elimination via the kidney we formulated a simple first order reaction (Eq. 3.3),

$$v = V_{tissue} \cdot k \cdot [S] \quad (3.3)$$

with k being a constant and $[S]$ the 1-hydroxymidazolam concentration in the arterial blood outside the kidney.

All reactions in the tissue models are scaled via the respective tissue volumes V_{tissue} . All reaction rates v are in $\frac{mmole}{min}$.

For each reaction, parameter, metabolite and compartment units were defined. This way model-outputs are comparable among each other and correct conversion factors and interfaces can be ensured during the hierarchical model composition. Importantly, the complete unit annotation allowed automatic checking of units to prevent errors when defining reaction rates and allowed for automatic unit conversion of data to models in the simulations.

The hierarchical PBPK model consisting of the whole-body model with the coupled liver, intestine and kidneys was flattened is available in SBML.

3.2.2 Model parameterization

In the next step the model had to be parameterized. Model parameters were (i) either taken from the existing whole-body PBPK model (physiological parameters such as blood flows, organ volumes or heart rate), (ii) are physio-chemical constants retrieved from data bases (such as molecular weights), (iii) were manually set to reasonable values (for instance Michaelis-Menten constants of transport reactions), (iv) or fitted based on parameter optimization (as described in Sec. 3.2.3). An overview of all model parameters of the final model is provided on the git repository https://github.com/YannickDuport/midazolam_model, in the form of the final SBML file.

3.2.3 Parameter fitting

The next step was to fit the model (Sec. 3.2) to the curated datasets (Sec. 3.1), i.e., to adjust the model parameters so that the distance between model predictions and experimental time courses is minimized. A total of 27 studies from all 43 curated studies were used in parameter fitting. Studies were chosen according to the following criteria: (i) they must provide time courses from healthy individuals, (ii) the time courses must be based on group data, i.e. no time courses from single individuals, and (iii) the study protocol should be relatively simple consisting of single applications of midazolam either orally or intravenously (i.e. more complicated protocols such as simultaneous administration of intravenous and oral midazolam, or multiple dosing studies, were excluded). Most studies were excluded because they either did not provide any time course information or the time courses came from single individuals. Furthermore, only the subset of time courses under control conditions (no CYP3A4 induction or inhibition) were used in optimizing the reference model (control condition).

In total 12 model parameters were fitted, partaking in the absorption, distribution and elimination of midazolam:

- **Ka_dis_mid** and **Ka_abs_mid**, describe the dissolution and absorption of orally administered midazolam.
- **ftissue_mid** and **ftissue_mid1oh**, control the distribution of midazolam and 1-hydroxymidazolam into tissues.
- **LI_MIDIM_Vmax**, **LI_MID1OHEX_Vmax**, **GU_MIDIM_Vmax** and **GU_MID1OHEX_Vmax**, the maximum reaction rates (v_{max}) of midazolam and 1-hydroxymidazolam transport reactions in the liver and intestine.

- **LI_MIDOH_Vmax** and **GU_MIDOH_Vmax**, the maximum reaction rates (v_{max}) of the metabolic reactions in the liver and intestine (CYP3A4).
- **MIDOH_Km**, the common Michaelis-Menten constant for the metabolic reactions in both liver and intestine (CYP3A4).
- **KI_MID1OHEX_k**, the rate constant which controls the elimination of 1-hydroxymidazolam via the kidneys.

For all studies simulation experiments were encoded using the curated study protocols (e.g., 10 mg midazolam applied orally) and further the time course data from the study mapped on the respective observables in the model. E.g., if a time course of plasma midazolam concentration was measured in a study it was mapped on the variable 'Cve_mid', corresponding to the predicted midazolam concentration in the model. Unit conversions were performed automatically between model and data, using the curated data and model units and the molecular weights. The resulting mappings between the reference time course data and model observables were then used for parameter fitting by minimizing the distance between references and corresponding observables.

In a first step, the model was fitted against each study individually. This allowed us to check if the model with the given parameter bounds is capable of reproducing the individual time courses (data not shown). All studies succeeded (i.e., a good fit could be achieved) except for Pentikis2007 [71], which was excluded from all subsequent fittings.

The next step was to fit the model against the time courses from the complete data of the remaining 26 studies via a non-linear least squares optimization using a multi-start approach (Sec. 2.3.2).

The overview of the parameter fitting performance is provided in the form of Waterfall plots and the individual optimization traces of the optimizers in Fig. 6. The main quantity for evaluation of the optimization is the cost, which provides a measure of the distance between data references and observables in the respective model simulations. The total cost is the sum of the weighted individual cost of all individual time courses from the various studies. All optimizers in the multi-start approach reduced the overall cost.

In total 69 time courses from 26 studies were used in the optimization with the individual costs before and after parameter fitting depicted in Fig. 7. The optimization could improve the overall agreement between data and model as can be seen by the reduction in cost (shift of histogram to the left)

The resulting optimal parameters are listed in Tab. 7. In the following we refer to the model with optimal parameters as 'reference model'. If not otherwise stated all simulations were performed with the reference model. If additional parameters were adjusted these are mentioned in the respective simulations and figures.

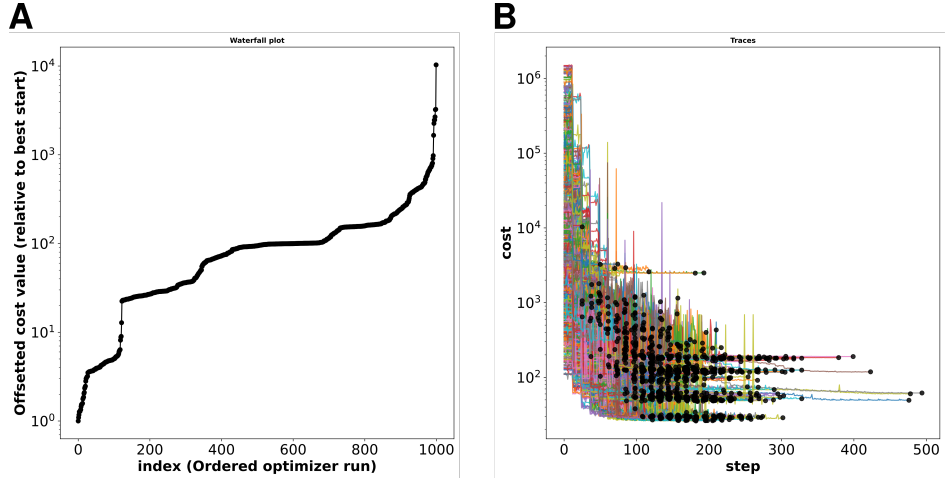


Figure 6: (A) Waterfall plot. Shows the final costs relative to the smallest cost, sorted by cost for each optimization run. (B) Illustrates the traces of each optimization run. It shows the costs at each step of an optimization run.

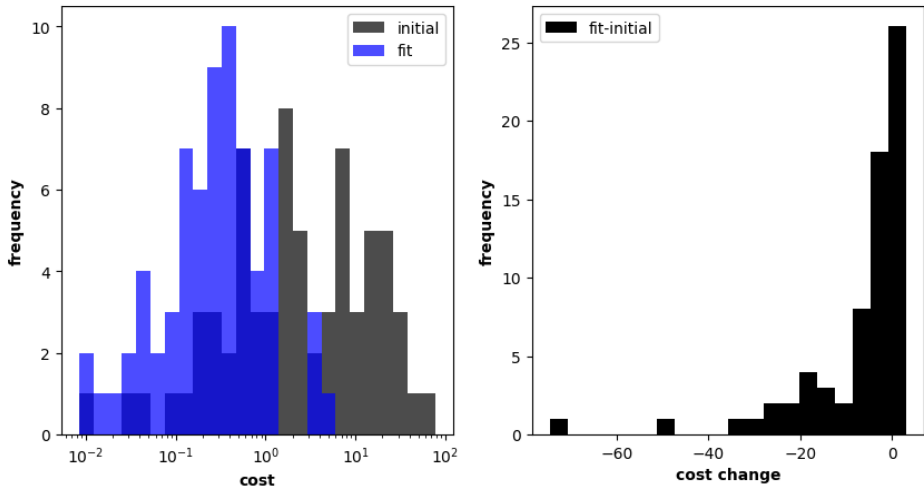


Figure 7: The plot shows the histogram of costs for each of the 69 timecourses before (grey) and after (blue) model optimization. The histogram of differences in costs (fit-initial) is depicted in black. The cost is reduced in parameter optimization for almost all timecourses.

Table 7: Parameters included in the parameter fitting and their optimal values (rounded to four digits). It lists the parameter name as represented in the model, a short description of the parameter, the optimal value after fitting, and the unit.

Parameter	Description	Value	Unit
Ka_dis_mid	Midazolam dissolution rate	2.409	$\frac{1}{\text{hour}}$
Ka_abs_mid	Midazolam absorption rate	4.463	$\frac{1}{\text{hour}}$
ftissue_mid	Midazolam distribution rate into tissues	916.0	$\frac{l}{\text{min}}$
ftissue_mid1oh	1-hydroxymidazolam distribution rate into tissues	0.1124	$\frac{l}{\text{min}}$
LI_MIDIM_Vmax	v_{\max} of midazolam transport in the liver	0.001465	$\frac{\text{mmole}}{\text{min}}$
LI_MID1OHEX_Vmax	v_{\max} of 1-hydroxymidazolam transport in the liver	0.04864	$\frac{\text{mmole}}{\text{min}}$
LI_MIDOH_Vmax	v_{\max} of liver CYP3A4 conversion of midazolam into 1-hydroxymidazolam	0.01049	$\frac{\text{mmole}}{\text{min}}$
GU_MIDIM_Vmax	v_{\max} of midazolam transport in the intestine	0.9884	$\frac{\text{mmole}}{\text{min}}$
GU_MID1OHEX_Vmax	v_{\max} of 1-hydroxymidazolam transport in intestine	2.379e-6	$\frac{\text{mmole}}{\text{min}}$
GU_MIDOH_Vmax	v_{\max} of intestine CYP3A4 conversion of midazolam into 1-hydroxymidazolam	0.1130	$\frac{\text{mmole}}{\text{min}}$
MID1OH_Km	K_m of CYP3A4 conversion of midazolam to 1-hydroxymidazolam in liver and intestine	0.100	$\frac{\text{mmole}}{\text{min}}$
KI_MID1OHEX_k	v_{\max} of 1-hydroxymidazolam kidney excretion	1.303	$\frac{1}{\text{min}}$

3.2.4 Model performance

The fitted model was used to predict all simulation experiments for the 26 studies. Representative simulations with the 'reference model' are provided in Fig. 8, Fig. 9 and Fig. 10. The full set of simulations is depicted in the supplementary Sec. A.3.

Importantly, we established a workflow which allowed to run the complete analysis consisting of all 26 simulation experiments after changes to the model. This allowed, in an iterative manner, to improve the agreement between model predictions and reference data.

The fitted model showed good performance in predicting midazolam time courses after intravenous bolus injections, after infusions, as well as oral administration in various forms (e.g. tablet, solution). The large majority of data points was within the uncertainty range (Sec. 2.4). The overall kinetics of midazolam

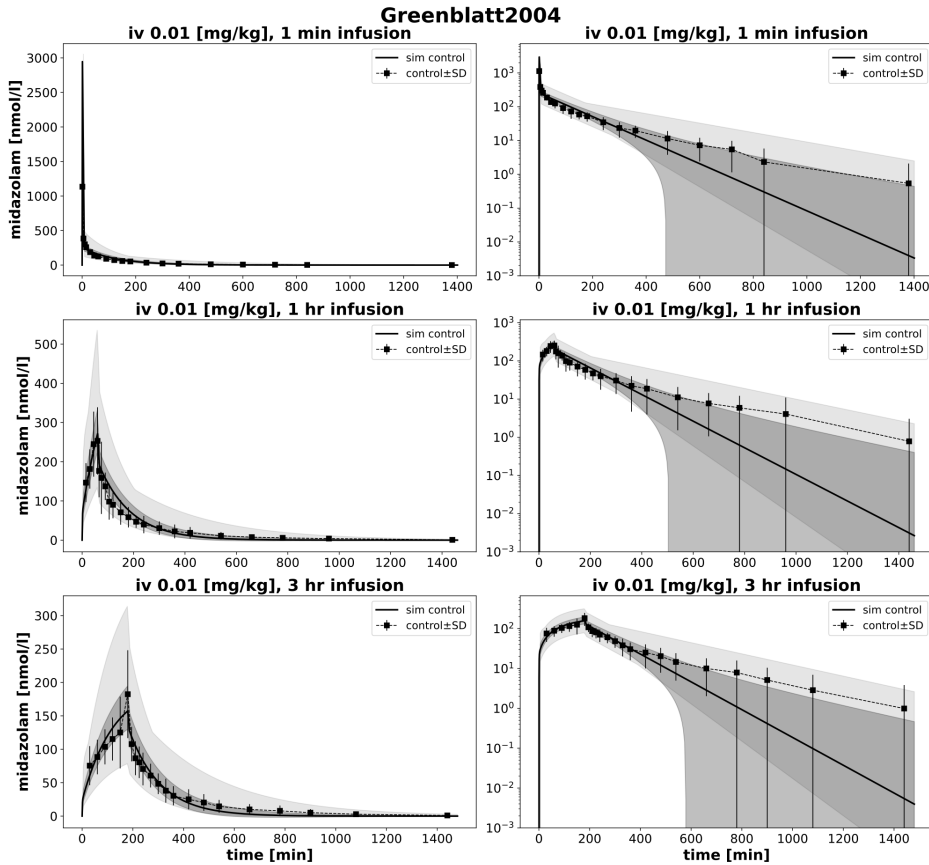


Figure 8: Simulation experiment Greenblatt2004. The figure shows the reported time courses (dashed) from Greenblatt2004 [56] and time course predictions by the reference model (solid) after an intravenous midazolam dose of 0.01 mg/kg, infused over 1 min, 1 hour and 3 hours. The shaded areas around the model predictions depict the SD (dark) and the full range (light) from the uncertainty analysis (Sec. 2.4). Reported time course data are mean \pm SD. Each time course is plotted on a linear y-axis (left) and a logarithmic y-axis (right)

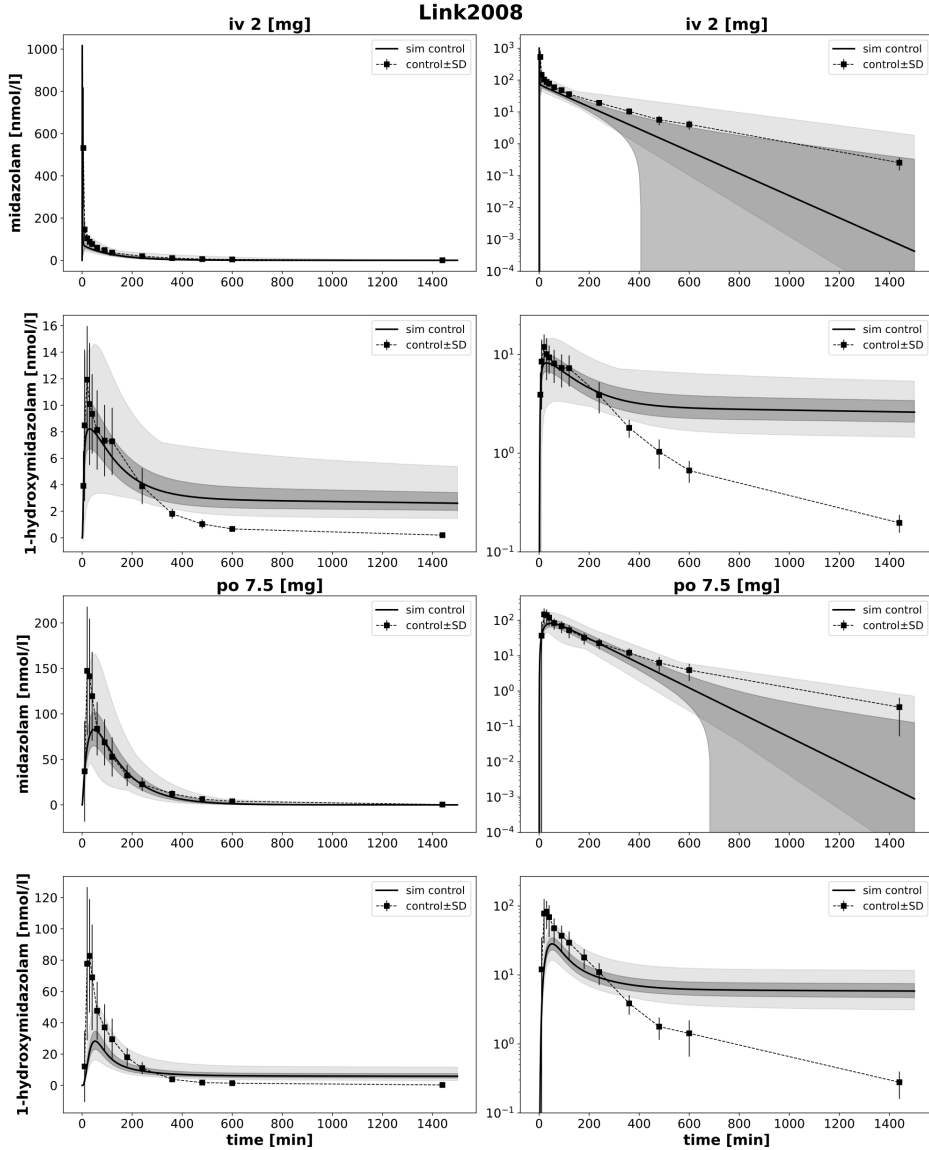


Figure 9: Simulation experiment Link2008. The figure shows the reported time courses (dashed) from Link2008 [63] and time course predictions by the reference model (solid) of midazolam and 1-hydroxymidazolam after an intravenous dose of 2 mg and an oral dose of 7.5 mg midazolam. The shaded areas around the model predictions depict the SD (dark) and the full range (light) from the uncertainty analysis (Sec. 2.4). Reported time course data are mean \pm SD. Each time course is plotted on a linear y-axis (left) and a logarithmic y-axis (right)

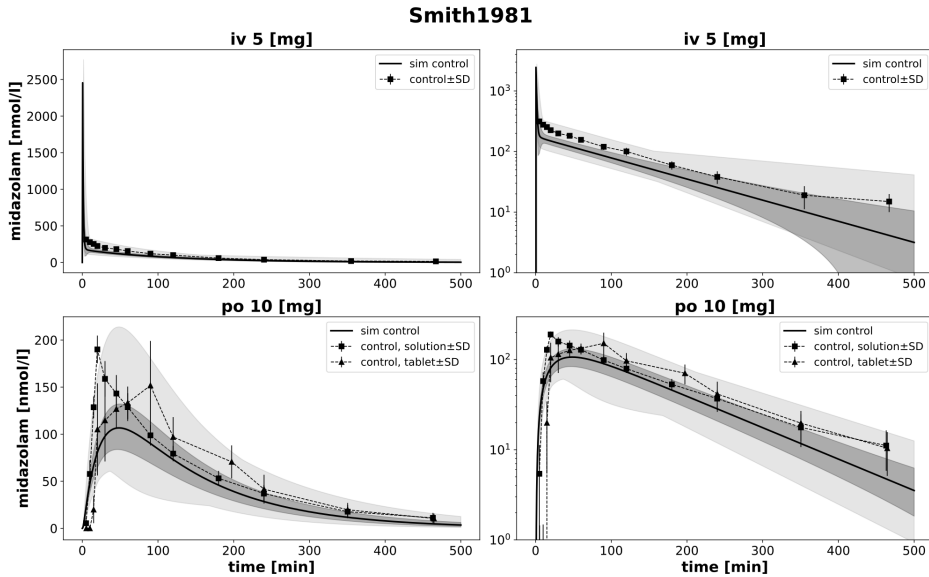


Figure 10: Simulation experiment Smith1981. The figure shows the reported time courses (dashed) from Smith1981 [75] and time course predictions by the reference model (solid) of midazolam after an intravenous dose of 5 mg and an oral dose (solution (square) and tablet (triangle)) of 10 mg midazolam. The shaded areas around the model predictions depict the SD (dark) and the full range (light) from the uncertainty analysis (Sec. 2.4). Reported time course data are mean \pm SD. Each time course is plotted on a linear y-axis (left) and a logarithmic y-axis (right)

was described very well in the 26 studies.

However, for 1-hydroxymidazolam the results were mixed. The overall predicted dynamics of 1-hydroxymidazolam was in good agreement with the experimental data. While for some experiments the predictions were close to the reported time course data, the model often underestimated the concentrations for other experiments. A recurring issue was that the model could not eliminate 1-hydroxymidazolam in a reasonable time frame and return back to baseline (Fig. 9).

To validate the model performance, pharmacokinetic parameters not used for model fitting were used as a validation data set (this included data from the full set of 43 curated studies). Oral and intravenous doses were changed step-wise in the model and subsequently pharmacokinetic parameters were calculated from the predicted time courses as described in Sec. 2.1. The predicted dose-dependency of the pharmacokinetic parameters of midazolam were then used and compared to the available data base to validate the model (Fig. 11) (corresponding data for 1-hydroxymidazolam in supplementary Sec. A.4).

The model predictions showed very good agreement for most of the pharmacokinetic parameters for midazolam under oral and intravenous dosing (e.g. AUC). Only the predicted C_{max} for intravenous application is much higher than the reported values, which can be explained due to the sampling issues with most intravenous studies. More specifically, often no very early time points are recorded after iv midazolam administration so that the actual C_{max} peak is not detected, and too low C_{max} values of later time points are reported.

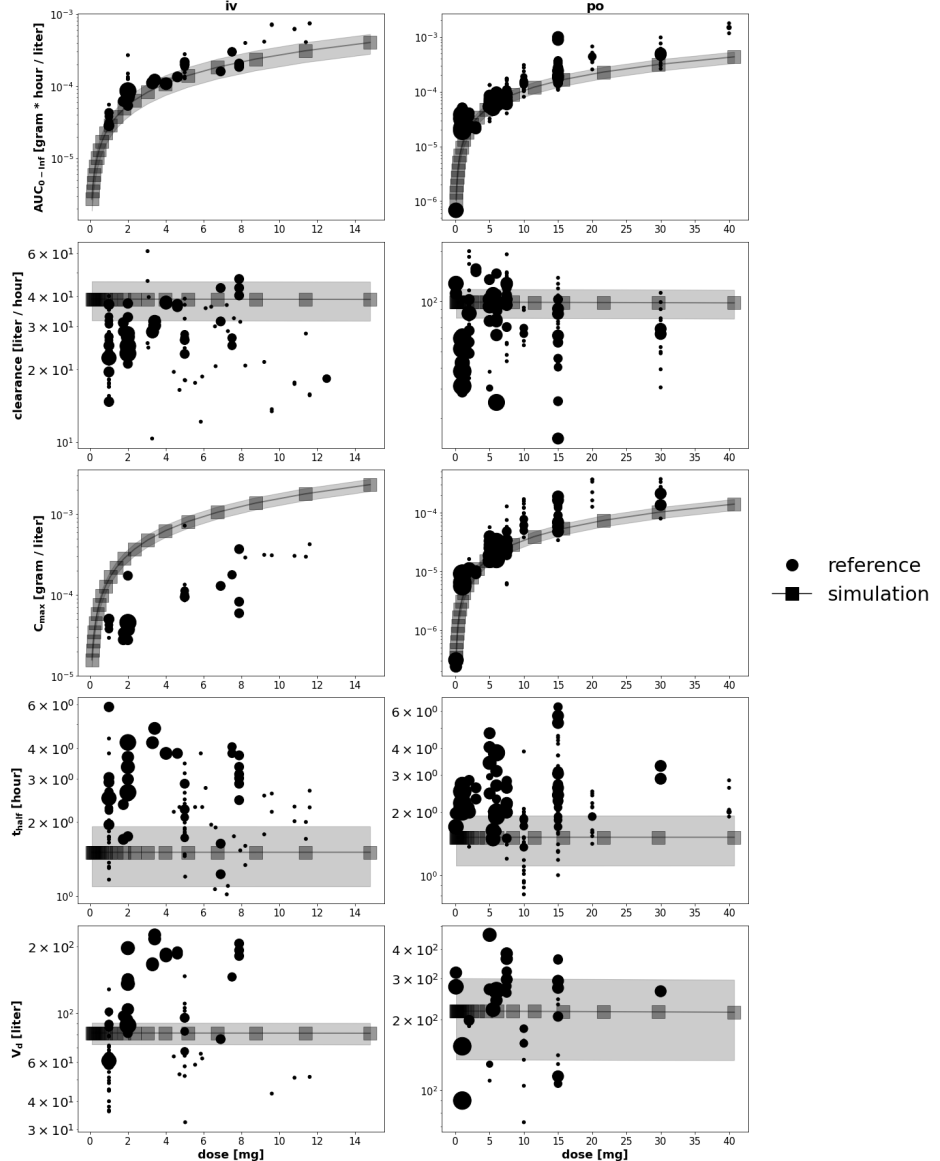


Figure 11: Predicted dose-dependency of pharmacokinetic parameters ($AUC_{0-\infty}$, clearance, C_{max} , t_{half} and V_d) compared to the pharmacokinetic parameters from the 43 curated studies. Oral (po) and intravenous (iv) doses were changed step-wise in the reference model, and pharmacokinetic parameters were calculated from the predicted time courses (squares) and plotted together with the collected data from the curated studies (circles). The shaded areas around the lines depict the SD from the uncertainty analysis.

In summary, the reference model predicted very well the time courses and pharmacokinetics of midazolam under control conditions, with more mixed results for 1-hydroxymidazolam.

3.2.5 Sensitivity analysis

In the next step the role of the individual model parameters on the pharmacokinetic parameters was analyzed systematically using sensitivity analysis (Sec. 2.5).

The effect of model parameters on midazolam and 1-hydroxymidazolam is depicted in Fig. 12. Pharmacokinetic parameters are strongly influenced by parameters effecting blood flow (e.g. blood flow rates, heart rate, blood volume) and therefore the distribution and elimination of midazolam and 1-hydroxymidazolam. In addition to these parameters, pharmacokinetic parameters of midazolam are controlled by the rate of midazolam metabolism in the intestine (GU_MIDOH_Vmax and MIDOH_Km) and in case of C_{max} and t_{max} also by the absorption of midazolam after oral administration (Ka_dis_mid, Ka_abs_mid). On the other hand, the pharmacokinetics of 1-hydroxymidazolam is very sensitive to changes in the transportation rates of midazolam and 1-hydroxymidazolam in the liver and intestine (LI/GU_MIDIM/MID1OHEX_Vmax) and the elimination via the kidney (KI_MID1OHEX_k). While changes in the rate of midazolam metabolism in the intestine has a strong effect on 1-hydroxymidazolam pharmacokinetics, the same reaction in the liver has no effect at all.

3.3 Effect of inhibitors and inducers

3.3.1 CYP3A4 induction and inhibition

To evaluate the effect of CYP3A4 induction and inhibition on midazolam metabolism and pharmacokinetics the v_{max} values of the respective liver and intestinal CYP3A4 were either increased (induction) or reduced (inhibition) by a single factor f . We determined the respective factors by manually adjusting f for each condition (induction, inhibition, intestinal inhibition) by comparing the predicted pharmacokinetic parameters against the collected pharmacokinetics data in our database.

As a final result we determined a 15- and a 0.05-fold change of v_{max} in liver and intestine to be appropriate for CYP3A4 induction and inhibition, respectively. In case of intestinal inhibition the v_{max} parameter in the intestine was changed by a factor of 0.5, while it was left unchanged in the liver. The resulting dose-dependency of the predicted pharmacokinetic parameters under induction and inhibition in comparison to the data is depicted in Fig. 13.

Overall, the model predicted very well the dose dependency of the midazolam pharmacokinetics under induction and inhibition. Induction after an oral dose of midazolam (po) resulted in a marked reduction in $AUC_{0-\infty}$, C_{max} and t_{half} and an increase in clearance and V_d . Inhibition after oral midazolam had the respective opposite effect. In the case of intravenous midazolam $AUC_{0-\infty}$ was only increased by inhibitors, but no marked effect could be observed for induction. The discrepancy between intravenous C_{max} model prediction has been discussed before and is due to sampling effects in the data. The increase in t_{half} under inhibition and decrease under induction was nicely reproduced by the model. Overall, the clinical data has a large variability, which is partly due to the highly variable clinical protocols (dosing amount and schema for inducers and inhibitors) and due to the pooling of multiple substances within the induction and inhibition classes. Despite this large data variance the general effects of induction and inhibition of CYP3A4 could be nicely reproduced with the developed model and the constant induction and inhibition factors.

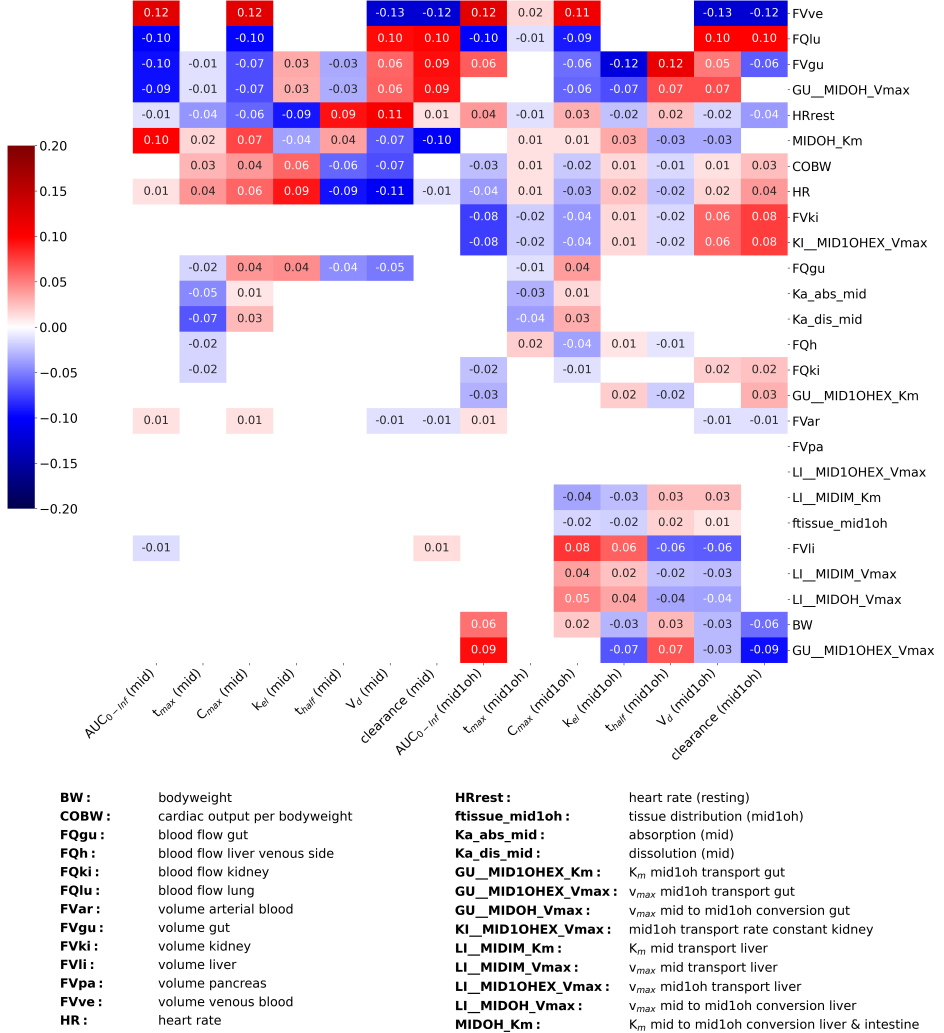


Figure 12: The sensitivity heatmap shows the effect of small changes ($\pm 10\%$) in model parameters (y-axis) on the pharmacokinetic parameters (x-axis). The values show the fractional change of the pharmacokinetic parameter after changing the corresponding model parameter. Positive values (red) indicate a positive correlation, i.e., an increase in the model parameter increases the pharmacokinetic parameter, while negative values (blue) indicate a negative correlation, i.e., an increase in the model parameter decreases the pharmacokinetic parameter. Changes smaller than a threshold of 0.01 were excluded from the heatmap (white). Model parameters which have no, or sub-threshold effects on the pharmacokinetic parameters were removed from the heatmap.

With the model now being capable of predicting pharmacokinetics under different conditions we ran the simulation experiments under activated and inhibited conditions. A representative slice of the results is shown in Fig. 14, Fig. 15 and Fig. 16. The complete set of simulation experiments can be found in the supplementary Sec. A.3.

The model adjusted to CYP3A4 induction, inhibition and intestinal inhibition showed mixed results. Overall, if the reference model under control conditions

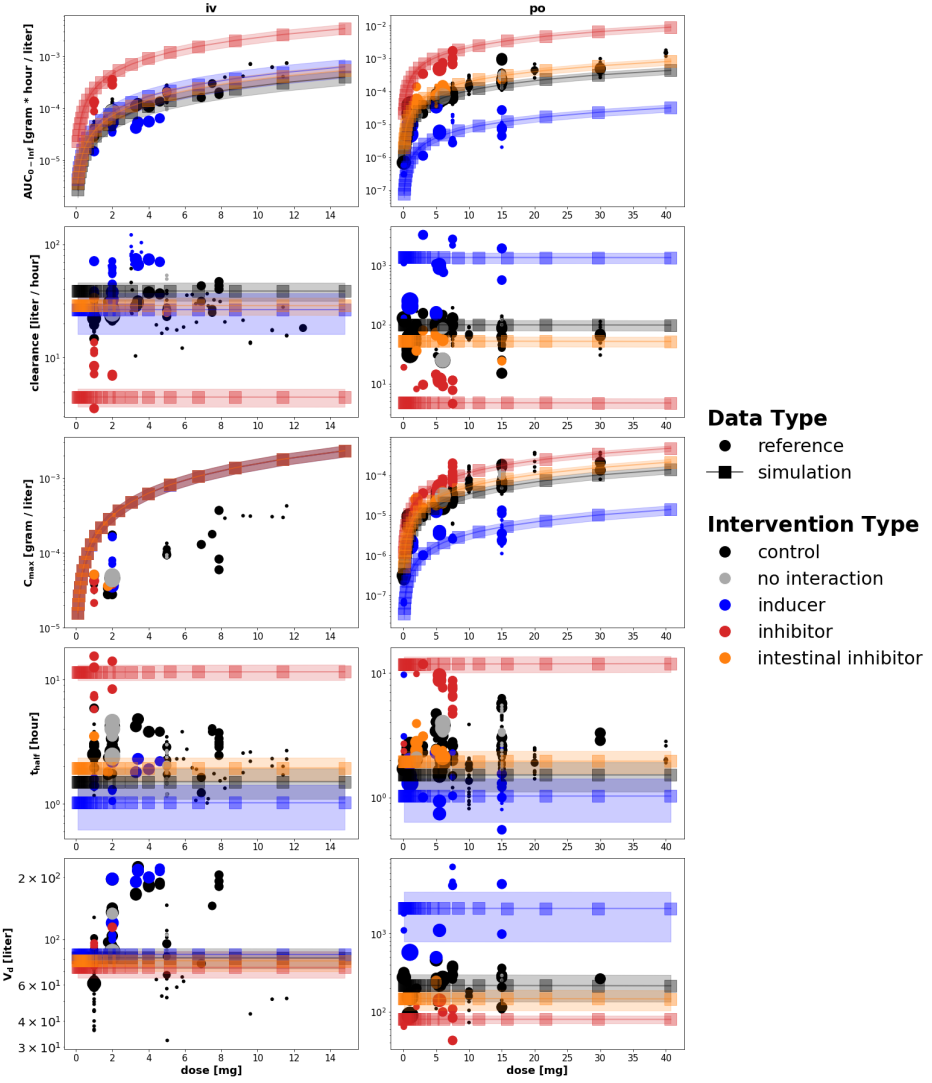


Figure 13: Dose-dependency of midazolam pharmacokinetic parameters $AUC_{0-\infty}$, clearance, C_{max} , t_{half} and V_d . The reference model was adjusted to control (black), inducer (blue), inhibitor (red) and intestinal inhibitor (orange) conditions by changing the f factors for the v_{max} of intestinal and hepatic CYP3A4. Oral and intravenous doses were changed step-wise in the adjusted model, and subsequently pharmacokinetic parameters were calculated from the predicted time courses (squares) and plotted together with the collected data (circles) from the curated studies. The shaded areas around the lines depict the SD from the uncertainty analysis.

made a good prediction for midazolam, the adjusted model was also in agreement under inhibition or induction condition. Especially, under the intestinal inhibition the predictions worked well.

The predictions for 1-hydroxymidazolam performed not very well, mainly because discrepancies existed already for simulations under control conditions. Without a correct baseline the subsequent induction and inhibition also resulted in incorrect predictions.

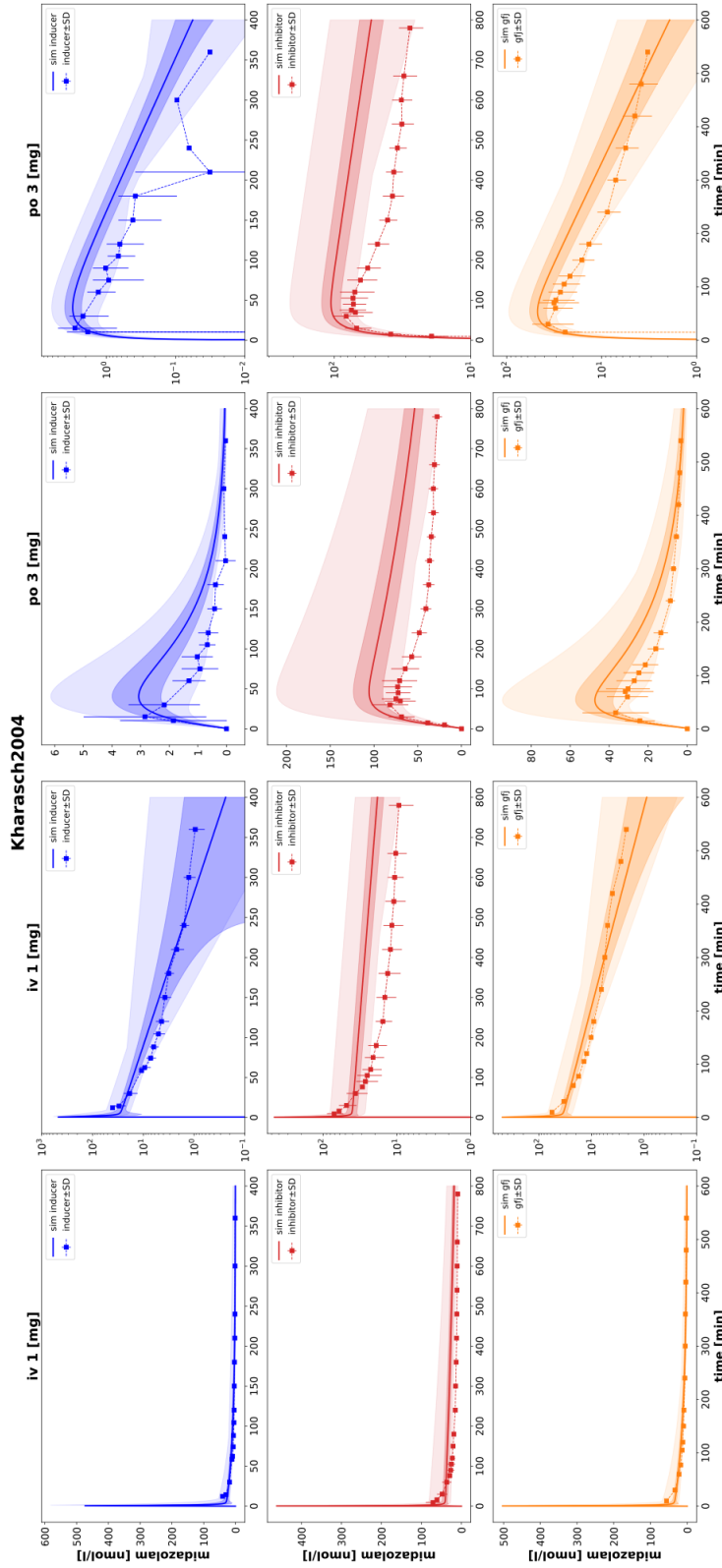


Figure 14: Simulation experiment Kharash2004. The figure shows the reported time courses (dashed) from Kharash2004 [23] and time course predictions by our model (solid) adjusted to inhibitor (red), intestinal inhibitor (orange) and inducer conditions (blue) for midazolam. Midazolam was administered as an intravenous dose of 1 mg and an oral dose of 3 mg. The inhibitor, intestinal inhibitor and inducer used in this study was Troleandomycin, grapefruit juice and rifampin, respectively. The shaded areas around the model predictions depict the SD (dark) and the full range (light) from the uncertainty analysis (Sec. 2.4). Reported time course data are mean \pm SD. Each time course is plotted on a linear y-axis (left) and a logarithmic y-axis (right).

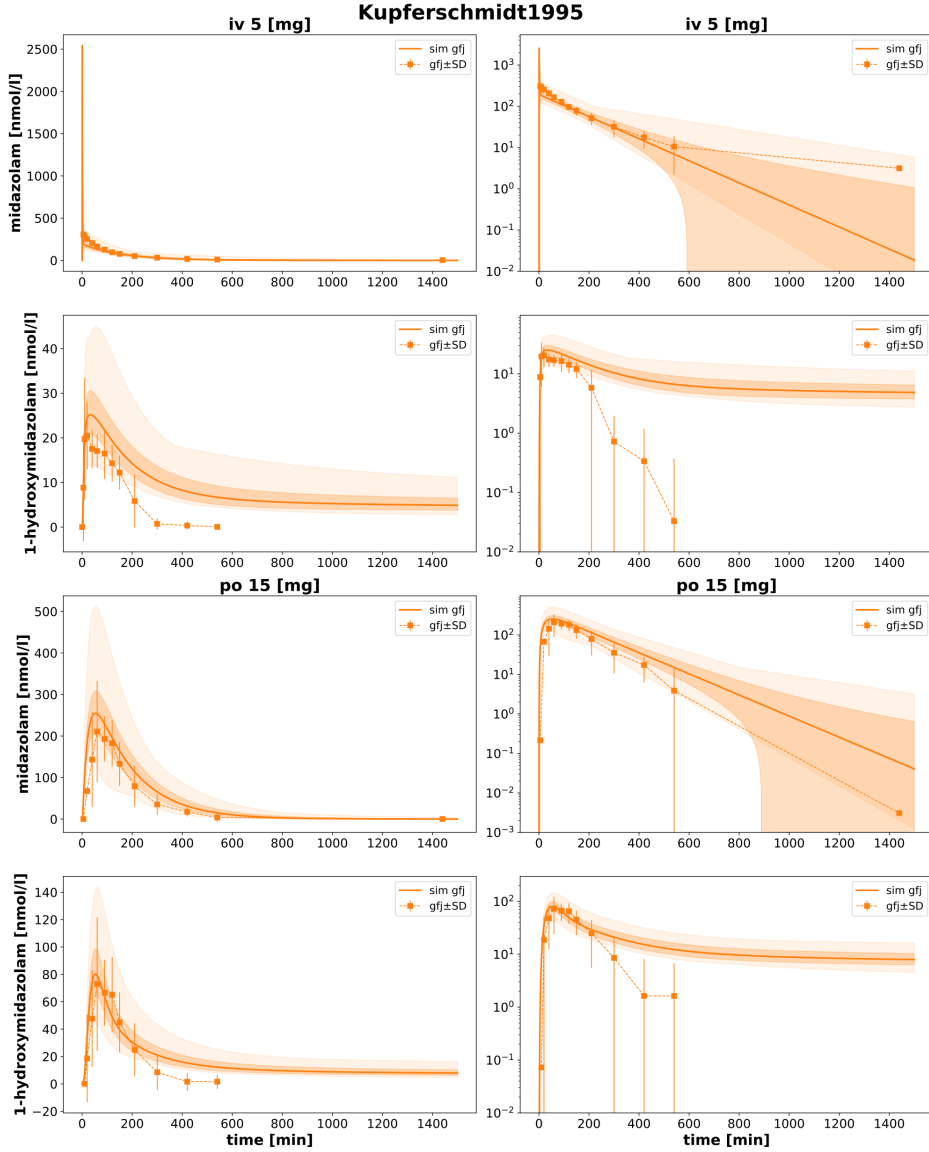


Figure 15: Simulation experiment Kupferschmidt1995. The figure shows the reported time courses (dashed) from Kupferschmidt1995 [25] and time course predictions by our model (solid), adjusted to intestinal inhibitor conditions (orange), for midazolam and 1-hydroxymidazolam. Midazolam was administered, together with grapefruit juice, as an intravenous dose of 5 mg and an oral dose of 15 mg. The shaded areas around the model predictions depict the SD (dark) and the full range (light) from the uncertainty analysis (Sec. 2.4). Reported time course data are mean \pm SD. Each time course is plotted on a linear y-axis (left) and a logarithmic y-axis (right).

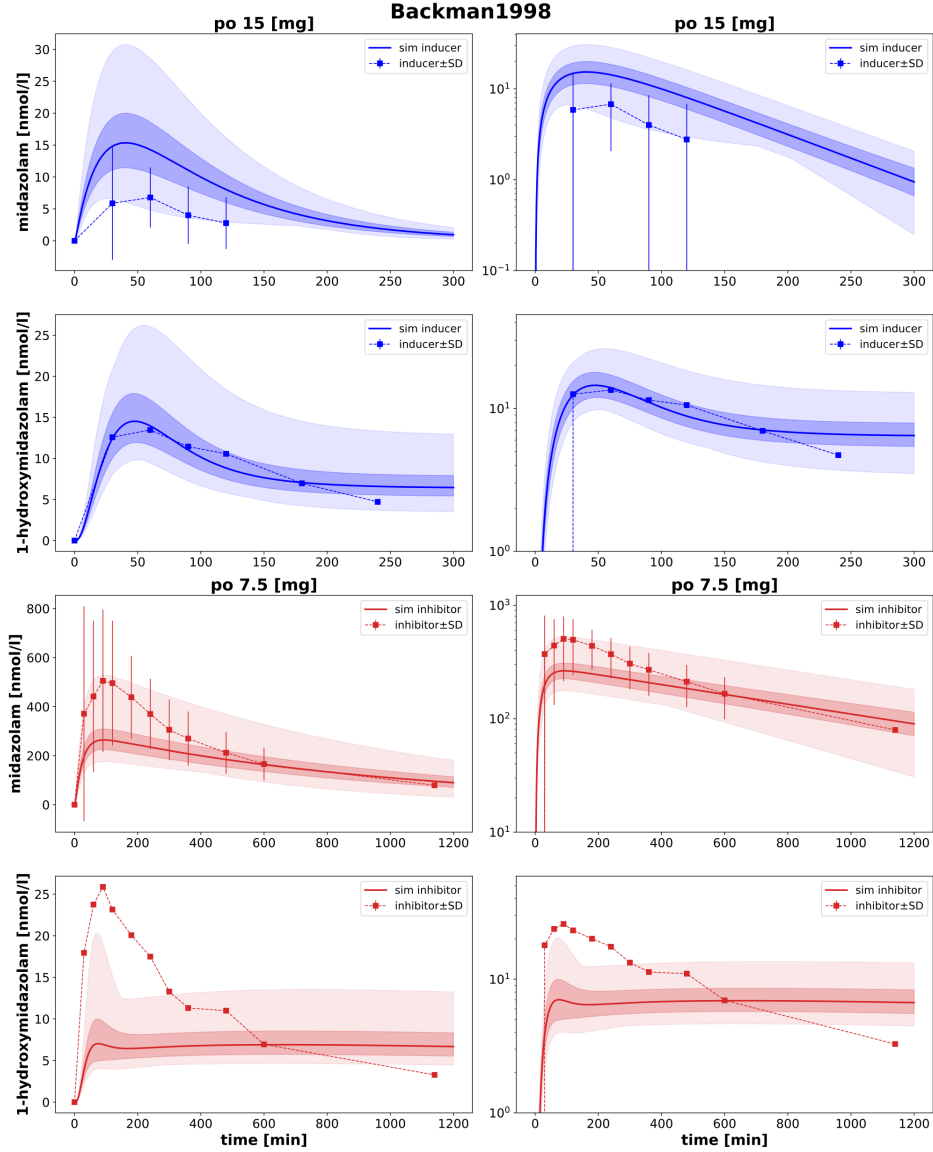


Figure 16: Simulation experiment Backman1998. The figure shows the reported time courses (dashed) from Backman1998 [43] and time course predictions by our model (solid), adjusted to inhibitor (red) and inducer (blue) conditions, for midazolam and 1-hydroxymidazolam. Midazolam was administered an oral dose of 7.5 mg (inhibitor) and 15 mg (inducer). The inhibitors and inducers used in this study were itraconazole and rifampin, respectively. The shaded areas around the model predictions depict the SD (dark) and the full range (light) from the uncertainty analysis (Sec. 2.4). Reported time course data are mean \pm SD. Each time course is plotted on a linear y-axis (left) and a logarithmic y-axis (right).

3.3.2 Scan of CYP3A4 activity

To evaluate the effect of induction and inhibition of hepatic and intestinal CYP3A4 on the midazolam pharmacokinetics a systematic scan of the CYP3A4 v_{max} values was performed (whereas in Sec. 3.3.1 only single factors were studied). Three CYP3A4 v_{max} scans were performed for intravenous and oral administration: either changing hepatic and intestinal v_{max} individually, or both by the same factor (Fig. 17). In addition a 2D-scan of intestinal versus hepatic v_{max} was performed (Fig. 18). CYP3A4 scans for the remaining pharmacokinetic parameters and 1-hydroxymidazolam are provided in the supplementary Sec. A.5.

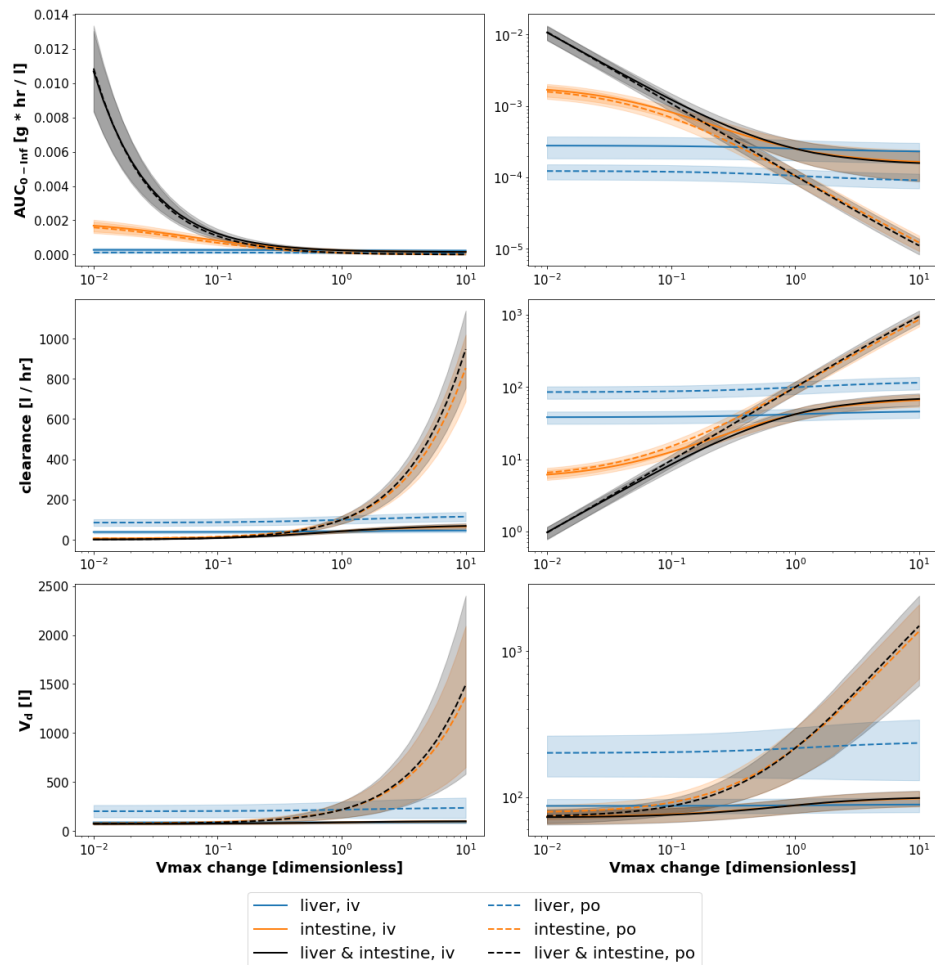


Figure 17: 1-D scans of CYP3A4 activity. A systematic scan of CYP3A4 activity was performed by adjusting v_{max} by some factor f either in the liver (blue), intestine (orange) or in both by the same value (black). The models with the adjusted v_{max} were then used to predict pharmacokinetic parameters ($AUC_{0-\infty}$, clearance, V_d) after intravenous (solid) and oral (dashed) midazolam administration, which we plotted against the corresponding change of v_{max} .

Changing hepatic CYP3A4 activity left the pharmacokinetics ($AUC_{0-\infty}$, clearance, V_d) mostly unchanged, opposed to intestinal CYP3A4, which had a strong

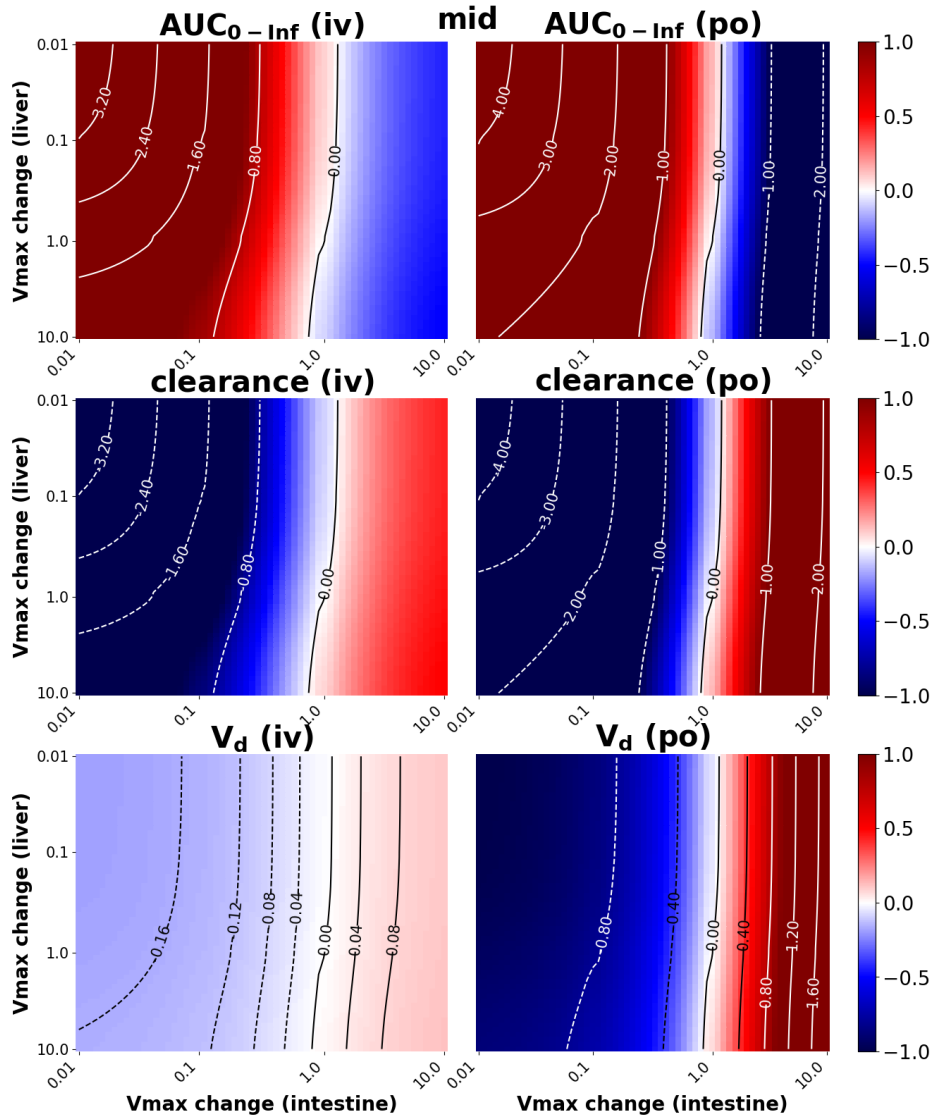


Figure 18: 2-D scans of CYP3A4 activity. A systematic scan of CYP3A4 activity was performed by step-wise adjusting v_{max} by a factor f in both the liver (y-axis) and intestine (x-axis). The models with the adjusted v_{max} were then used to predict pharmacokinetic parameters ($AUC_{0-\infty}$, clearance, V_d) after intravenous (iv) and oral (po) midazolam administration. The heatmap depicts the log-change of the resulting pharmacokinetic parameter compared to the reference pharmacokinetic parameter predicted by the reference model. Positive values (red) indicate an increase and negative values (blue) a decrease of the pharmacokinetic parameter compared to the reference.

effect on the pharmacokinetics. This effect was increased even further after oral midazolam administration. A clear strength-dependency of induction and inhibition on pharmacokinetics parameters could be observed, i.e., the stronger the induction or inhibition the stronger the change in pharmacokinetics (if the parameter had an effect).

3.4 Summary

In this work we established a unique database of midazolam pharmacokinetics based on reported data from 43 clinical studies. Based on these data we developed and optimized a PBPK model capable of simulating midazolam metabolism. The model was then extended to predict the effects of CYP3A4 inhibition and induction on midazolam pharmacokinetics by scaling the reaction rate of midazolam to 1-hydroxymidazolam conversion. We then systematically analyzed the effects of model parameter changes via sensitivity analysis and the effects of change in CYP3A4 activity on midazolam pharmacokinetics.

4 Discussion

Within this work a detailed physiological-based pharmacokinetics model of midazolam was created and applied to study the effects of induction and inhibition of hepatic and intestinal CYP3A4 on clearance and other pharmacokinetic parameters of midazolam metabolism.

Gaining a better understanding of these effects is a highly relevant clinical question. Midazolam is a widely applied medication for anesthesia and procedural sedation, as well as treating trouble sleeping and severe agitation [3], and correct dosing within the therapeutic range is crucial. In addition midazolam is an important probe drug for phenotyping of CYP3A4. For both applications a better understanding of the effects of induction and inhibition can provide important insights and elucidate underlying mechanisms. In addition, the presented work is highly relevant for a better characterisation of drug-drug interactions affecting CYP3A4 drugs.

Pharmacokinetic data: As part of this work the first high-quality dataset of midazolam pharmacokinetics data has been established. This in itself is a unique resource for studying midazolam metabolism and its pharmacokinetics. The focus of data curation was on pharmacokinetics studies providing information on induction and inhibition of midazolam metabolism. The complete dataset is made accessible as FAIR (findable, accessible, interoperable, reusable) data [41] in a standardized open accessible database (<https://pk-db.com>). Thereby we facilitate future studies on the pharmacokinetics and metabolism of midazolam.

A limitation of the database is that only a subset of relevant information was reported by the respective studies. The heterogeneity in reporting can be seen in the supplementary study overview (Tab. 8) as well as in the time course overview (Tab. 6) and pharmacokinetics overview (Tab. 4/5). For instance most of the studies report aggregated information for groups, but seldom for individuals.

As seen in Tab. 4/5, no measurements from urine were provided, only one study reported pharmacokinetics of 4-hydroxymidazolam and, compared to midazolam, remarkable less data on 1-hydroxymidazolam. All these could help getting a better insight into midazolam metabolism and elimination and could improve modeling.

Overall, the large heterogeneity between the studies, and lack of some crucial information posed a challenge for model building. On the other hand, access to complementary data from multiple studies with partial overlap (especially in the midazolam data) allowed to integrate data from multiple sources in a single model. Thereby, a much larger database could be used for model building.

Using data from various sources is especially important in the clinical context to achieve transferability of the results. Large variability between different study cohorts and issues such as inter-lab variability can make it difficult to transfer results. By using data from a wide range of studies we could include this variability in the modeling process.

Model scope: Within this work a PBPK model of midazolam and 1-hydroxymidazolam with focus on available plasma time course and pharmacokinetics data was established.

The model does not include the secondary metabolic route of midazolam, i.e. the conversion of midazolam to 4-hydroxymidazolam (see Sec. 1.2.1). We did not

include this pathway, because (i) it only plays a very minor role, and (ii) only very limited pharmacokinetics data is available on 4-hydroxymidazolam. In our literature curation we could only find a single study which reported time courses and pharmacokinetics information (see Tab. 6 and Tab. 4/5). Elimination of midazolam only happens via metabolization and then excretion of its metabolite 1-hydroxymidazolam into the urine via the kidney. While excretion of unmetabolized midazolam does happen *in-vivo*, it's such small amounts [79] that we decided to omit it from the model.

To imitate different application methods improved injection and absorption kinetics were implemented. This way the model is capable of simulating intravenous bolus injections, intravenous infusions over a given time and oral administration. In theory the model is even capable of simulating different forms of administration, i.e. solution or tablet. However, within this work we did not differentiate between the two forms.

With the introduction of additional scaling factors in each the metabolic reactions, we implemented a simple form of changing the metabolic reaction rates. This way the model can simulate CYP3A4 inhibition and induction both in liver and intestine independent from each other.

Parameter fitting: A major challenge of the work was the parameter fitting using a large set of clinical data from heterogeneous sources and being limited to aggregated group data. To test that the model is able to fit the various data sources, first, all single studies were fitted individually. All studies, with exception of Pentikis2007 [71], provided good fits with individual parameter sets. Subsequently, the model was fitted using the complete data set. Despite the challenges a large subset of the data could be fitted with a single parameter set.

Major difficulties in fitting were (i) weighting of individual data points in a time course; (ii) weighting of different metabolites relative to each other (midazolam and 1-hydroxymidazolam); and (iii) weighting time courses from different studies relative to each other. All three weightings can strongly influence the contribution of the residuals to the overall cost function and thereby the optimization results. Early time points with large concentrations often had a strong impact on the optimization methods, due to their larger contribution to the overall cost. We could solve this by weighting each data point locally, according to their error (SD), if errors were provided (the larger the error, the smaller the weight). In a similar vein, reported midazolam blood concentration were always considerably higher than 1-hydroxymidazolam, which introduced a bias for midazolam. To circumvent this, residuals of each experiment were globally weighted relative to the average reported concentration of the corresponding experiment. This global weighting also solved the issue of making time courses from different studies comparable.

Model validation: Predictions of the dose dependency of pharmacokinetics were used for validation of the fitted model (Fig. 13).

None of the reported pharmacokinetic parameters used in validation were used in fitting of the model. When studies reported time courses as well as pharmacokinetics parameters, the parameters were included for model validation. As a consequence a subset of the pharmacokinetics parameters used for validation was also used indirectly in the fitting of the model in induced and inhibited

conditions.

Validation revealed good prediction of midazolam pharmacokinetics in the reference state (control). However, certain problems exist in the prediction of 1-hydroxymidazolam pharmacokinetics. In it's current state, the model can not fully account for the large inter-individual variation in CYP3A4 activity. Therefore, the model often over- or underestimates 1-hydroxymidazolam concentrations, compared to the respective data. The metabolism in the liver compartment is currently limited by the rate of midazolam import into the compartment. The actual metabolic reaction therefore only has limited influence on the rate of conversion of midazolam to 1-hydroxymidazolam, which can be seen in Fig. 18. Similarly, 1-hydroxymidazolam concentration in blood is heavily controlled by it's export from the intestine. The v_{max} of said reaction is currently fitted to very low values which results in accumulation of the metabolite in the intestine. This explains why the concentration does not return back to the baseline fast enough. Setting tighter bounds for these parameters solved these problems, but resulted in 'bad' predictions.

Effect of inducers and inhibitors: A main target of this work was to get a better insight into the effects of induction and inhibition of CYP3A4 and it's effects on the metabolism of midazolam.

To fit the model for CYP3A4 induction and inhibition we adjusted the rates of the metabolic reactions by scaling their corresponding v_{max} accordingly. The values were adjusted so that they fit the reported pharmacokinetic parameters in our collected dataset. Only a single induction and inhibition and intestinal inhibition factor was manually determined for every class. We did not distinguish between different inhibitors or inducers, and also did not account for differences between the study protocol (often varying dosing and dosings schemas for inhibitors and inducers). It would make sense to fit these factors individually, i.e., on a per substance and per study basis in an automatic manner. The prediction worked very well for the dose-dependency of the pharmacokinetics parameters under induction and inhibition. The prediction of the individual time courses for the single studies gave much more heterogeneous results. Whereas, due to the data integration in the dose-dependency, an overall factor for induction and inhibition worked well, individual adjusted factors would have given much better results for the individual simulation experiments.

Further, the metabolic reaction in the liver only has limited influence on the rate of conversion from midazolam to 1-hydroxymidazolam. Therefore, adjusting the v_{max} in the liver does not have the desired effect. To properly simulate the effect of CYP3A4 induction and inhibition, we would have to fix the issues with the parameter fitting first.

Overall,

Summary: Within this work we've built a large high-quality dataset of midazolam pharmacokinetics. To our knowledge, a dataset of this extent has not been established yet. Some crucial information about the metabolism and elimination of midazolam is still missing or underrepresentend in this dataset (e.g. urinary data, data on 4-hydroxymidazolam), but it can be easily added at a later point.

Based on this data we've constructed a model that is can simulating mida-

zolam metabolism. It can simulate different routes and forms of application and can adjust for CYP3A4 activation/inhibition. For model optimization weighting schemes were established to account for the large variability between the studies.

The final model is capable of predicting midazolam pharmacokinetics under reference conditions (control). Some problems with the prediction of 1-hydroxymidazolam pharmacokinetics still exist, partially due to unrealistic parameter choices in transport reactions. However, this problem could be overcome with a further improved optimization method.

The model can be adjusted for inhibition and induction of CYP3A4. However, the current model can not fully account for the large inter-individual variability of CYP3A4 phenotypes. This is crucial to properly predict the effects of inhibition and induction. Although, by further collection data and gaining a better understanding of midazolam metabolism and all the sources of said inter-individual variability, it should be possible to further extend the model to make proper predictions about CYP3A4 induction and inhibition.

5 Outlook

We established unique database and parameterized model for the prediction of midazolam kinetics and for the evaluation of midazolam as liver function probe.

Importantly, within this work we could establish the complete workflow for building PBPK models from a wide range of heterogeneous data: (i) data curation in standardized formats; (ii) building of PBPK models from existing template models; (iii) creating simulation experiments and parameter fitting problems semi-automatically from existing data and models; (iv) parameter fitting with weighting schemas to account for inter-study variability; (v) application of the model to biological question (effect of induction and inhibition).

Certain limitations exist which can be addressed in future work. For instance, an important extension would be a more complex parameter fitting setup in which the overall dataset is used to fit prior parameter distributions which are subsequently used for fitting the parameters for the individual datasets. I.e., one should allow a certain amount of variability in the parameters to account for the differences between studies. Such an approach could also account for the inter-individual variation in CYP3A4 activity and would result in much better fits of the individual study data (as indicated by the individual fit of the studies). Furthermore, it should be possible to define constraints between certain parameters. This way we could ensure that the metabolic reactions in liver and intestine are the limiting factors in midazolam metabolism, instead of the transport reactions.

Within this work we focused on the use of plasma concentration profiles. No urinary excretion data of midazolam or midazolam metabolites were utilized. To better understand the elimination of midazolam, future work could extend the presented model to account for urinary excretion data.

6 Acknowledgements

I would like to express my deepest gratitude to my supervisor Dr. Matthias König for all his help and guidance during my time in his group. You taught me a lot about how to properly conduct scientific research and computational modeling. Both things, which will be extremely valuable in my future career. It was a real pleasure to work with you. Further, I want to thank all the other group members, Adrian Kölle, Florian Bartsch and especially Jan Gregorzewski for their help and providing such a pleasant working atmosphere, while we could still work in the office. Last but not least, I want to thank my wife for all her moral support during this time and her help on some of the figures.

Acronyms

- ADME** Absorption, distribution, metabolism, elimination
- AUC** Area under the curve
- C_{max}** Maximum concentration in a time course
- CYP** Cytochrome P450
- FAIR** Findable, accessible, interoperable, reusable
- iv** Intravenous
- k_{el}** Fractional elimination rate
- K_m** Michaelis-Menten constant
- ODE** Ordinary differential equation
- PBPK** Physiological-based pharmacokinetic (model)
- po** oral (*per orem*)
- SBML** Systems biology markup language
- SD** Standard deviation
- SE** Standard error
- t_{max}** Time at which C_{max} occurs
- thalf** Half-life of substance
- V_d** Volume of distribution
- v_{max}** Maximum reaction rate (Michaelis-Menten kinetics)

References

- [1] Thomas J Pallasch. "Principles of pharmacotherapy: II. Pharmacokinetics." In: *Anesthesia progress* 35.4 (1988), pp. 133–46.
- [2] D. J. (Donald John) Birkett. *Pocket guide : pharmacokinetics made easy*. McGraw-Hill Education Australia, 2010, p. 120.
- [3] Sean Patrick Nordt and Richard F. Clark. "Midazolam: A review of therapeutic uses and toxicity". In: *The Journal of Emergency Medicine* 15.3 (May 1997), pp. 357–365.
- [4] World Health Organization et al. *World Health Organization model list of essential medicines: 21st list 2019*. Tech. rep. World Health Organization, 2019.
- [5] Armin Walser et al. "Quinazolines and 1,4-benzodiazepines. 84. Synthesis and reactions of imidazo[1,5-a][1,4]benzodiazepines". In: *The Journal of Organic Chemistry* 43.5 (Mar. 1978), pp. 936–944.
- [6] M. Gerecke. "Chemical structure and properties of midazolam compared with other benzodiazepines." In: *British journal of clinical pharmacology* 16 Suppl 1.S1 (Feb. 1983), 11S–16S.
- [7] A. Kupietzky and M. I. Houpt. "Midazolam: a review of its use for conscious sedation of children." In: *Pediatric dentistry* 15.4 (1993), pp. 237–41.
- [8] K. T. Olkkola and J. Ahonen. "Midazolam and other benzodiazepines." In: *Handbook of experimental pharmacology* 182.182 (2008), pp. 335–60.
- [9] J. G. Reves et al. "Midazolam: pharmacology and uses." In: *Anesthesiology* 62.3 (Mar. 1985), pp. 310–24.
- [10] George K. Dresser, J. David Spence, and David G. Bailey. "Pharmacokinetic-pharmacodynamic consequences and clinical relevance of cytochrome P450 3A4 inhibition." In: *Clinical pharmacokinetics* 38.1 (Jan. 2000), pp. 41–57.
- [11] Saskia N. de Wildt et al. "Cytochrome P450 3A: ontogeny and drug disposition." In: *Clinical pharmacokinetics* 37.6 (Dec. 1999), pp. 485–505.
- [12] F. Peter Guengerich. "Cytochrome P-450 3A4: regulation and role in drug metabolism." In: *Annual review of pharmacology and toxicology* 39.1 (Apr. 1999), pp. 1–17.
- [13] T. Kronbach et al. "Oxidation of midazolam and triazolam by human liver cytochrome P450IIIA4." In: *Molecular pharmacology* 36.1 (July 1989), pp. 89–96.
- [14] Hylke De Jonge et al. "Impact of CYP3A5 genotype on tacrolimus versus midazolam clearance in renal transplant recipients: New insights in CYP3A5-mediated drug metabolism". In: *Pharmacogenomics* 14.12 (Sept. 2013), pp. 1467–1480.
- [15] Kyung-Sang Yu et al. "Effect of the CYP3A5 genotype on the pharmacokinetics of intravenous midazolam during inhibited and induced metabolic states." In: *Clinical pharmacology and therapeutics* 76.2 (Aug. 2004), pp. 104–12.

- [16] Antonius E. van Herwaarden, Robert A B van Waterschoot, and Alfred H. Schinkel. “How important is intestinal cytochrome P450 3A metabolism?” In: *Trends in pharmacological sciences* 30.5 (May 2009), pp. 223–7.
- [17] K S Lown, M Ghosh, and P B Watkins. “Sequences of intestinal and hepatic cytochrome P450 3A4 cDNAs are identical.” In: *Drug metabolism and disposition: the biological fate of chemicals* 26.2 (Feb. 1998), pp. 185–7.
- [18] Kenneth E. Thummel et al. “Oral first-pass elimination of midazolam involves both gastrointestinal and hepatic CYP3A-mediated metabolism.” In: *Clinical pharmacology and therapeutics* 59.5 (May 1996), pp. 491–502.
- [19] E L Michalets. “Update: clinically significant cytochrome P-450 drug interactions.” In: *Pharmacotherapy* 18.1 (1998), pp. 84–112.
- [20] Kenneth A. Bachmann. “Genotyping and phenotyping the cytochrome p-450 enzymes.” In: *American journal of therapeutics* 9.4 (July 2002), pp. 309–16.
- [21] Guillermo Alberto Keller et al. “In vivo Phenotyping Methods: Cytochrome P450 Probes with Emphasis on the Cocktail Approach.” In: *Current pharmaceutical design* 23.14 (May 2017), pp. 2035–2049.
- [22] Ellen Chung et al. “Comparison of midazolam and simvastatin as cytochrome P450 3A probes.” In: *Clinical pharmacology and therapeutics* 79.4 (Apr. 2006), pp. 350–61.
- [23] Evan D Kharasch et al. “Intravenous and oral alfentanil as in vivo probes for hepatic and first-pass cytochrome P450 3A activity: noninvasive assessment by use of pupillary miosis.” In: *Clinical pharmacology and therapeutics* 76.5 (Nov. 2004), pp. 452–66.
- [24] David J. Greenblatt et al. “Effect of age, gender, and obesity on midazolam kinetics.” In: *Anesthesiology* 61.1 (July 1984), pp. 27–35.
- [25] Hugo H.T. Kupferschmidt et al. “Interaction between grapefruit juice and midazolam in humans.” In: *Clinical pharmacology and therapeutics* 58.1 (July 1995), pp. 20–8.
- [26] Holger Petri. “Arzneimitteltherapiesicherheit: Das Interaktionspotenzial hormoneller Kontrazeptiva”. In: *Dtsch Arztebl International* 117.7 (2020), A–328–.
- [27] F. Peter Guengerich. “Role of cytochrome P450 enzymes in drug-drug interactions.” In: *Advances in pharmacology (San Diego, Calif.)* 43.C (1997), pp. 7–35.
- [28] Janne T. Backman, Klaus T. Olkkola, and Pertti J. Neuvonen. “Rifampin drastically reduces plasma concentrations and effects of oral midazolam.” In: *Clinical pharmacology and therapeutics* 59.1 (Jan. 1996), pp. 7–13.
- [29] David G. Bailey, George Dresser, and J. Malcolm O. Arnold. “Grapefruit-medication interactions: Forbidden fruit or avoidable consequences?” In: *Canadian Medical Association Journal* 185.4 (Mar. 2013), pp. 309–316.

- [30] HM Jones and K. Rowland-Yeo. “Basic concepts in physiologically based pharmacokinetic modeling in drug discovery and development.” In: *CPT: pharmacometrics & systems pharmacology* 2.8 (Aug. 2013), e63.
- [31] Richard N. Upton, David J R Foster, and Ahmad Y. Abuhelwa. “An introduction to physiologically-based pharmacokinetic models.” In: *Paediatric anaesthesia* 26.11 (Nov. 2016). Ed. by Brian Anderson, pp. 1036–1046.
- [32] Jan Grzegorzewski et al. “PK-DB: Pharmacokinetics DataBase for Individualized and Stratified Computational Modeling”. In: *bioRxiv* (Jan. 2019), p. 760884.
- [33] Jan Grzegorzewski and Matthias König. *matthiaskoenig/pkdb_analysis: pkdb-analysis-v0.1.6a2*. Version 0.1.6a2. Aug. 2020.
- [34] M. Hucka et al. “The systems biology markup language (SBML): a medium for representation and exchange of biochemical network models”. In: *Bioinformatics* 19.4 (Mar. 2003), pp. 524–531.
- [35] Michael Hucka et al. “The Systems Biology Markup Language (SBML): Language Specification for Level 3 Version 2 Core Release 2”. In: *Journal of Integrative Bioinformatics* 16.2 (June 2019).
- [36] Matthias König. *matthiaskoenig/sbmlutils: sbmlutils-v0.3.8: python utilities for SBML*. Jan. 2020.
- [37] Matthias König. *matthiaskoenig/sbmlsim: sbmlsim-v0.1.0: SBML simulation made easy*. Jan. 2020.
- [38] Endre T. Somogyi et al. “libRoadRunner: a high performance SBML simulation and analysis library.” In: *Bioinformatics (Oxford, England)* 31.20 (Oct. 2015), pp. 3315–21. arXiv: 1503.01095.
- [39] Lucian P.aul Smith et al. “SBML Level 3 package: Hierarchical Model Composition, Version 1 Release 3.” In: *Journal of integrative bioinformatics* 12.2 (Sept. 2015), p. 268.
- [40] Pauli Virtanen et al. “SciPy 1.0: fundamental algorithms for scientific computing in Python”. In: *Nature Methods* 17.3 (Mar. 2020), pp. 261–272.
- [41] Mark D. Wilkinson et al. “The FAIR Guiding Principles for scientific data management and stewardship.” In: *Scientific data* 3.1 (Mar. 2016), p. 160018.
- [42] Hannu Allonen, Gismar Ziegler, and Ulrich Klotz. “Midazolam kinetics.” In: *Clinical pharmacology and therapeutics* 30.5 (Nov. 1981), pp. 653–61.
- [43] J. T. Backman et al. “The area under the plasma concentration-time curve for oral midazolam is 400-fold larger during treatment with itraconazole than with rifampicin.” In: *European journal of clinical pharmacology* 54.1 (Mar. 1998), pp. 53–8.
- [44] L. D. Bornemann et al. “Dose dependent pharmacokinetics of midazolam.” In: *European journal of clinical pharmacology* 29.1 (1985), pp. 91–5.

- [45] Harshvardhan N Chaobal and Evan D Kharasch. “Single-point sampling for assessment of constitutive, induced, and inhibited cytochrome P450 3A activity with alfentanil or midazolam.” In: *Clinical pharmacology and therapeutics* 78.5 (Nov. 2005), pp. 529–39.
- [46] Mona Darwish et al. “Interaction profile of armodafinil with medications metabolized by cytochrome P450 enzymes 1A2, 3A4 and 2C19 in healthy subjects.” In: *Clinical pharmacokinetics* 47.1 (2008), pp. 61–74.
- [47] Madelé van Dyk et al. “Validation of a 3-h Sampling Interval to Assess Variability in Cytochrome P450 3A Phenotype and the Impact of Induction and Mechanism-Based Inhibition Using Midazolam as a Probe Substrate.” In: *Frontiers in pharmacology* 10.SEP (Sept. 2019), p. 1120.
- [48] Chin B Eap et al. “Oral administration of a low dose of midazolam (75 microg) as an in vivo probe for CYP3A activity.” In: *European journal of clinical pharmacology* 60.4 (June 2004), pp. 237–46.
- [49] Stéphane L. Eeckhoudt et al. “Sensitive assay for midazolam and its metabolite 1'-hydroxymidazolam in human plasma by capillary high-performance liquid chromatography.” In: *Journal of chromatography. B, Biomedical sciences and applications* 710.1-2 (June 1998), pp. 165–71.
- [50] S L Eeckhoudt et al. “Midazolam and cortisol metabolism before and after CYP3A induction in humans.” In: *International journal of clinical pharmacology and therapeutics* 39.7 (July 2001), pp. 293–9.
- [51] Nielka P. van Erp et al. “Marginal increase of sunitinib exposure by grapefruit juice.” In: *Cancer chemotherapy and pharmacology* 67.3 (Mar. 2011), pp. 695–703.
- [52] Dora Farkas et al. “Pomegranate juice does not impair clearance of oral or intravenous midazolam, a probe for cytochrome P450-3A activity: comparison with grapefruit juice.” In: *Journal of clinical pharmacology* 47.3 (Mar. 2007), pp. 286–94.
- [53] J. Christopher Gorski et al. “The effect of age, sex, and rifampin administration on intestinal and hepatic cytochrome P450 3A activity”. In: *Clinical Pharmacology and Therapeutics* 74.3 (Sept. 2003), pp. 275–287.
- [54] D. J. Greenblatt et al. “Absence of interaction of cimetidine and ranitidine with intravenous and oral midazolam.” In: *Anesthesia and analgesia* 65.2 (Feb. 1986), pp. 176–80.
- [55] David J Greenblatt et al. “Time course of recovery of cytochrome p450 3A function after single doses of grapefruit juice.” In: *Clinical pharmacology and therapeutics* 74.2 (Aug. 2003), pp. 121–9.
- [56] David J. Greenblatt et al. “Kinetics and EEG effects of midazolam during and after 1-minute, 1-hour, and 3-hour intravenous infusions.” In: *Journal of clinical pharmacology* 44.6 (June 2004), pp. 605–11.
- [57] P. Heizmann, M. Eckert, and W H Ziegler. “Pharmacokinetics and bioavailability of midazolam in man.” In: *British journal of clinical pharmacology* 16 Suppl 1.S1 (Feb. 1983), 43S–49S.
- [58] Jussi H Kanto. “Midazolam: the first water-soluble benzodiazepine. Pharmacology, pharmacokinetics and efficacy in insomnia and anesthesia.” In: *Pharmacotherapy* 5.3 (May 1985), pp. 138–55.

- [59] Marina Kawaguchi-Suzuki et al. “Effect of Low-Furanocoumarin Hybrid Grapefruit Juice Consumption on Midazolam Pharmacokinetics.” In: *Journal of clinical pharmacology* 57.3 (Mar. 2017), pp. 305–311.
- [60] Evan D Kharasch et al. “The role of cytochrome P450 3A4 in alfentanil clearance. Implications for interindividual variability in disposition and perioperative drug interactions.” In: *Anesthesiology* 87.1 (July 1997), pp. 36–50.
- [61] Ulrich Klotz and Gismar Ziegler. “Physiologic and temporal variation in hepatic elimination of midazolam.” In: *Clinical pharmacology and therapeutics* 32.1 (July 1982), pp. 107–12.
- [62] Jang-Ik Lee et al. “Application of semisimultaneous midazolam administration for hepatic and intestinal cytochrome P450 3A phenotyping.” In: *Clinical pharmacology and therapeutics* 72.6 (Dec. 2002), pp. 718–28.
- [63] Bettina Link et al. “Pharmacokinetics of intravenous and oral midazolam in plasma and saliva in humans: usefulness of saliva as matrix for CYP3A phenotyping.” In: *British journal of clinical pharmacology* 66.4 (Oct. 2008), pp. 473–84.
- [64] Bo Liu et al. “The absorption kinetics of ketoconazole plays a major role in explaining the reported variability in the level of interaction with midazolam: Interplay between formulation and inhibition of gut wall and liver metabolism”. In: *Biopharmaceutics & Drug Disposition* 38.3 (Apr. 2017), pp. 260–270.
- [65] Joseph D. Ma et al. “Lack of effect of subject posture on intravenous midazolam clearance: implications for hepatic cytochrome P450 3A phenotyping.” In: *British journal of clinical pharmacology* 67.3 (Mar. 2009), pp. 374–5.
- [66] J W Mandema et al. “Pharmacokinetic-pharmacodynamic modeling of the central nervous system effects of midazolam and its main metabolite alpha-hydroxymidazolam in healthy volunteers.” In: *Clinical pharmacology and therapeutics* 51.6 (June 1992), pp. 715–28.
- [67] Jacqueline McCrea et al. “Concurrent administration of the erythromycin breath test (EBT) and oral midazolam as in vivo probes for CYP3A activity.” In: *Journal of clinical pharmacology* 39.12 (Dec. 1999), pp. 1212–20.
- [68] Klaus T. Olkkola et al. “A potentially hazardous interaction between erythromycin and midazolam”. In: *Clinical Pharmacology and Therapeutics* 53.3 (Mar. 1993), pp. 298–305.
- [69] Klaus T Olkkola, Janne T Backman, and Pertti J Neuvonen. “Midazolam should be avoided in patients receiving the systemic antimycotics ketoconazole or itraconazole.” In: *Clinical pharmacology and therapeutics* 55.5 (May 1994), pp. 481–5.
- [70] P. J. Pentikäinen et al. “Pharmacokinetics of midazolam following intravenous and oral administration in patients with chronic liver disease and in healthy subjects.” In: *Journal of clinical pharmacology* 29.3 (Mar. 1989), pp. 272–7.

- [71] Helen S. Pentikis et al. “The effect of multiple-dose, oral rifaximin on the pharmacokinetics of intravenous and oral midazolam in healthy volunteers.” In: *Pharmacotherapy* 27.10 (Oct. 2007), pp. 1361–9.
- [72] J D Rogers et al. “Grapefruit juice has minimal effects on plasma concentrations of lovastatin-derived 3-hydroxy-3-methylglutaryl coenzyme A reductase inhibitors.” In: *Clinical pharmacology and therapeutics* 66.4 (Oct. 1999), pp. 358–66.
- [73] Stacy S. Shord et al. “Effects of oral clotrimazole troches on the pharmacokinetics of oral and intravenous midazolam”. In: *British Journal of Clinical Pharmacology* 69.2 (Feb. 2010), pp. 160–166.
- [74] S. Sjövall et al. “CSF penetration and pharmacokinetics of midazolam.” In: *European journal of clinical pharmacology* 25.2 (Aug. 1983), pp. 247–51.
- [75] M T Smith, M J Eadie, and T O’Rourke Brophy. “The pharmacokinetics of midazolam in man.” In: *European journal of clinical pharmacology* 19.4 (Mar. 1981), pp. 271–8.
- [76] S M Tsunoda et al. “Differentiation of intestinal and hepatic cytochrome P450 3A activity with use of midazolam as an in vivo probe: effect of ketoconazole.” In: *Clinical pharmacology and therapeutics* 66.5 (Nov. 1999), pp. 461–71.
- [77] J. Vanakoski, M. J. Mattila, and T. Seppälä. “Grapefruit juice does not enhance the effects of midazolam and triazolam in man.” In: *European journal of clinical pharmacology* 50.6 (July 1996), pp. 501–8.
- [78] Maria L. Veronese et al. “Exposure-dependent inhibition of intestinal and hepatic CYP3A4 in vivo by grapefruit juice.” In: *Journal of clinical pharmacology* 43.8 (Aug. 2003), pp. 831–9.
- [79] P Heizmann and W H Ziegler. “Excretion and metabolism of 14C-midazolam in humans following oral dosing.” In: *Arzneimittel-Forschung* 31.12a (1981), pp. 2220–3.

Appendices

A Figures and Tables

A.1 Midazolam studies overview

Table 8: Overview of all the information about groups, individuals and interventions provided by each study. The table provides information about the number of groups and individuals in each study, their sex, age, weight, height, bmi and ethnicity. Further, it lists whether the studies gave information about the study participants health, if they were on medication, their smoking status, if they had to fast prior to the trial and whether they drink alcohol. Finally, it shows if the study provided information about the dose, administration route and form of medication in each intervention. Either information for all groups/individuals/intervention was provided (✓), only partially (Ø) or not at all (whitespace).

pkdb	name	individuals	groups	sex	age	weight	height	bmi	ethnicity	healthy	medication	smoking	fast	alcohol	dose	route	form
PKDB00181	Allonen1981	6	1	✓	Ø	Ø				✓	✓	✓	✓	✓	✓	✓	
PKDB00227	Backman1996	10	1	✓	✓	✓				✓	✓	✓	✓	✓	✓	✓	
PKDB00228	Backman1998	9	1	✓						✓	✓	✓	✓	✓	✓	✓	
PKDB00251	Bornemann1985	12	1	✓	✓	✓				✓		✓	✓	✓	✓	✓	
PKDB00326	Chaobal2005	10	1							✓				✓	✓	Ø	
PKDB00243	Chung2006	19	6	✓	✓	✓				✓	✓	✓		✓	✓	✓	
PKDB00328	Darwishi2008	77	3	✓	✓					✓	Ø	✓	✓	✓	✓	Ø	
PKDB00308	Dyk2019	30	3	✓	Ø	Ø	Ø	Ø		✓	✓			✓	✓		
PKDB00327	Eap2004	21	4	✓	✓	✓				✓	✓	✓		✓	✓	✓	
PKDB00247	Eeckhoudt1998	9	0							✓				✓	✓	Ø	
PKDB00322	Eeckhoudt2001	8	1	✓	Ø	Ø				✓	✓	✓		✓	✓	Ø	
PKDB00249	Erp2011	8	0	✓	✓					✓	✓			✓	✓	✓	
PKDB00209	Farkas2007	13	1	✓	✓	✓				✓	✓	✓		✓	✓	Ø	
PKDB00205	Gorski2003	52	5	✓		Ø				Ø	Ø	✓		✓	✓	✓	
PKDB00179	Greenblatt1986	14	2	Ø						✓	✓			✓	✓	✓	
PKDB00254	Greenblatt2003	25	4	✓	✓					✓	✓	✓		✓	✓	✓	
PKDB00298	Greenblatt2004	8	1	✓	✓	✓	✓			✓	✓	✓		✓	✓	✓	
PKDB00178	Heizmann1983	6	3		Ø					✓		✓		✓	✓	✓	
PKDB00250	Kanto1985	207	17	Ø						✓				✓	✓	Ø	
PKDB00252	Kawaguchi-Suzuki2017	12	1	✓	✓					✓	✓	✓	✓	✓	✓	✓	
PKDB00245	Kharasch1997	9	1	✓	✓	✓				✓	✓	✓		✓	✓	✓	
PKDB00211	Kharasch2004	10	1	✓	✓	✓				✓	✓			✓	✓	Ø	
PKDB00203	Klotz1982	6	1	✓						✓	✓			✓	✓	Ø	
PKDB00207	Kupferschmidt1995	8	1	✓	✓	✓				✓				✓	✓	✓	
PKDB00306	Lee2002	12	2	✓	✓	Ø				✓	✓	✓	✓	✓	✓	Ø	
PKDB00248	Link2008	8	1	✓	✓	✓				✓		✓	✓	✓	✓	✓	
PKDB00305	Liu2017	15	2	✓						✓	✓			✓	✓	✓	
PKDB00325	Ma2009	13	2	✓						✓	✓			✓	✓	✓	
PKDB00206	Mandema1992	8	1	✓	✓	✓				✓	✓	✓	✓	✓	✓	✓	
PKDB00321	McCrea1999	12	3	✓	✓	✓				✓	✓	✓		✓	✓	Ø	
PKDB00246	Olkkola1993	12	2	✓						✓	✓			✓	✓	✓	
PKDB00307	Olkkola1994	9	1	✓						✓				✓	✓	Ø	
PKDB00269	Pentikainen1989	14	2	✓	✓	✓				✓	✓	✓	✓	✓	✓	Ø	
PKDB00244	Pentikis2007	27	12	✓	✓	✓	✓	✓		✓	✓			✓	✓	✓	
PKDB00208	Rogers1999	16	1	✓	✓	✓				✓	✓	✓		✓	✓	✓	
PKDB00323	Shord2010	10	1	✓		✓				✓	✓			✓	✓	✓	
PKDB00268	Sjoevall1983	57	4	✓	✓	✓	✓			✓	✓			✓	✓	Ø	
PKDB00199	Smith1981	6	1	✓	✓	✓				✓	✓	✓		✓	✓	✓	
PKDB00202	Thummel1996	20	3	✓	Ø	Ø				✓	✓	✓	✓	✓	✓	✓	
PKDB00201	Tsunoda1999	9	1	✓	✓	✓				✓	✓	✓	✓	✓	✓	✓	
PKDB00253	Vanakoski1996	120	1	✓						✓				✓	✓	✓	
PKDB00217	Veronese2003	24	2	✓	✓	✓				✓		✓	✓	✓	✓	✓	
PKDB00324	Yu2004	19	3	✓	✓	✓	✓			✓	✓			✓	✓	✓	

A.2 Meta-analysis

In this section we show the meta-analysis of the remaining pharmacokinetic parameters of midazolam (Fig. 19) and all parameters of 1-hydroxymidazolam (Fig. 20). For 1-hydroxymidazolam bioavailability, clearance and V_d are missing, since calculation of these parameters depend on an administration dose (see Sec. 2.1)

Figure description: Meta-analysis of pharmacokinetic parameters of midazolam/1-hydroxymidazolam in healthy subjects. Depicted are the respective parameters after intravenous (iv) and oral (po) midazolam administration, either for controls, pre-treatment with substances that have no influence on midazolam metabolism (no interaction), CYP3A4 inducers (induction), hepatic and intestinal CYP3A4 inhibitors (systemic inhibition), and inhibitors only affecting intestinal CYP3A4 (intestinal inhibition). Data points were either taken directly from the publication (from publication), transformed in absolute values with the respective bodyweight if given relative to bodyweight (from bodyweight) or calculated from time courses (from timecourse).

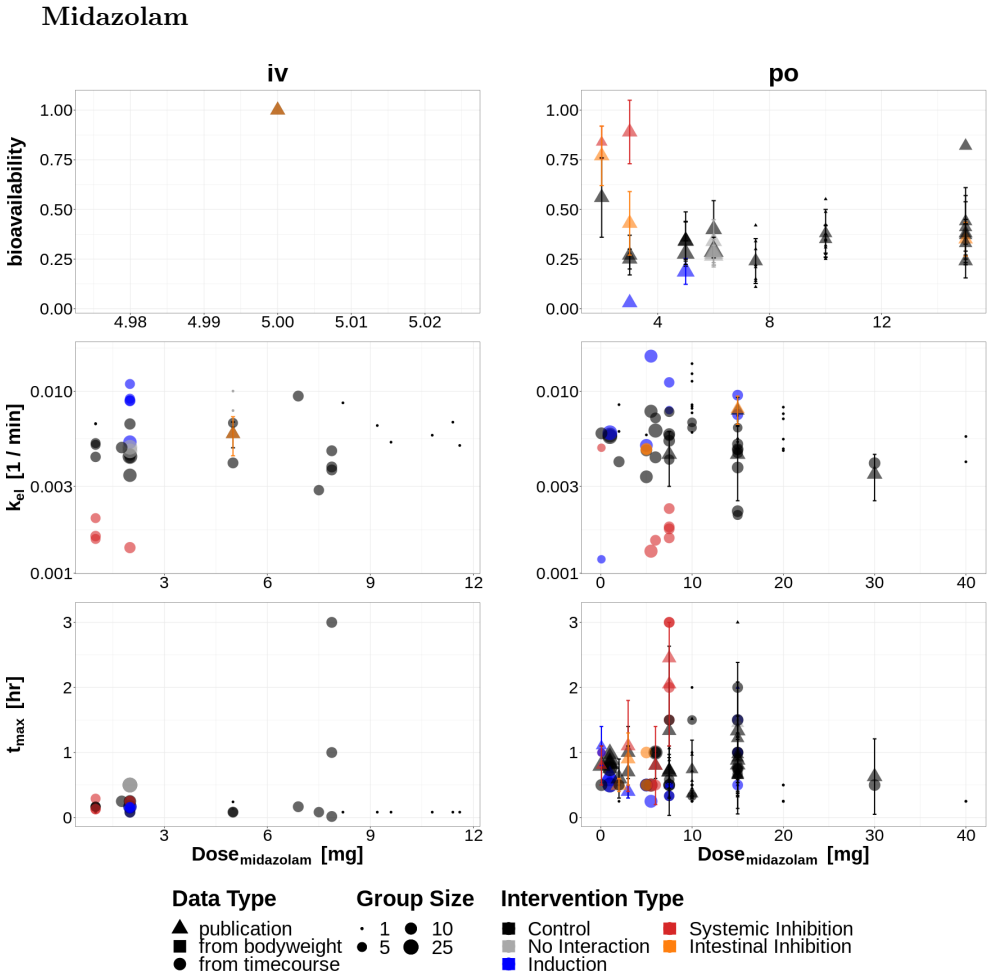


Figure 19: Meta-analysis of midazolam pharmacokinetics data.

1-hydroxymidazolam

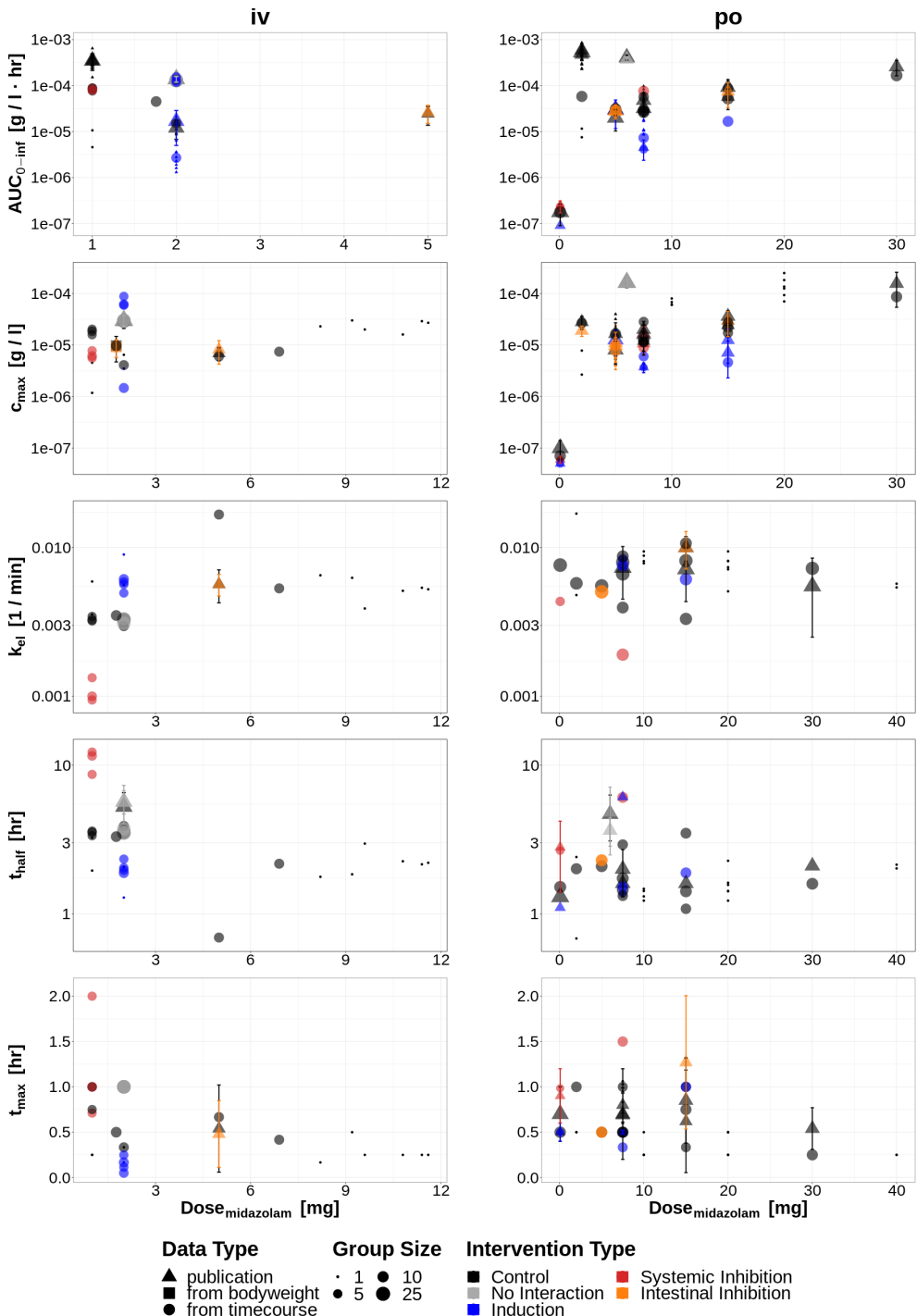


Figure 20: Meta-analysis of 1-hydroxymidazolam pharmacokinetics data.

A.3 Midazolam simulation experiments

In the following, model predictions of the complete set of 26 simulation experiments used in this work are depicted.

Figure description: Depicted are the simulation results for all 26 simulation experiments under control (black), inhibitor (red), intestinal inhibitor (orange) and inducer (blue) conditions. Each plot shows a reported time course (dashed; mean \pm SD) from a study and the corresponding model prediction (solid). The shaded areas around the model predictions depict the SD (dark) and the full range (light) from the uncertainty analysis. The study name and the experimental design, i.e route (iv - intravenous; po - oral) and dose, are listed in the respective plot titles and figure captions. Each time course is plotted on a linear y-axis (left) and logarithmic y-axis (right).

Allonen1981

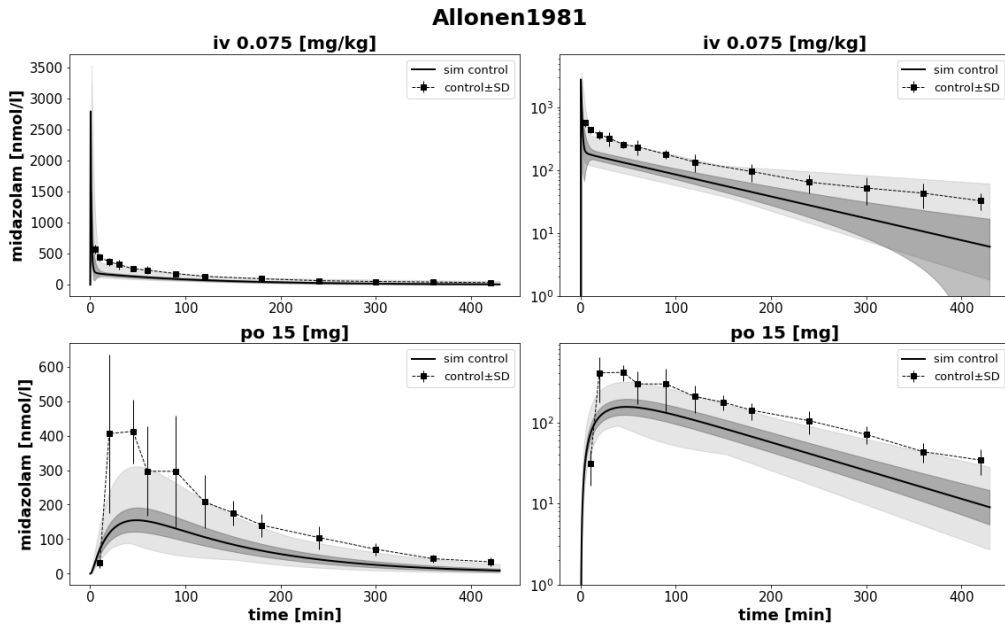


Figure 21: Allonen1981 [42]. Midazolam was administered intravenously (iv; 0.075 mg/kg) and orally (po; 15 mg)

Backman1996

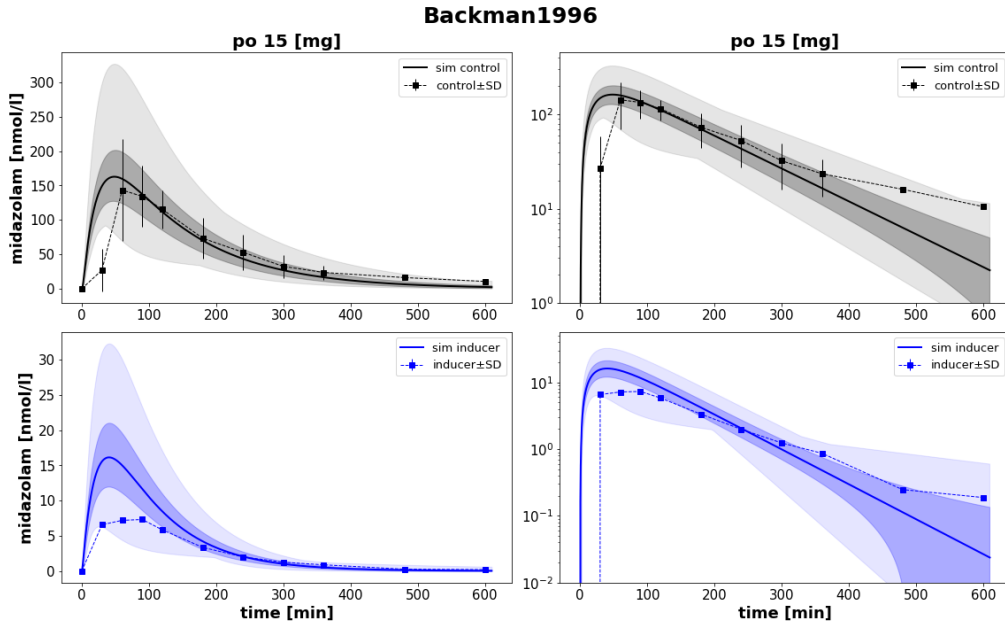


Figure 22: Backman1996 [28]. Midazolam was administered orally (15 mg) either alone (control; black) or with an inducer (blue).

Backman1998

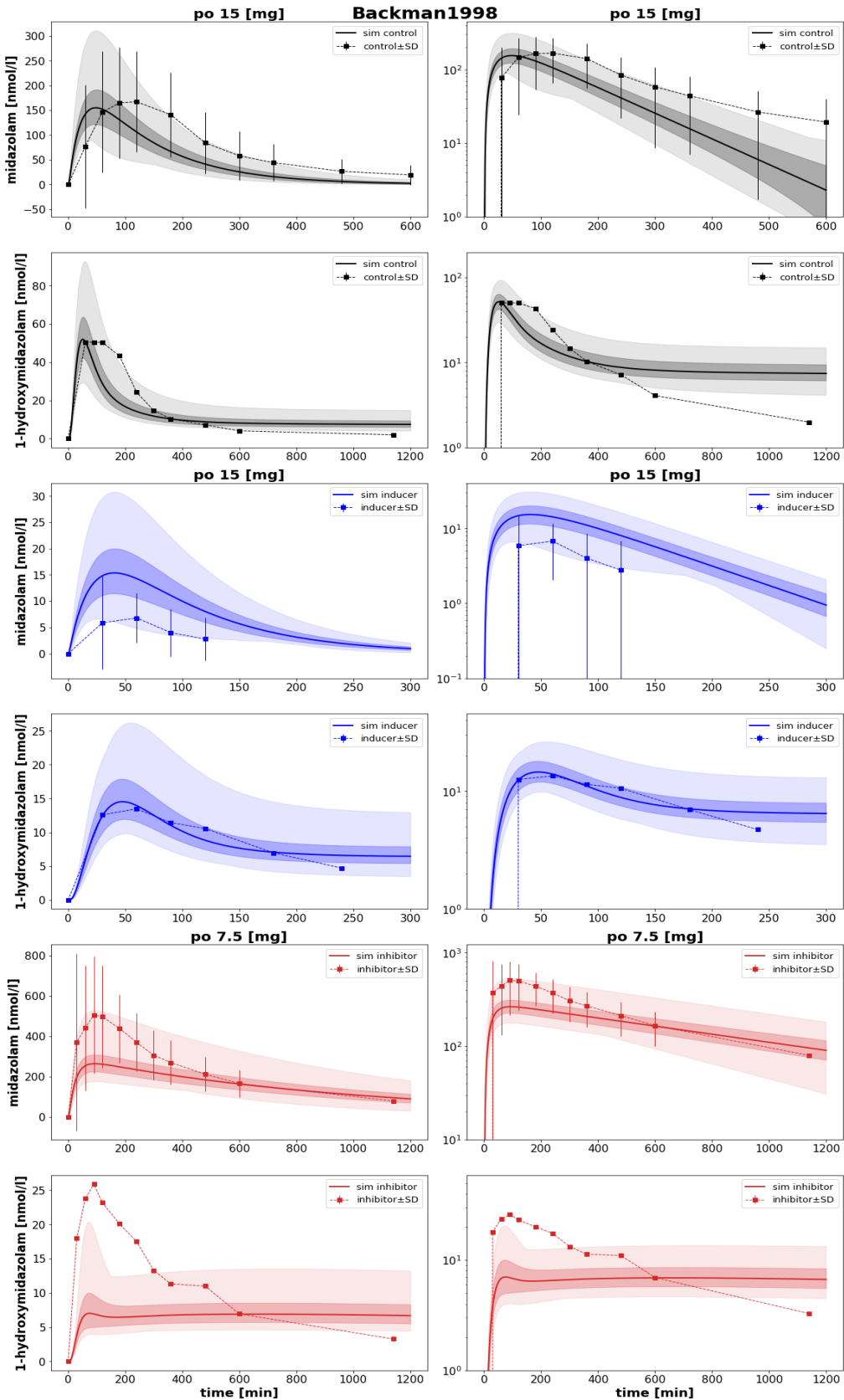


Figure 23: Backman1998 [43]. Midazolam was administered orally (15 mg) either under control (black) or inducer (blue) conditions. In addition, a dose of 7.5 mg was administered under inhibitor (red) condition.

Bornemann1985

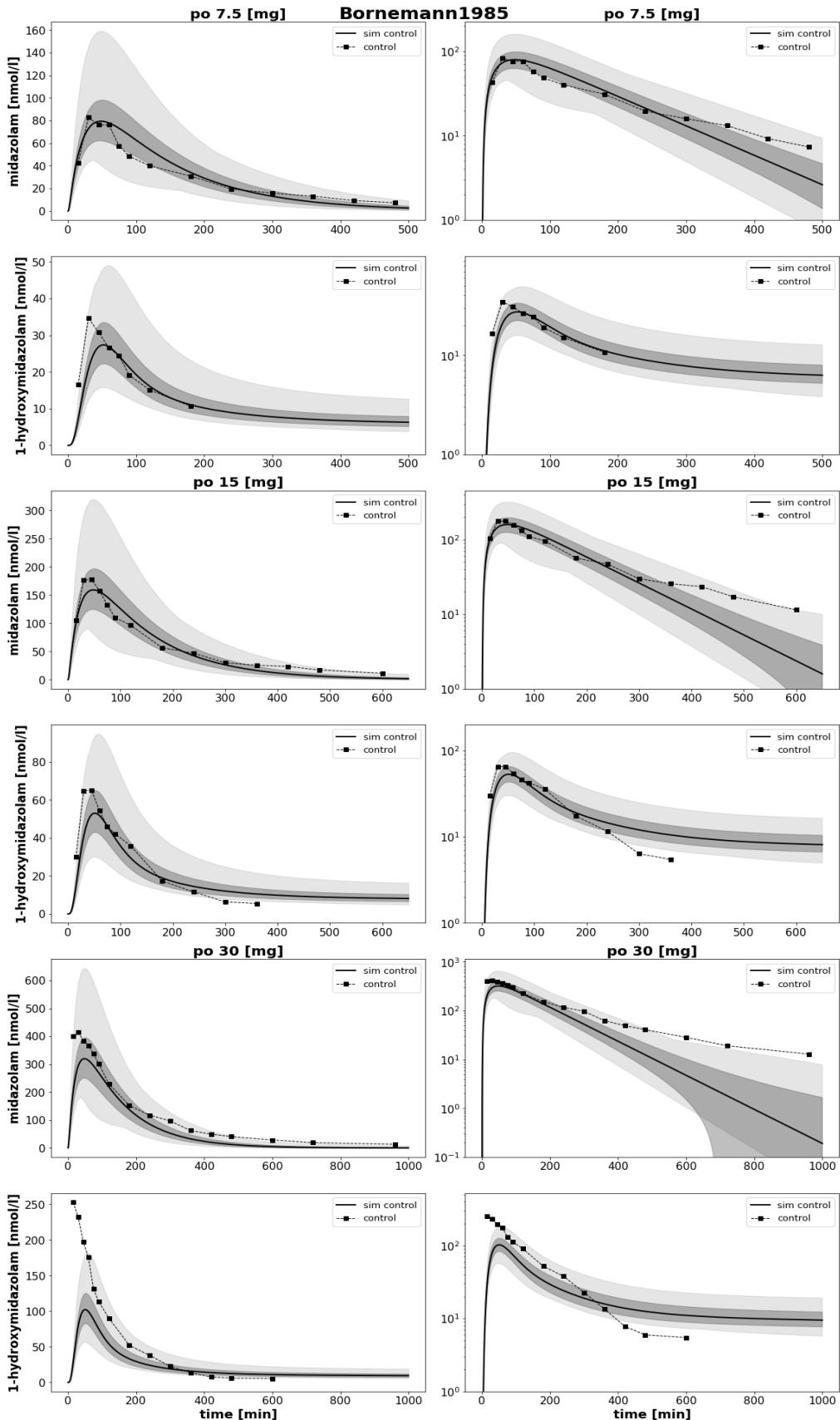


Figure 24: Bornemann1985 [44]. A midazolam dose of 7.5 mg, 15 mg or 30 mg was administered orally.

Chung2006

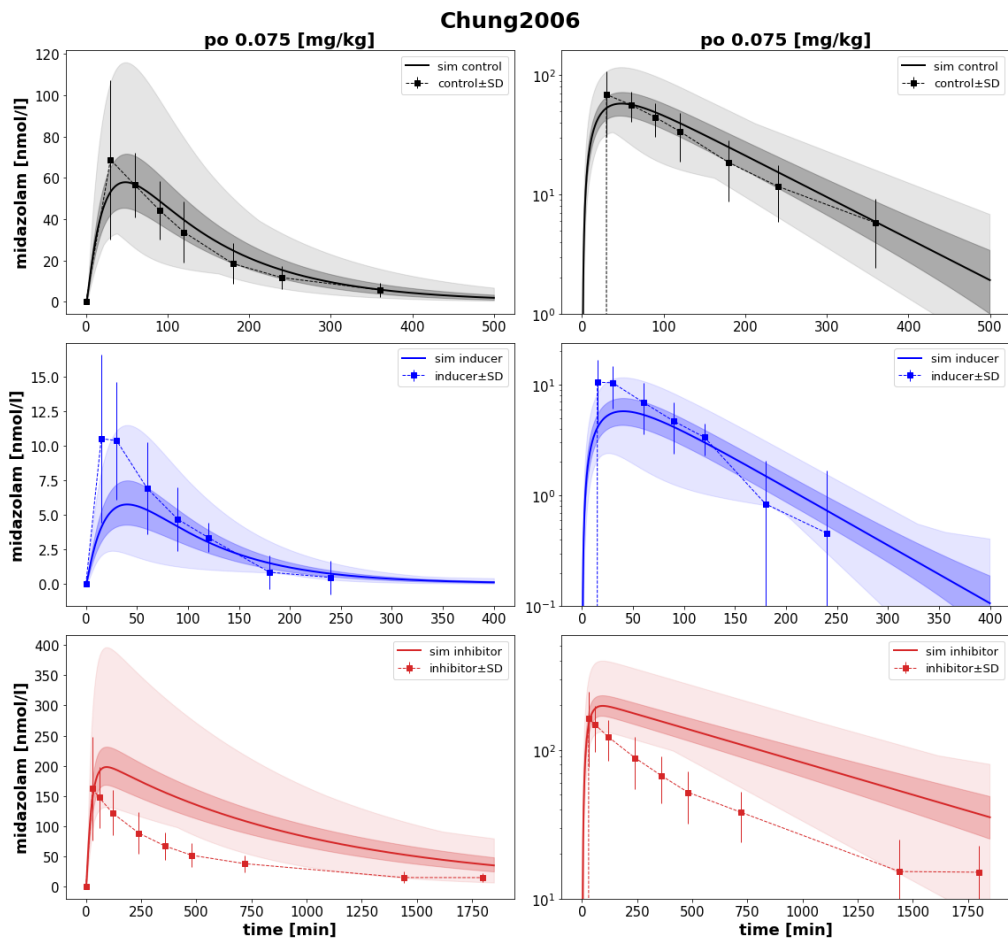


Figure 25: Chung2006 [22]. Midazolam was administered orally (0.075 mg/kg) either under control; (black), inducer (blue) or inhibitor conditions.

Darwish2008

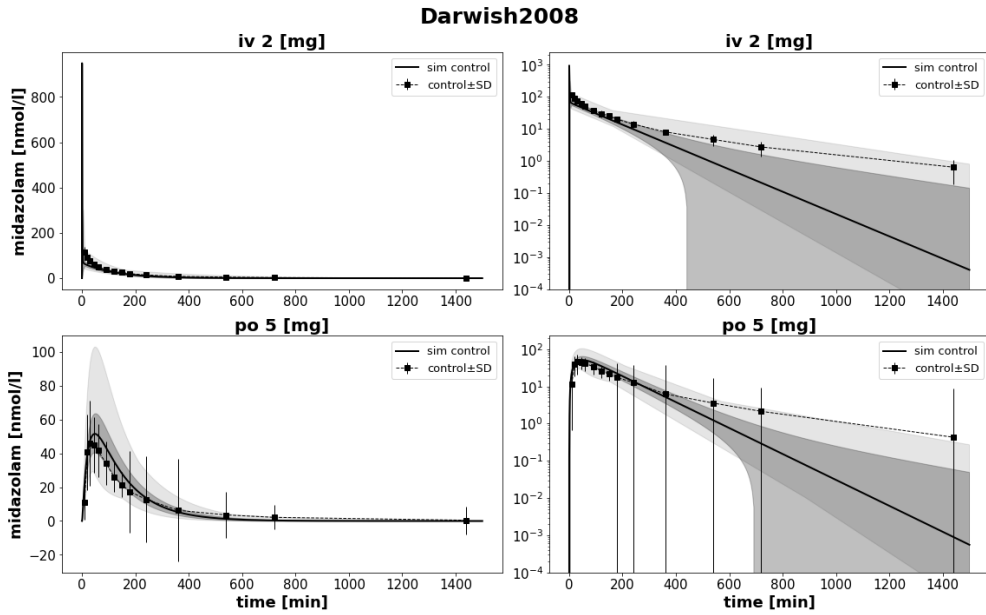


Figure 26: Darwish2008 [46]. Midazolam was administered intravenously (iv; 2 mg) or orally (po; 5 mg).

Dyk2019

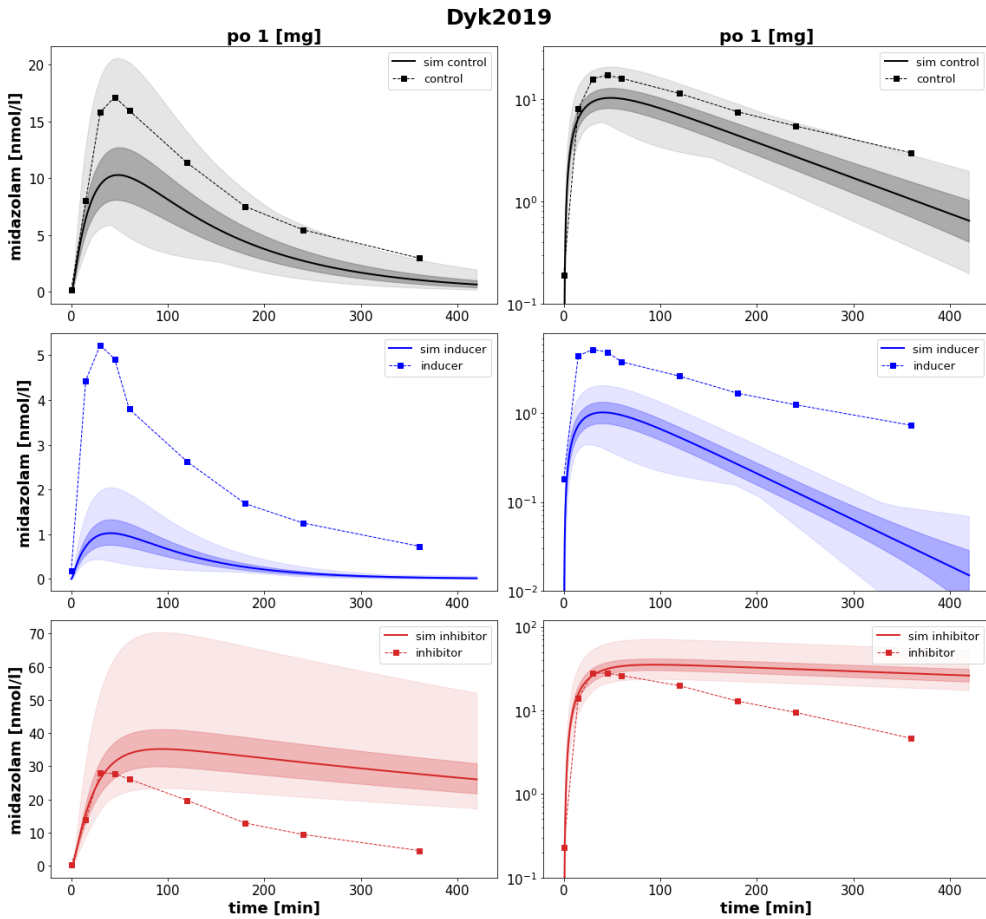


Figure 27: Dyk2019 [47]. Midazolam was administered orally (1 mg) either under control; (black), inducer (blue) or inhibitor (red) conditions.

Eap2004 (control)

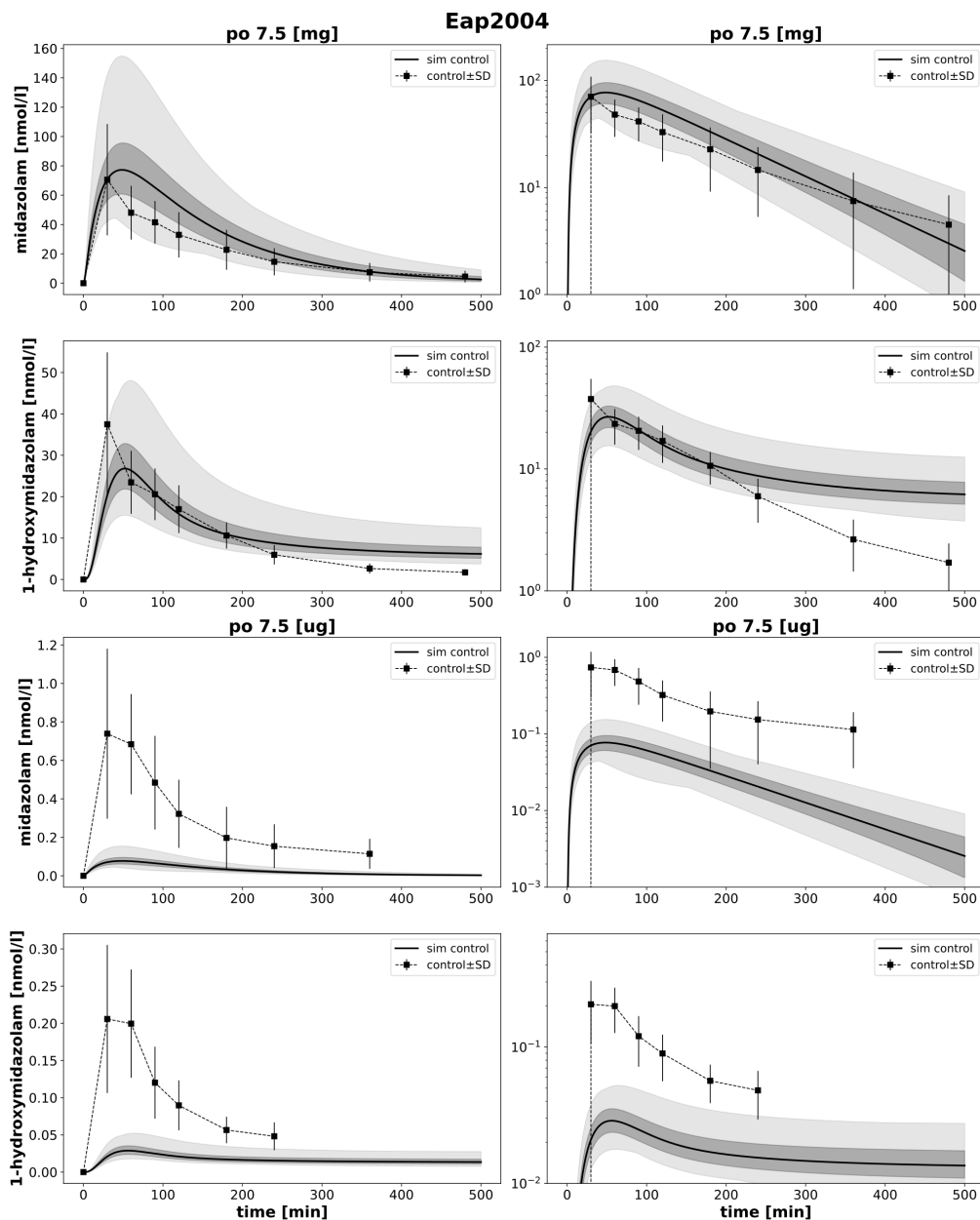


Figure 28: Eap2004 [48]. Oral doses of 7.5 mg and 7.5 μ g midazolam were administered.

Eap2004 (inhibitor & inducer)

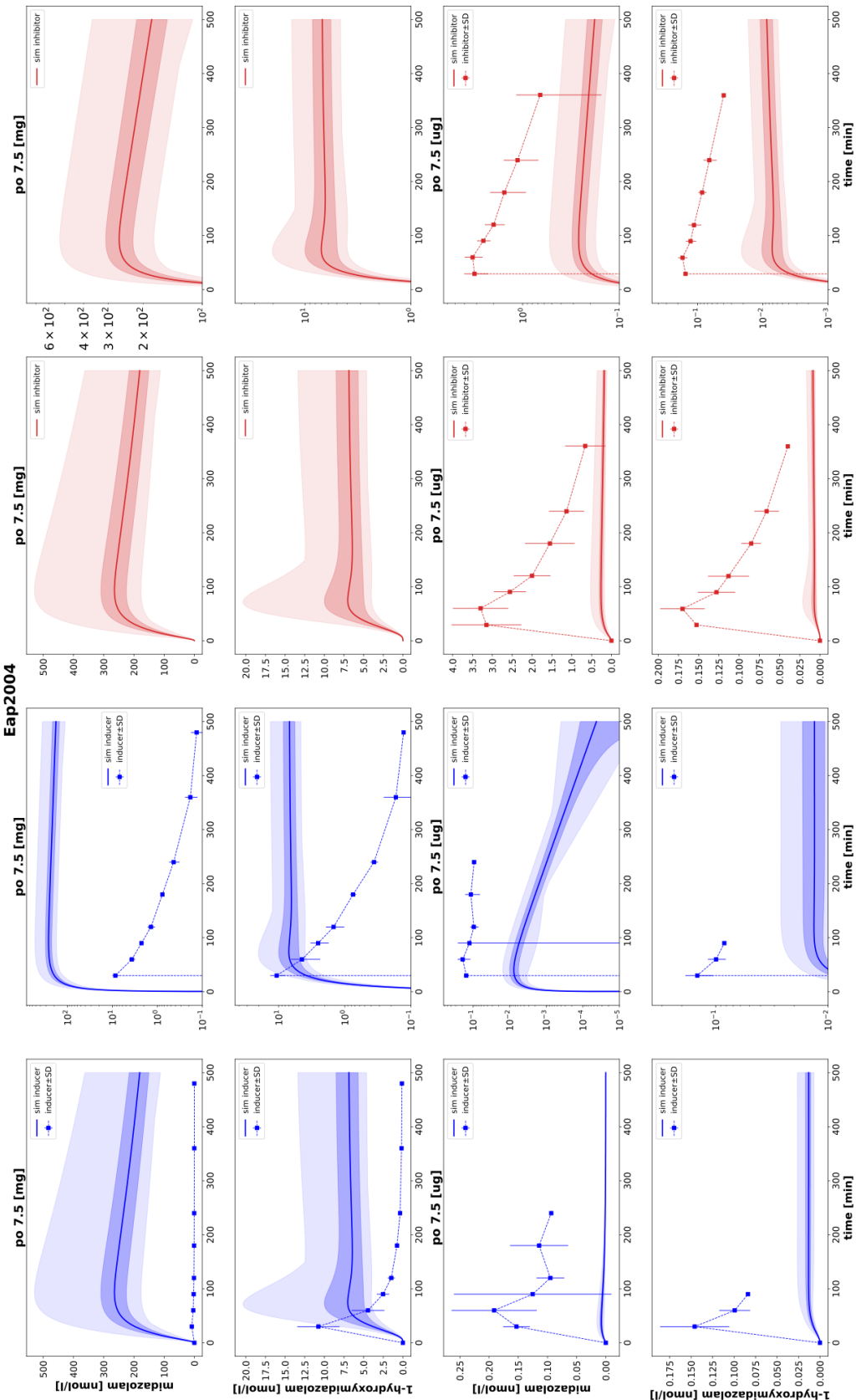


Figure 29: Eap2004 [48]. Oral doses of 7.5 mg and 7.5 µg midazolam were administered either under inducer (blue) or inhibitor (red) conditions. No data for the oral dose of 7.5 mg under inhibition was reported.

Farkas2007

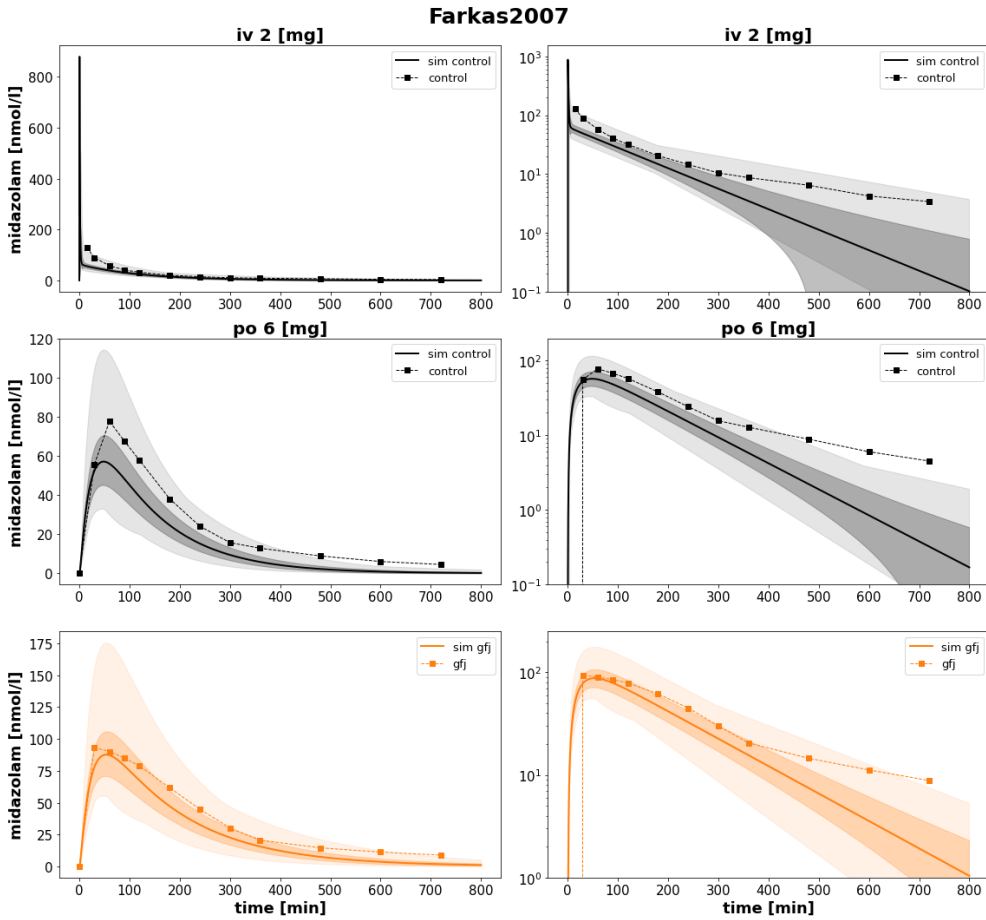


Figure 30: Farkas2007 [52]. Midazolam was administered intravenously (iv; 2 mg) or orally (po; 6 mg) either under control (black) or intestinal inhibitor conditions.

Greenblatt2003

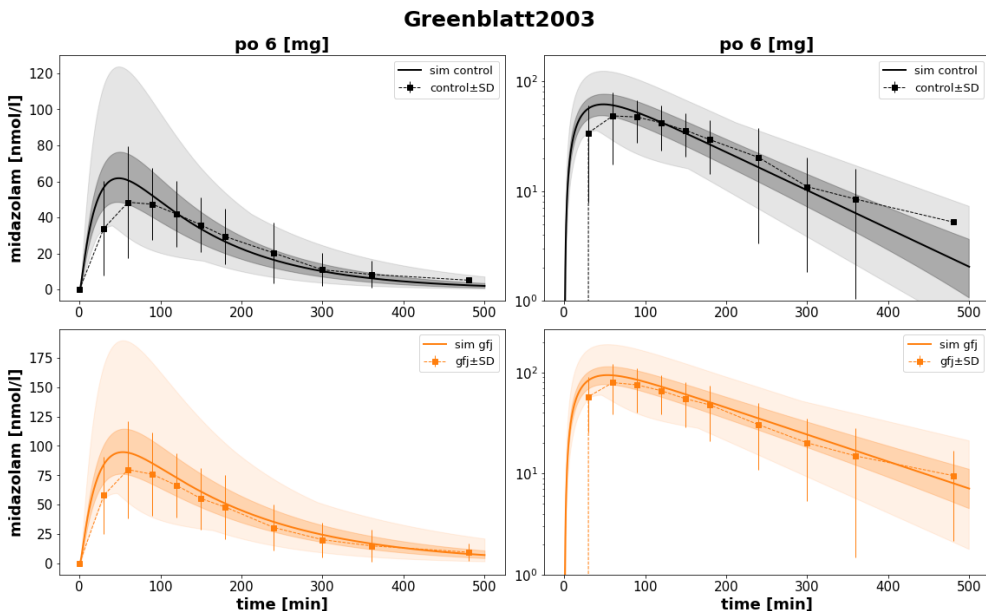


Figure 31: Greenblatt2003 [55]. Midazolam was administered orally (6 mg) either under control (black) or intestinal inhibitor (orange) conditions

Greenblatt2004

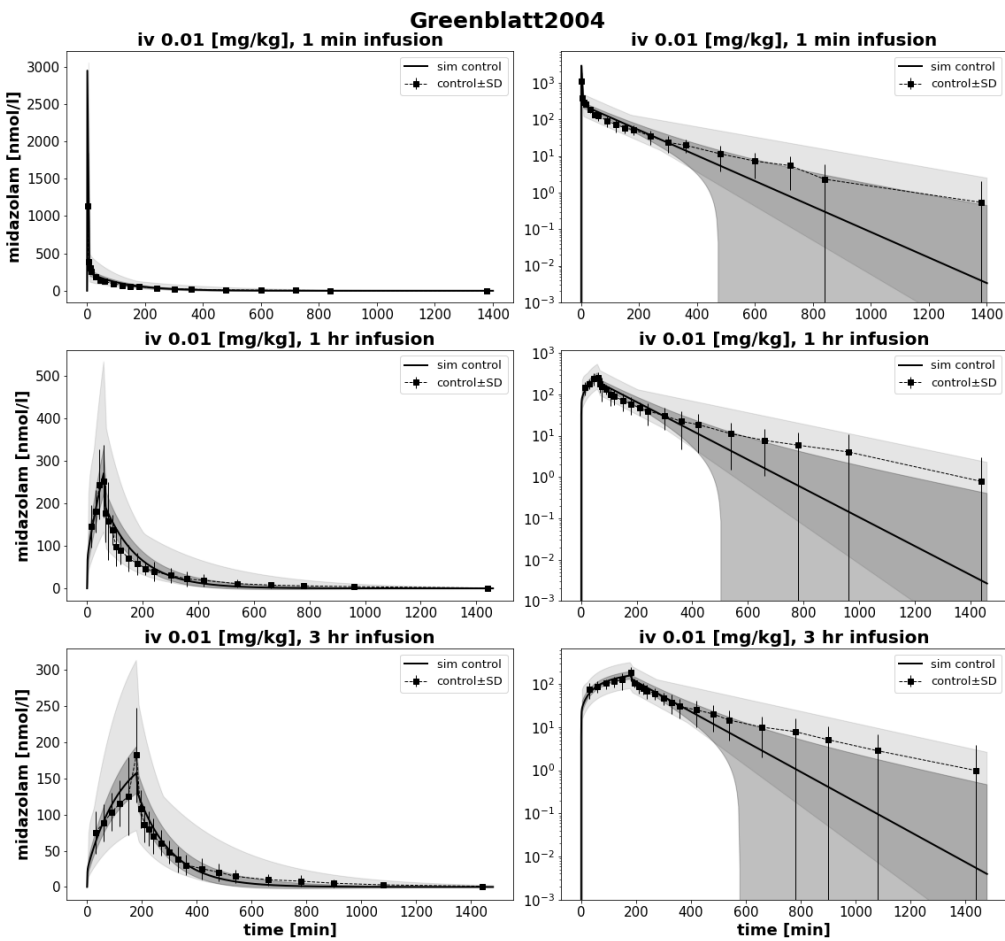


Figure 32: Greenblatt2004 [56]. A dose of 0.01 mg/kg midazolam was administered as an intravenous infusion over 1 min, 1 hr and 3 hr.

KawaguchiSuzuki2017

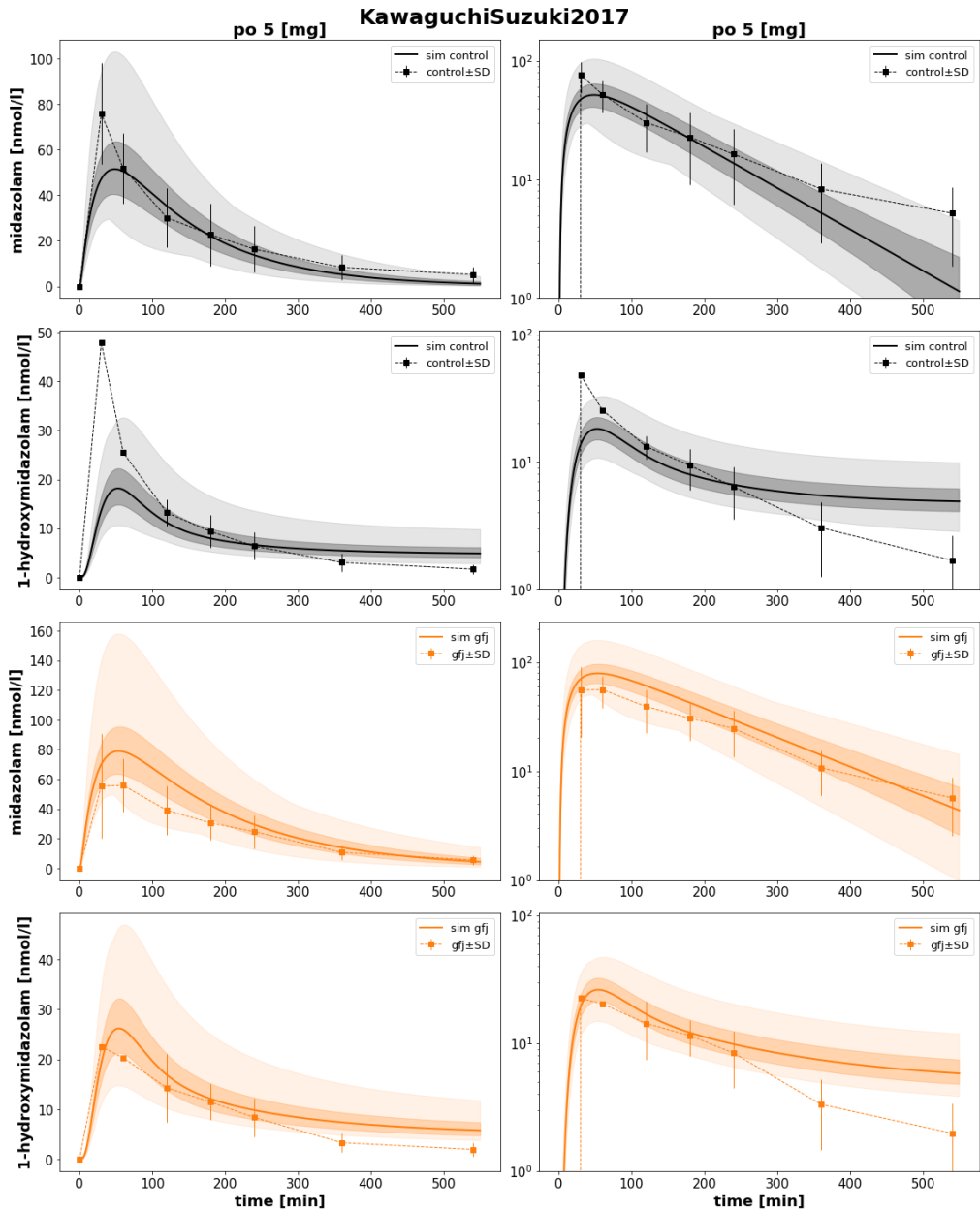


Figure 33: KawaguchiSuzuki2017 [59]. Midazolam was administered orally (5 mg) either under control (black) or intestinal inhibitor (orange) conditions

Kharash2004

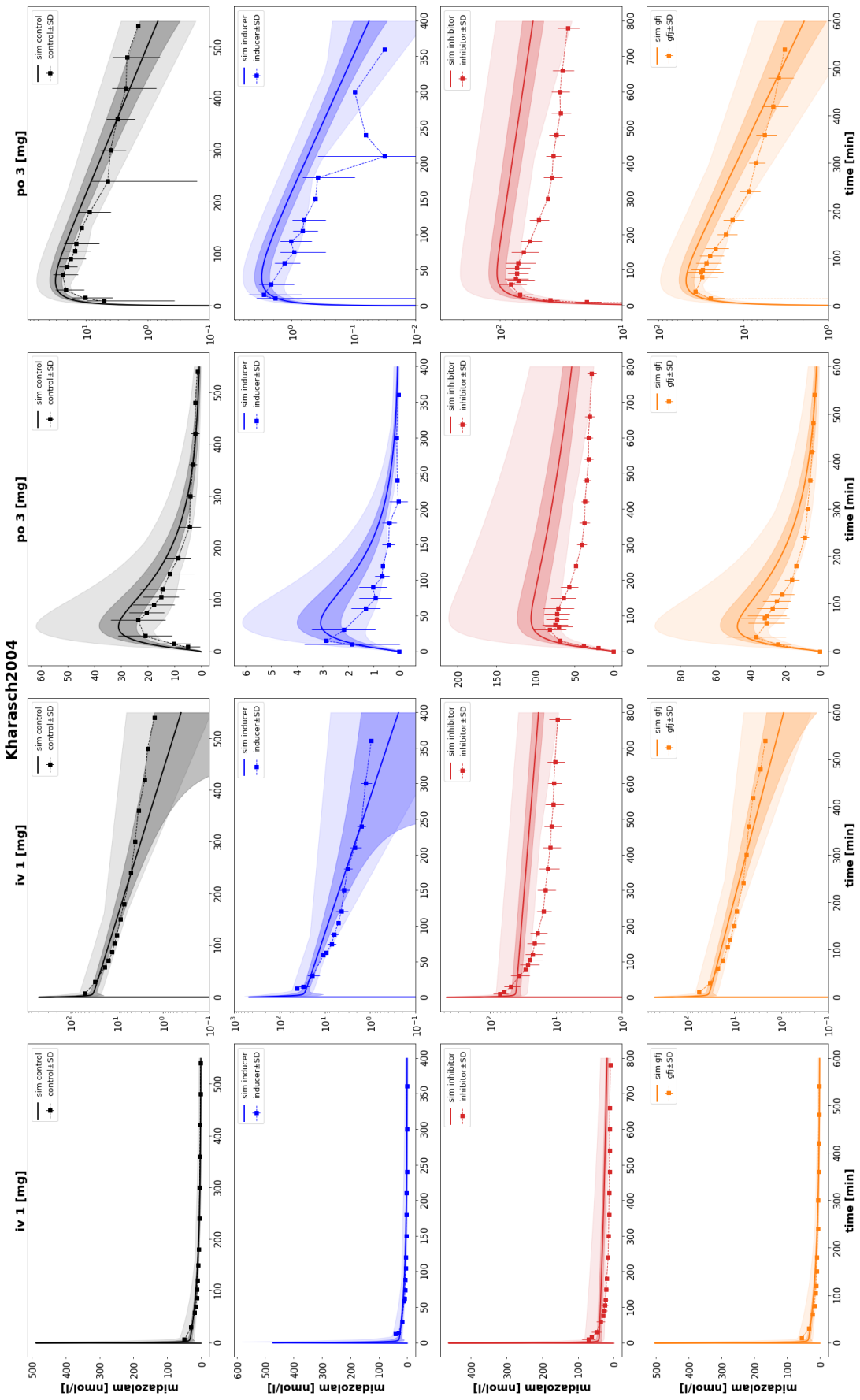


Figure 34: Kharash2004 [23]. Midazolam was administered intravenously (iv; 1 mg) and orally (po; 1 mg) either under control (black), inducer (blue), inhibitor (red) or intestinal inhibitor (orange) conditions.

Kupferschmidt1995

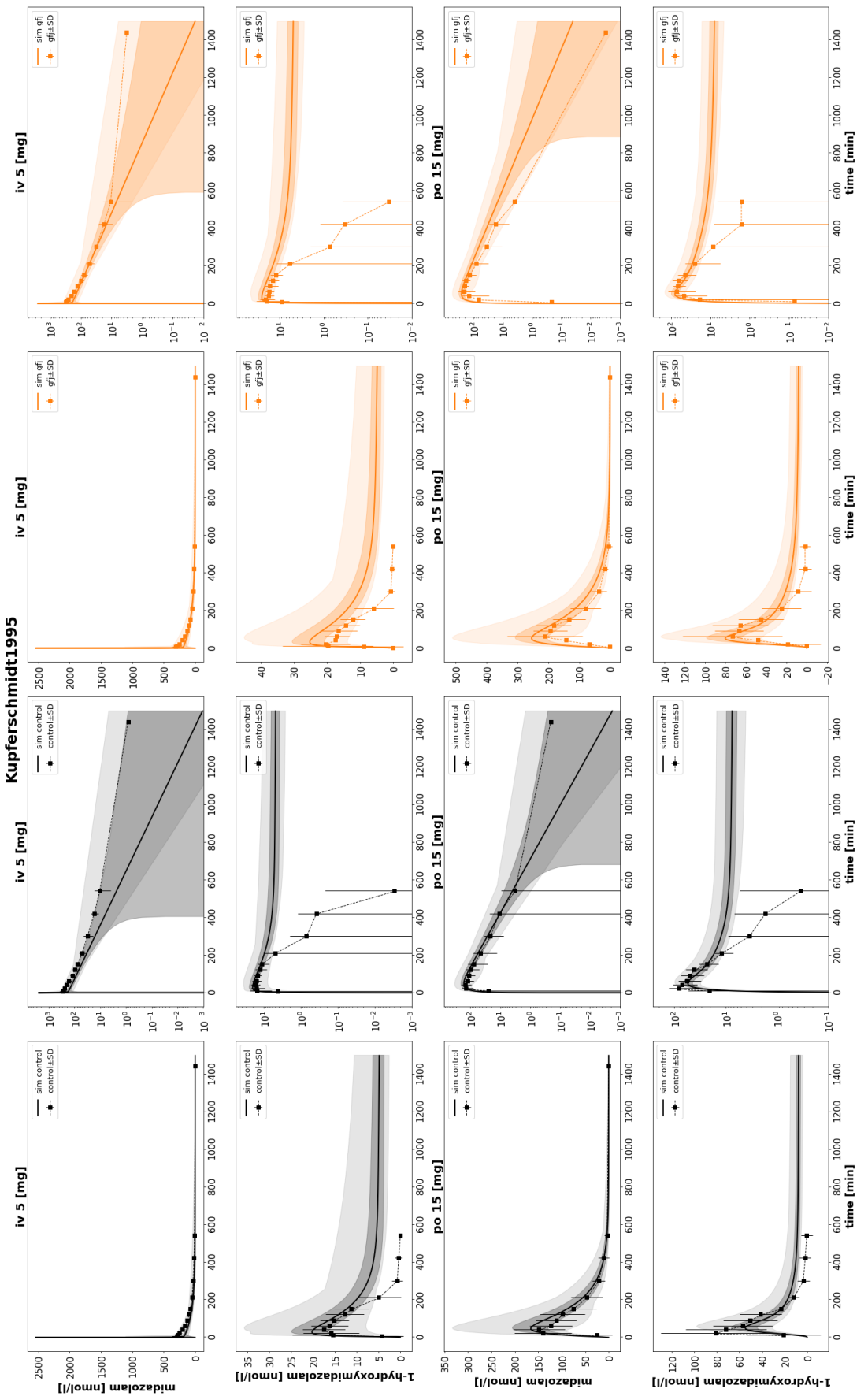


Figure 35: Kupferschmidt1995 [25]. Midazolam was administered intravenously (iv; 5 mg) and orally (po; 15 mg) either under control (black) or intestinal inhibitor (orange) conditions.

Lee2002

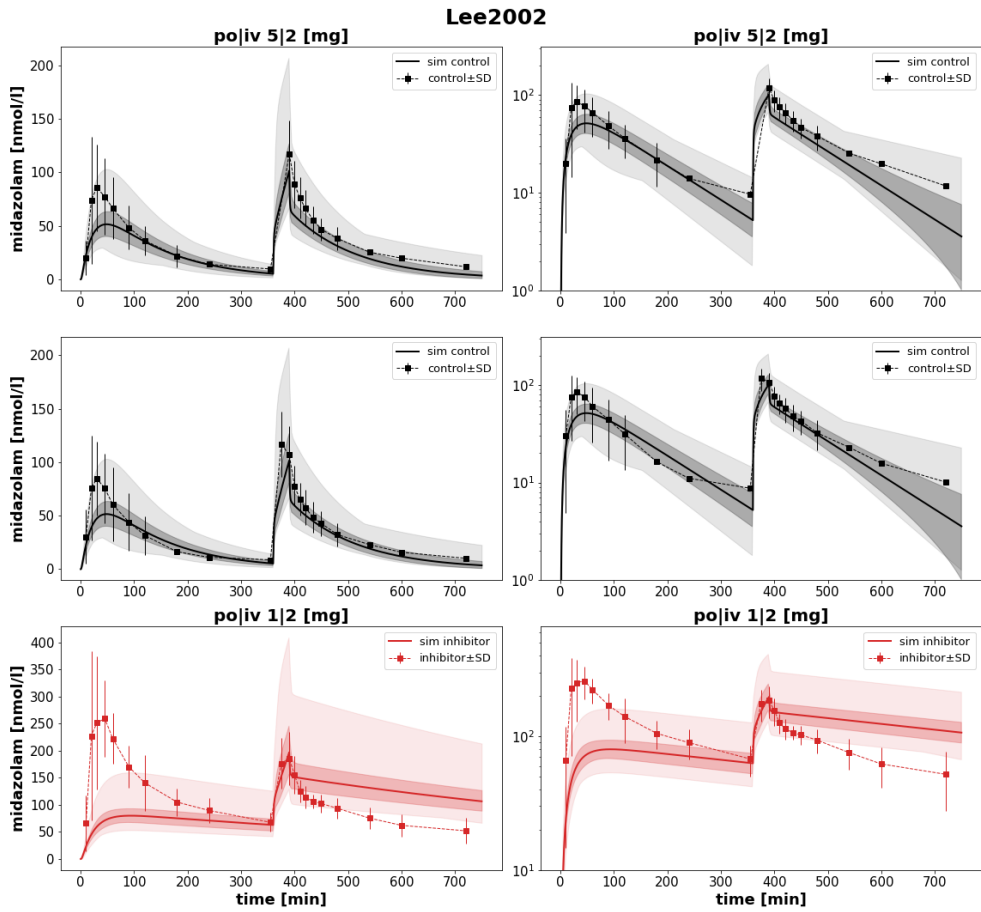


Figure 36: Lee2002 [62]. Oral (po) and intravenous (iv) midazolam was administered semisimultaneously (6 hours apart) under control (black), or inhibitor (red) conditions. Doses under control conditions were 5 mg (po) and 2 mg (iv), and 2 mg (po) and 1 mg (iv) under inhibitor conditions.

Ma2009

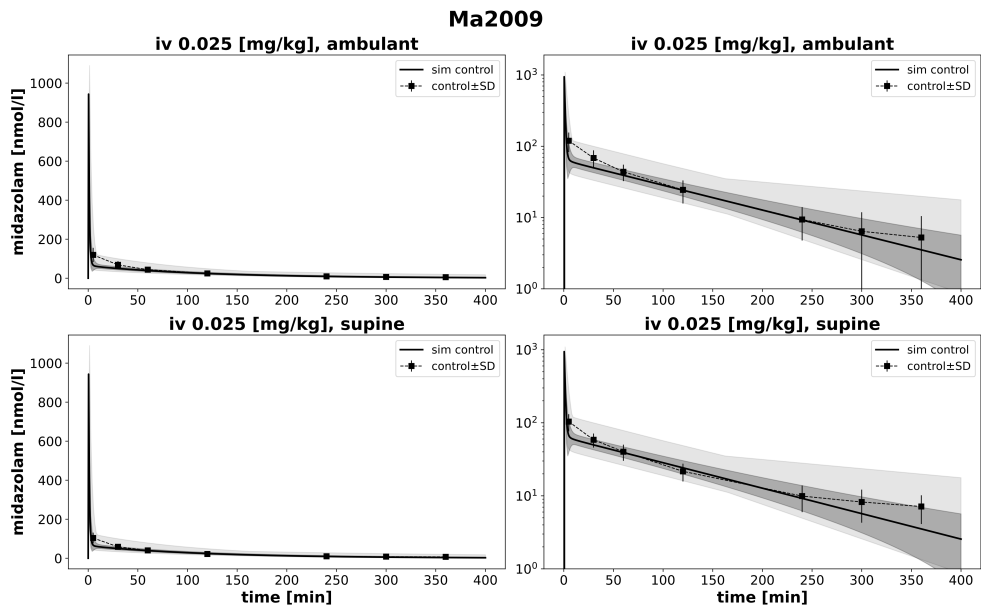


Figure 37: Ma2009 [65]. Midazolam was administered intravenously (0.025 mg/kg) in different body positions (ambulant and supine).

Link2008

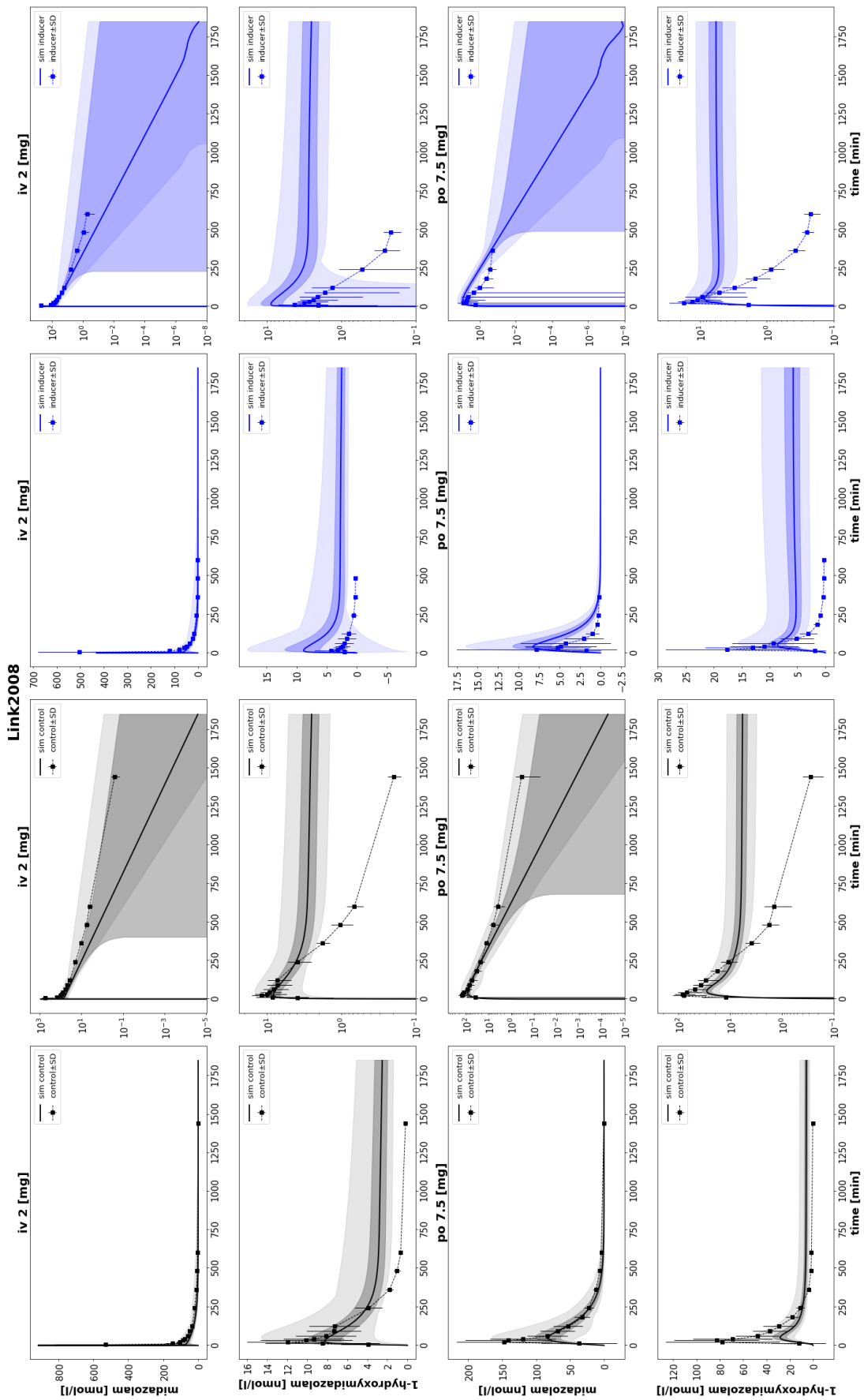


Figure 38: Link2008 [63]. Midazolam was administered intravenously (2 mg) and orally (7.5 mg) either under control; (black) or inducer (blue) conditions

Mandema1992

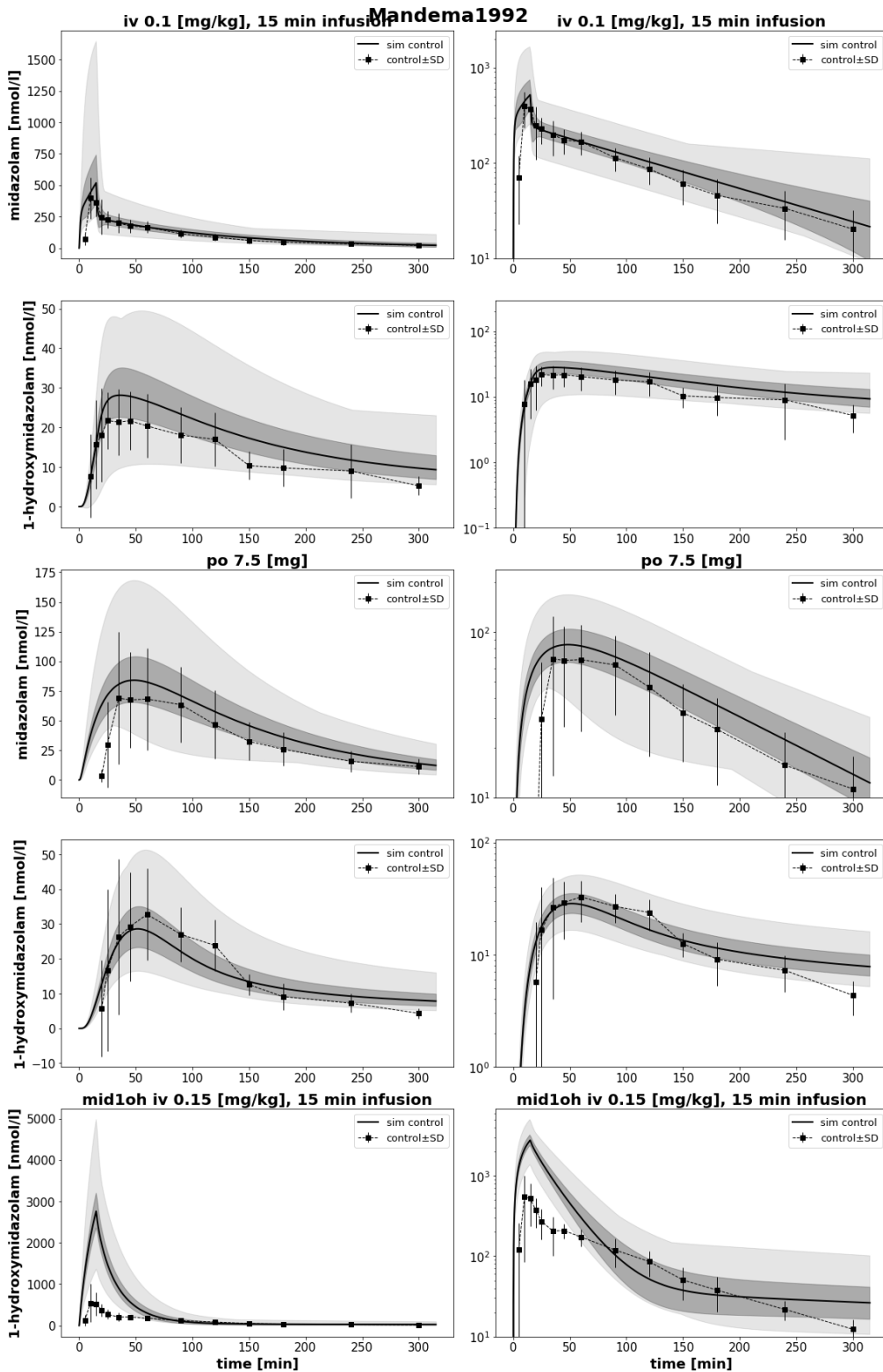


Figure 39: Mandema1992 [66]. Midazolam was administered intravenously as a infusion over 15 min (iv; 0.1 mg/kg) and orally (po; 7.5 mg). In addition, an intravenous dose of 0.15 mg/kg 1-hydroxymidazolam was administered.

McCrea1999

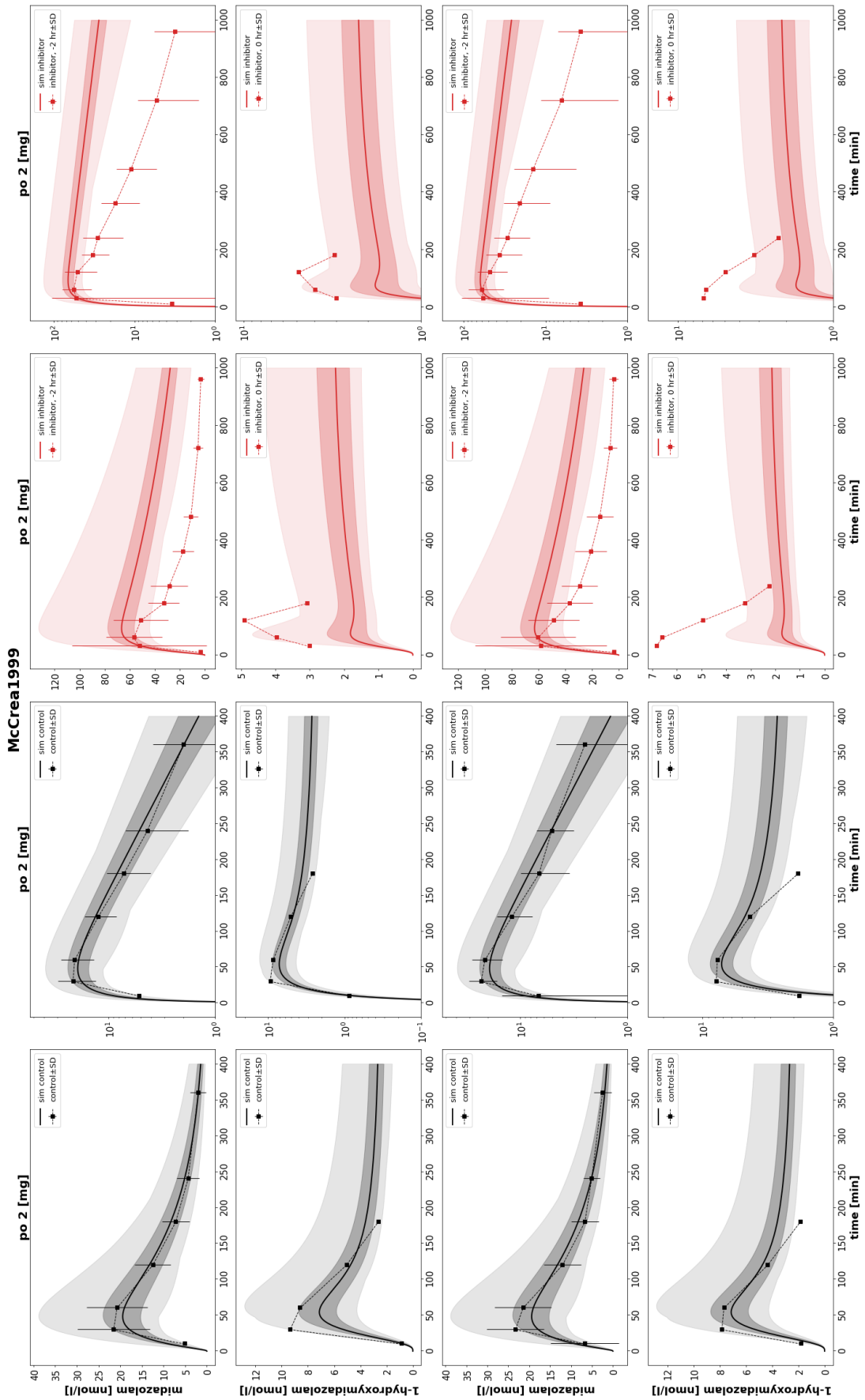


Figure 40: McCrea1999 [67]. Midazolam was administered orally (2 mg) either under control; (black) or inhibitor (red) conditions on 2 different days.

Olkkola1993

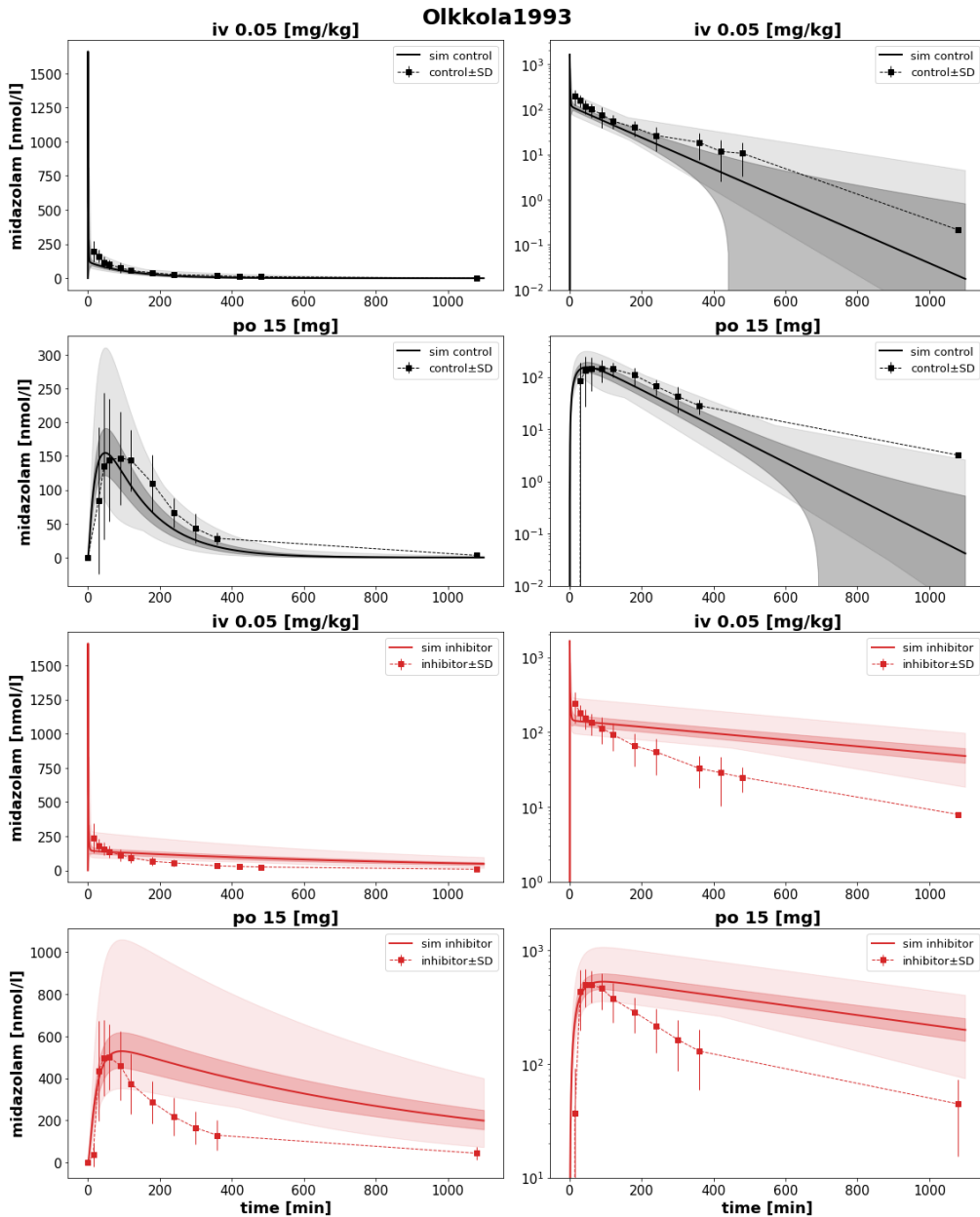


Figure 41: Olkkola1993 [68]. Midazolam was administered intravenously (iv; 0.05 mg/kg) and orally (po; 15 mg) either under control; (black) or inhibitor (red) conditions.

Olkkola1994

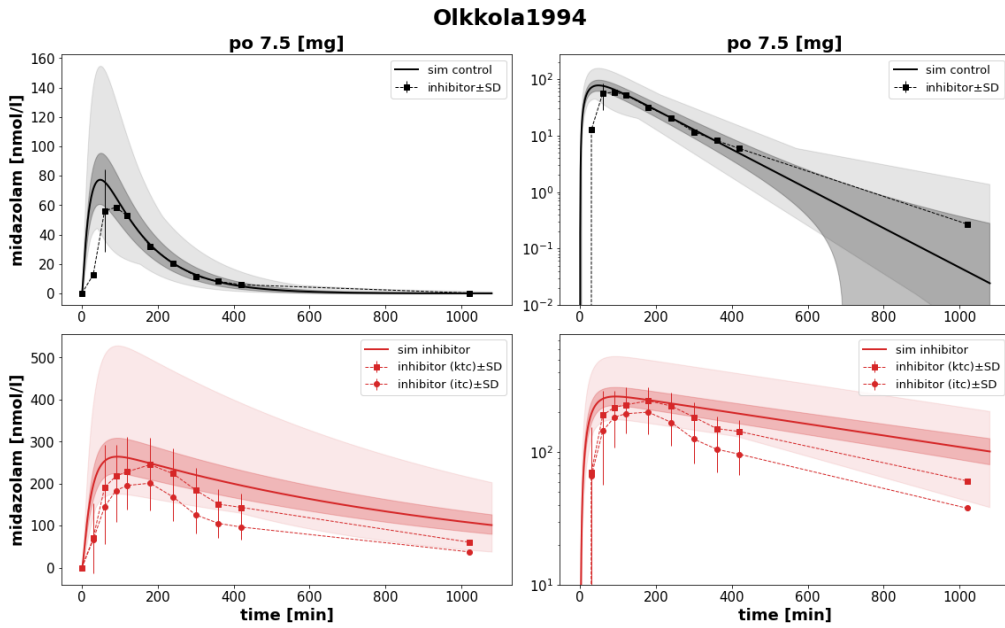


Figure 42: Olkkola1994 [69]. Midazolam was administered orally (7.5 mg) either under control; (black) or inhibitor (red) conditions.

Pentikaeinen1989

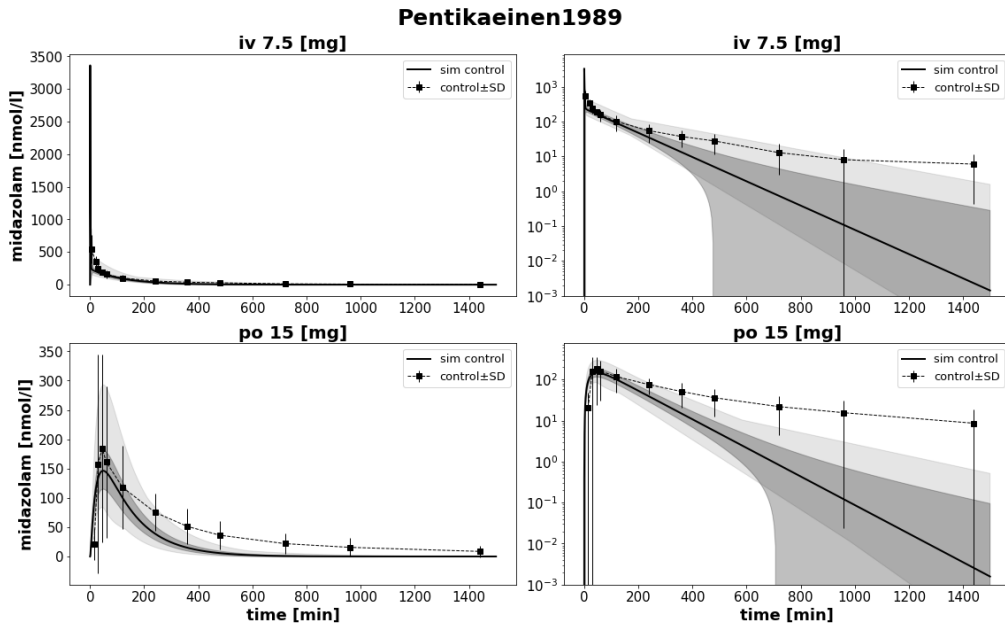


Figure 43: Pentikaeinen1989 [70]. Midazolam was administered intravenously (iv; 7.5 mg) and orally (po; 15 mg).

Shord2010

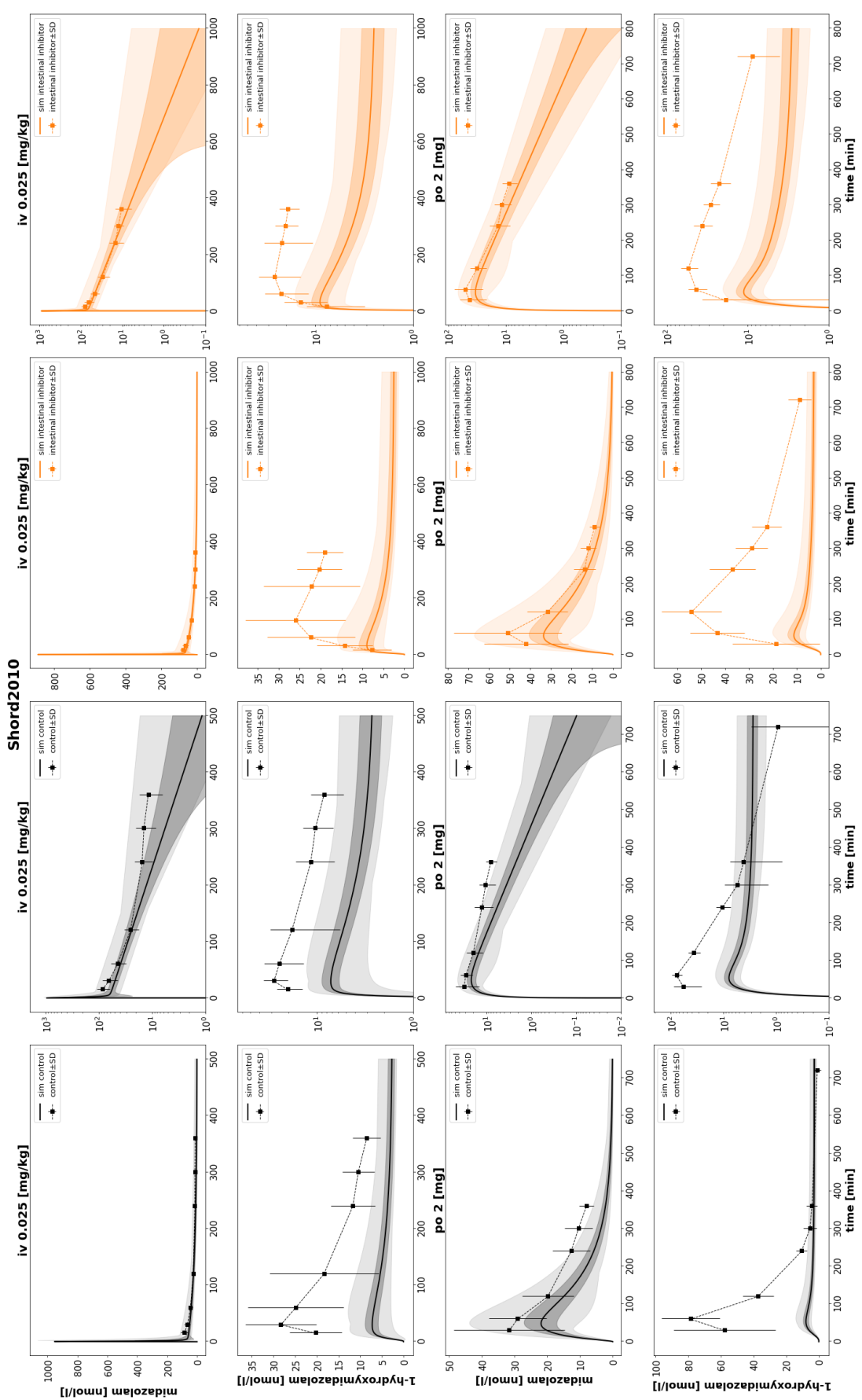


Figure 44: Shord2010 [73]. Midazolam was administered intravenously (iv; 0.025 mg/kg) and orally (po; 2 mg) either under control; (black) or intestinal inhibitor (orange) conditions.

Tsunoda1999

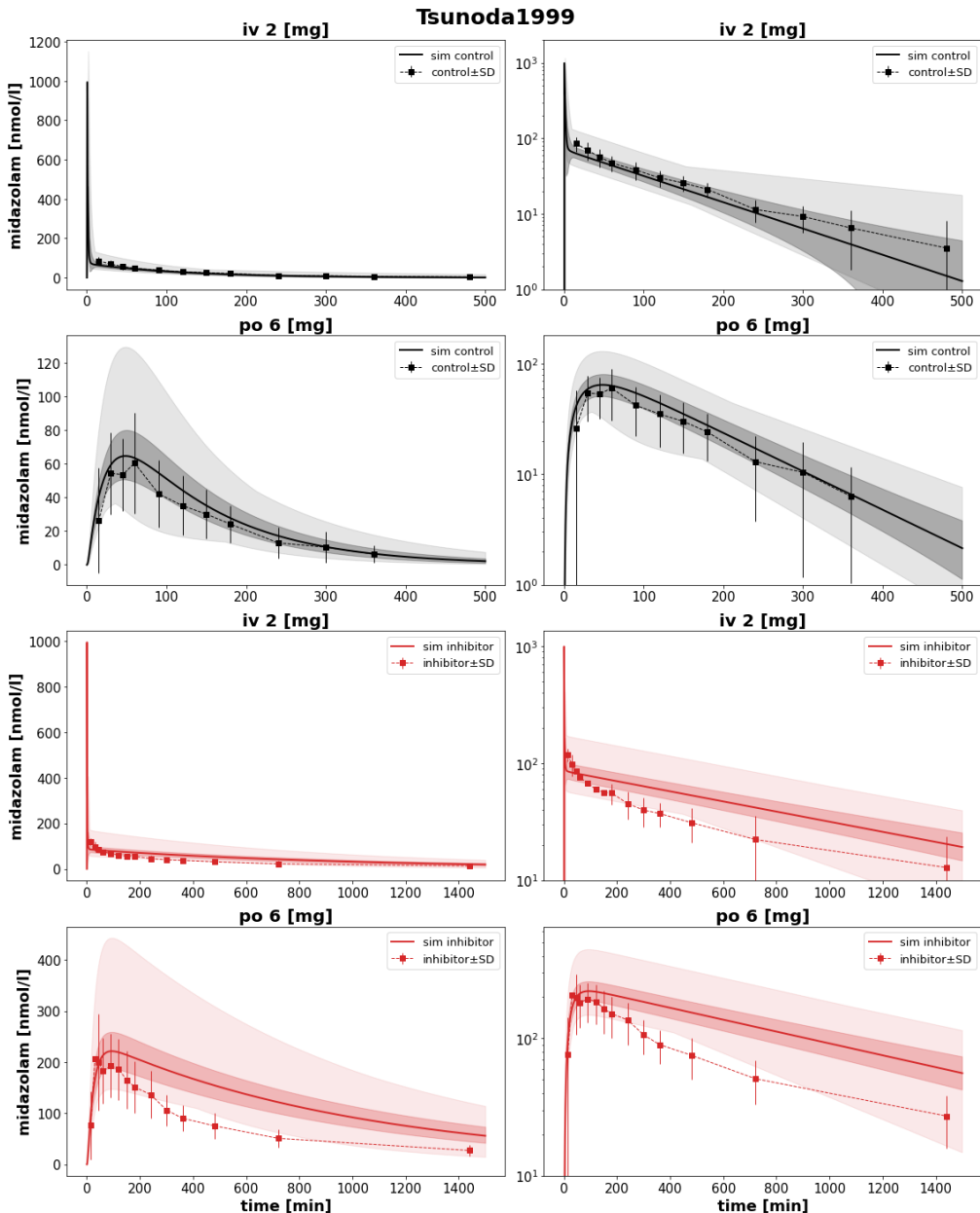


Figure 45: Tsunoda1999 [76]. Midazolam was administered intravenously (iv; 2 mg) and orally (po; 6 mg) either under control; (black) or inhibitor (red) conditions.

Smith1981

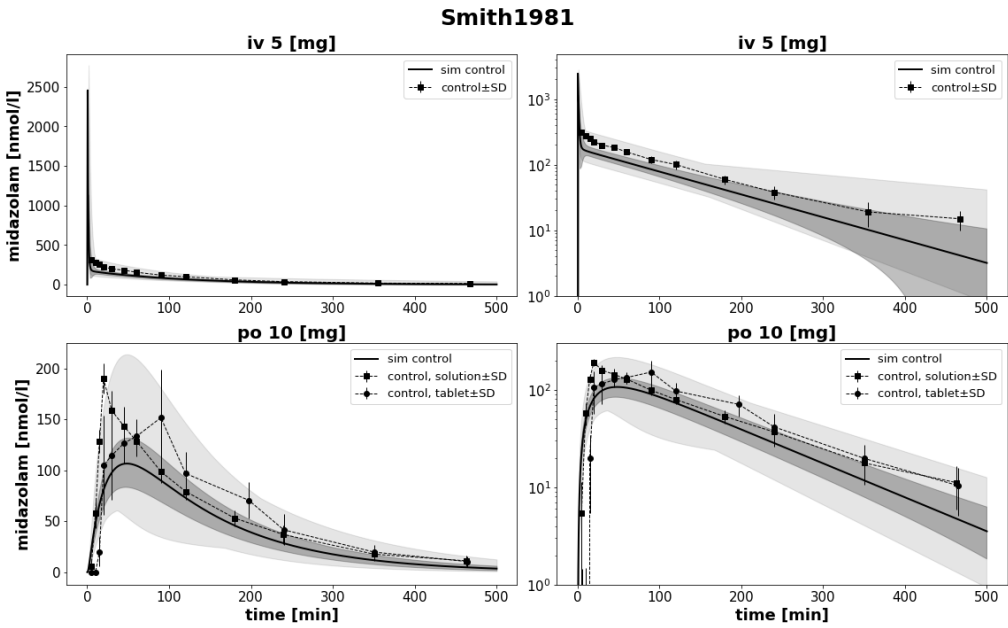


Figure 46: Smith1981 [75]. Midazolam was administered intravenously (iv; 5 mg) and orally (po). 10 mg). Oral doses were either in the form of a tablet (triangle) or solution (square)

Yu2004 (control)

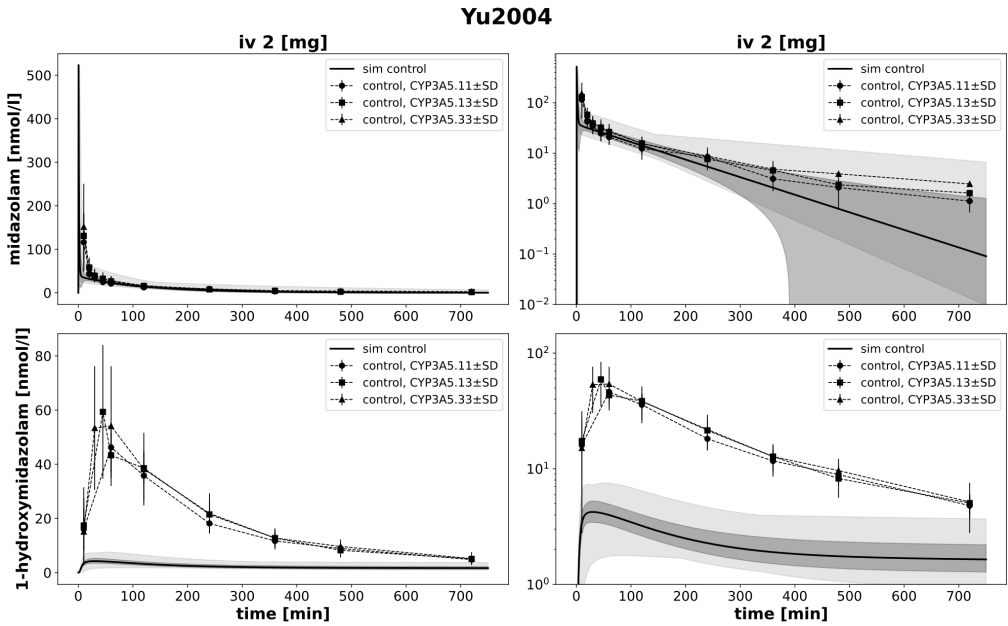


Figure 47: Yu2004 [15]. Midazolam was administered intravenously (2 mg). The study differentiated between different CYP3A5 genotypes.

Yu2004 (inhibitor & inducer)

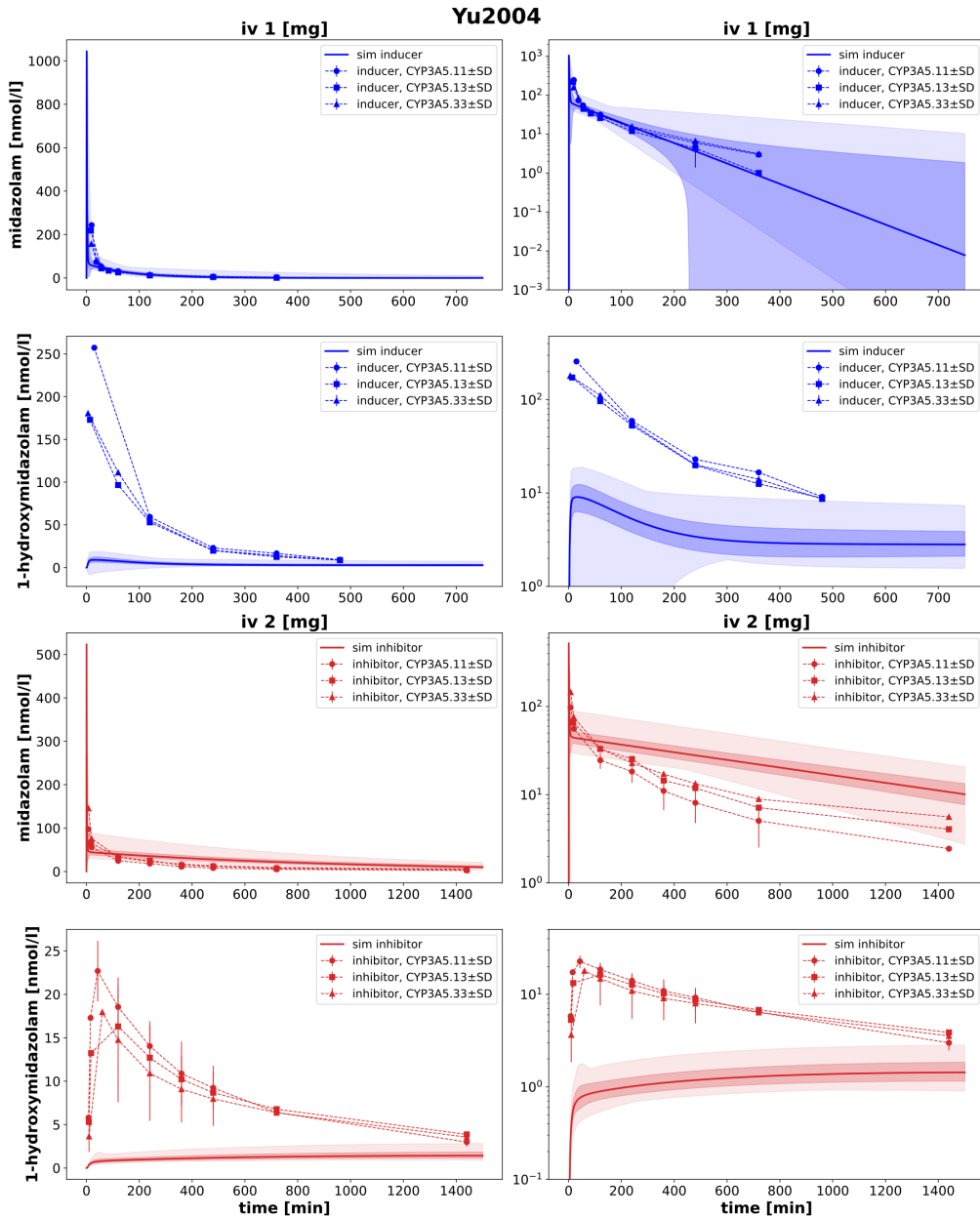


Figure 48: Yu2004 [15]. Midazolam was administered intravenously (2 mg) either under inducer (blue) or inhibitor (red) conditions. The study differentiated between different CYP3A5 genotypes.

A.4 Model validation

In this section we provide figures on the dose-dependency for the remaining pharmacokinetic parameters of midazolam (Fig. 49, Fig. 50) and 1-hydroxymidazolam (Fig. 51).

Figure description: Dose-dependency of midazolam/1-hydroxymidazolam pharmacokinetic parameters. The reference model was adjusted to control (black), inducer (blue), inhibitor (red) and intestinal inhibitor (orange) conditions by changing the f factors for the v_{max} of intestinal and hepatic CYP3A4. Oral and intravenous doses were changed step-wise in the adjusted models and subsequently, pharmacokinetic parameters were calculated from the predicted time courses (squares) and plotted together with the collected data from the curated studies (circles). The shaded areas around the lines depict the SD from the uncertainty analysis.

midazolam (control)

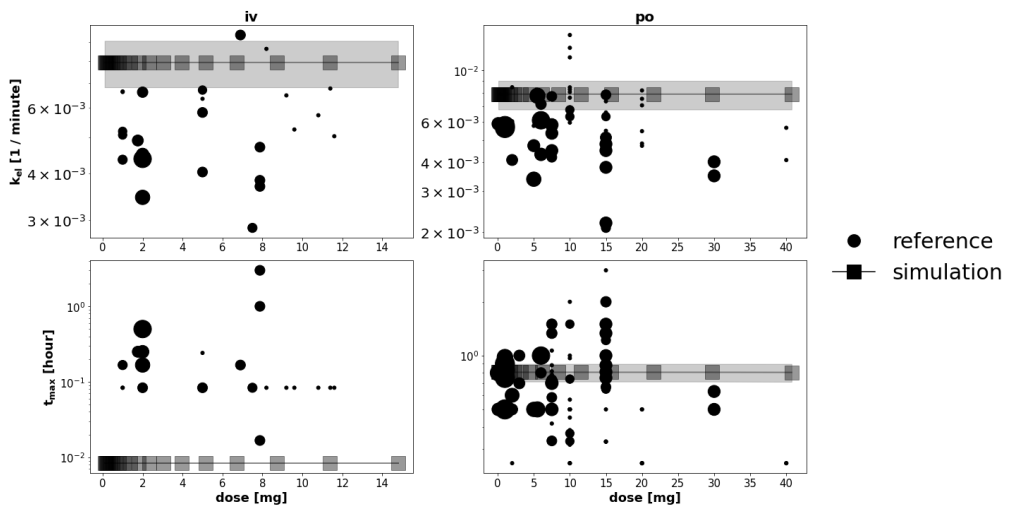


Figure 49: Dose dependency of pharmacokinetic parameters k_{el} and t_{max} of midazolam under control conditions.

midazolam (control, inducer, inhibitor, intestinal inhibitor)

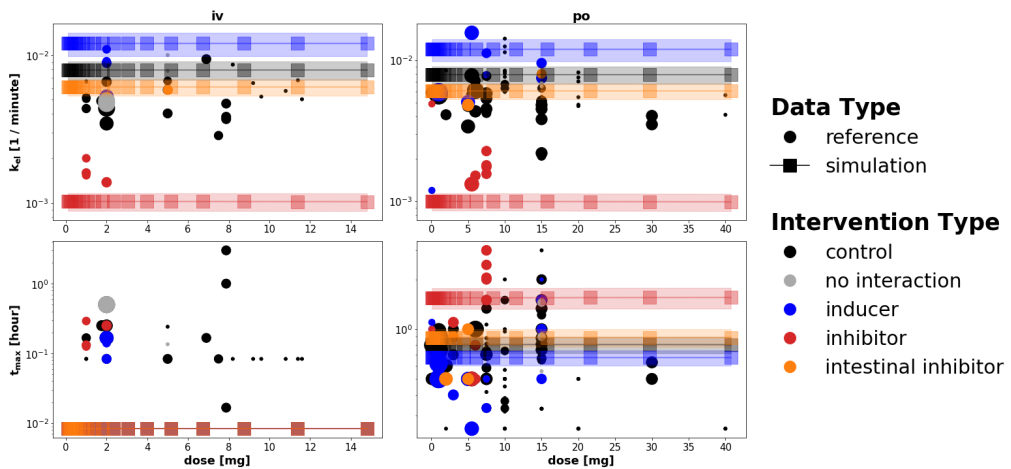


Figure 50: Dose dependency of pharmacokinetic parameters k_{el} and t_{max} of midazolam under control (black), inducer (blue), inhibitor (red) and intestinal inhibitor (orange) conditions.

1-hydroxymidazolam

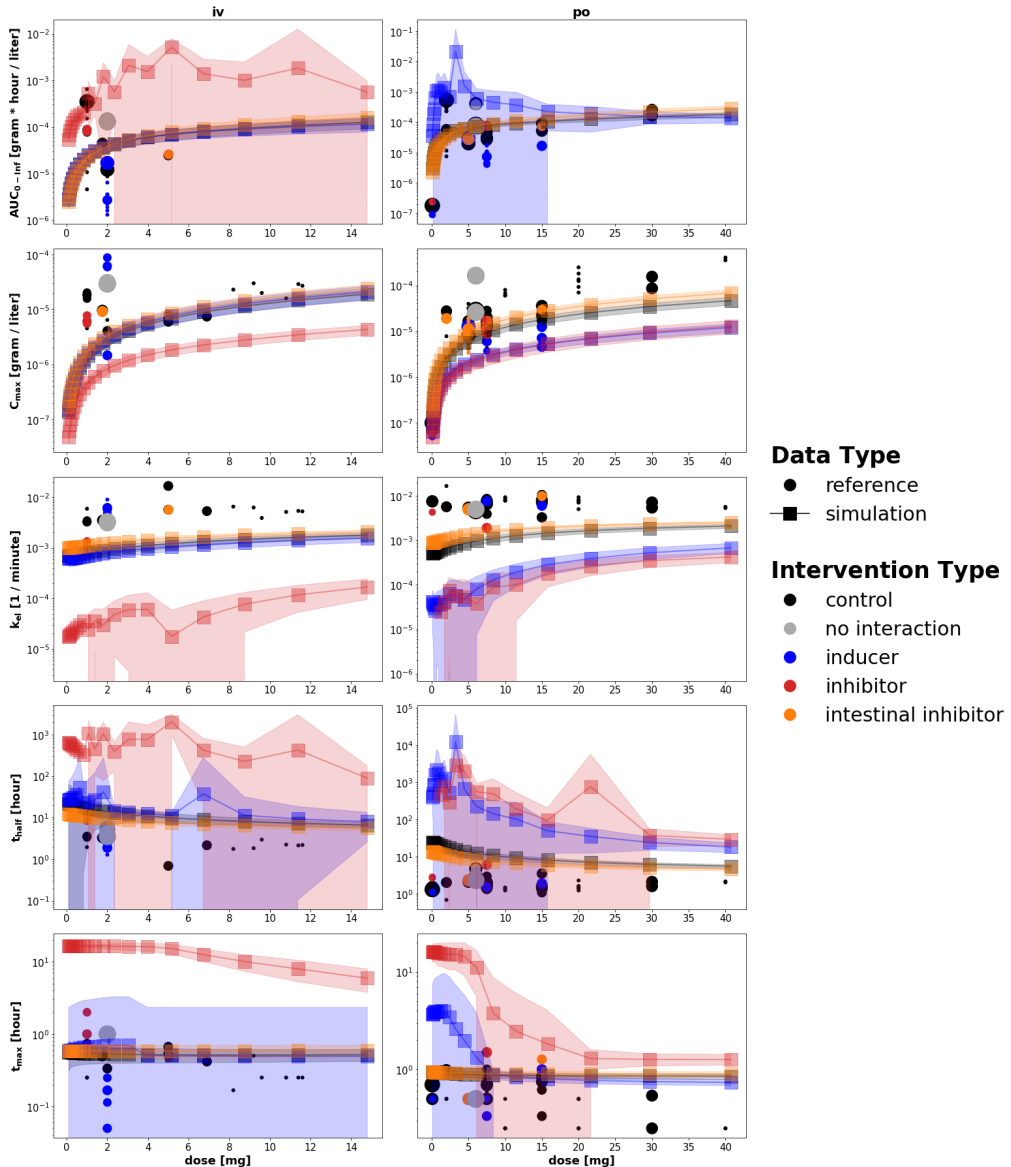


Figure 51: Dose dependency of pharmacokinetic parameters $AUC_{0-\infty}$, C_{max} , k_{el} , t_{max} and $t_{1/2}$ of 1-hydroxymidazolam under control (black), inducer (blue), inhibitor (red) and intestinal inhibitor (orange) conditions.

A.5 CYP3A4 scans

In the following we provide the CYP3A4 activity scans (1-D and 2-D) for the remaining pharmacokinetic parameters of midazolam (C_{max} , k_{el} , t_{half} and t_{max}) and 1-hydroxymidazolam ($AUC_{0-\infty}$, C_{max} , k_{el} , t_{half} and t_{max}).

Figure description 1-D scan (Fig. 52, Fig. 53): 1-D scans of CYP3A4 activity. A systematic scan of CYP3A4 activity was performed by adjusting v_{max} by some factor f , either in the liver (blue), intestine (orange) or in both by the same factor (black). The models with the adjusted v_{max} were then used to predict pharmacokinetic parameters after intravenous (solid) and oral (dashed) midazolam administration, which were plotted against the corresponding change of v_{max} (f).

Figure description 2-D scan (Fig. 54, Fig. 55): 2-D scans of CYP3A4 activity. A systematic scan of CYP3A4 activity was performed by step-wise adjusting v_{max} by a factor f in both the liver (y-axis) and intestine (x-axis). The models with the adjusted v_{max} were then used to predict pharmacokinetic parameters after intravenous (iv) and oral (po) midazolam administration. The heatmap depicts the log-change of the resulting pharmacokinetic parameter, compared to the reference pharmacokinetic parameter predicted by the reference model. Positive values (red) indicate an increase and negative values (blue) a decrease of the pharmacokinetic parameter compared to the reference. Missing values, due to calculation issues, are depicted in gray.

1-D scan midazolam

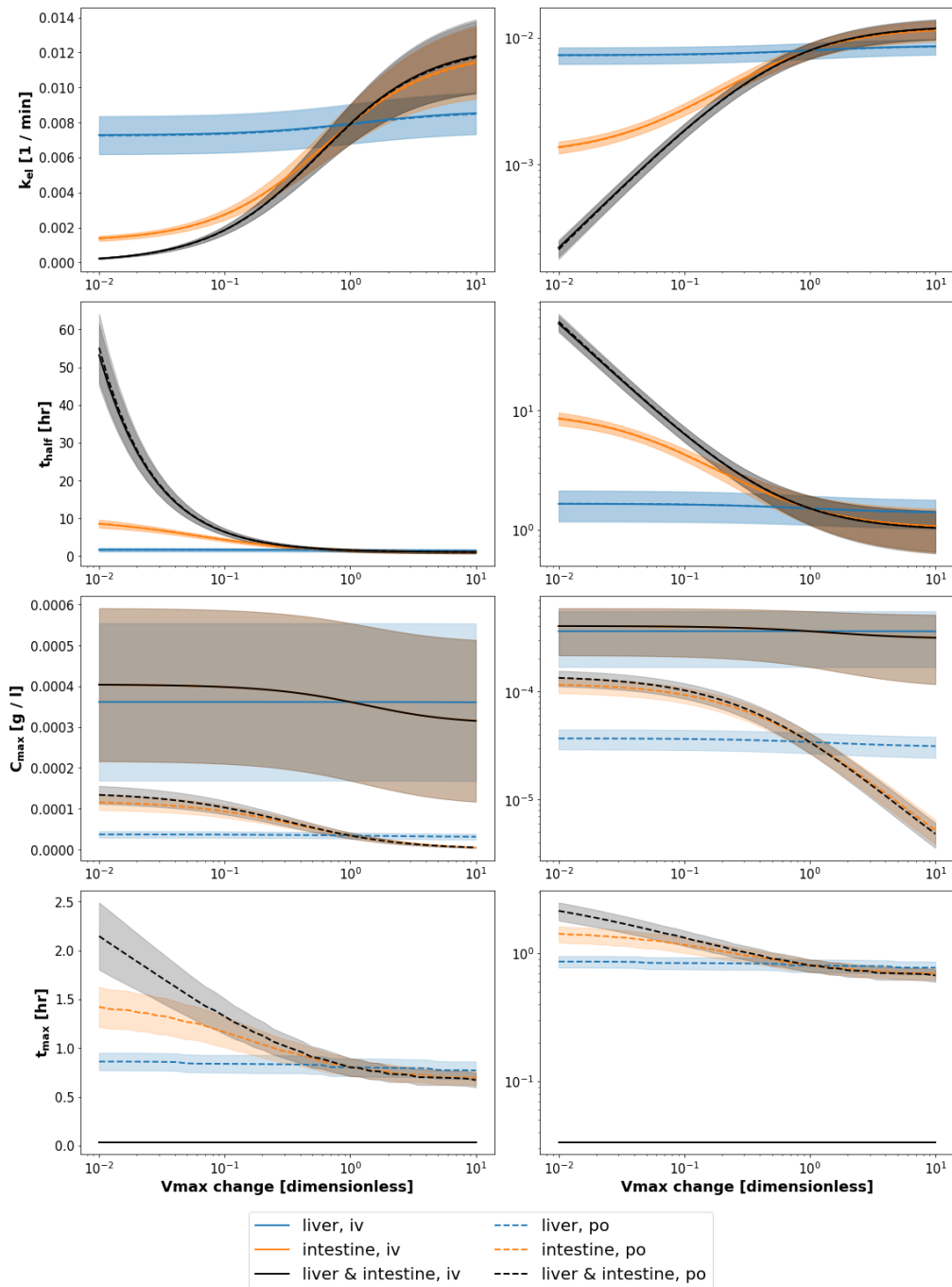


Figure 52: 1-D scan of CYP3A4 activity. Depicted are the pharmacokinetic parameters C_{max} , k_{el} , t_{half} and t_{max} of midazolam against the change of v_{max}

1-D scan 1-hydroxymidazolam

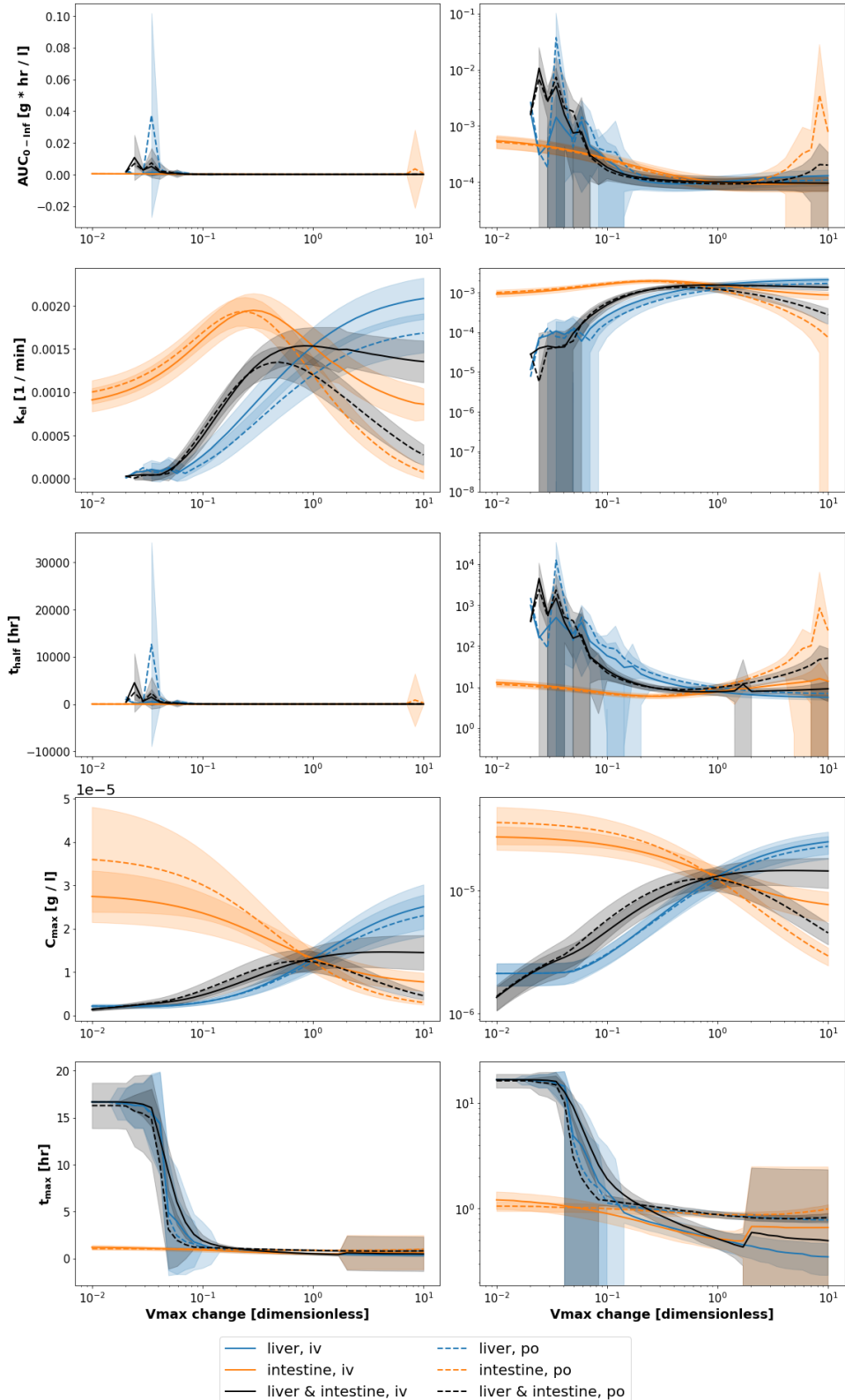


Figure 53: 1-D scan of CYP3A4 activity. Depicted are the pharmacokinetic parameters $AUC_{0-\infty}$, C_{max} , k_{el} , t_{half} and t_{max} of 1-hydroxymidazolam against the change of v_{max} .

2-D scan midazolam

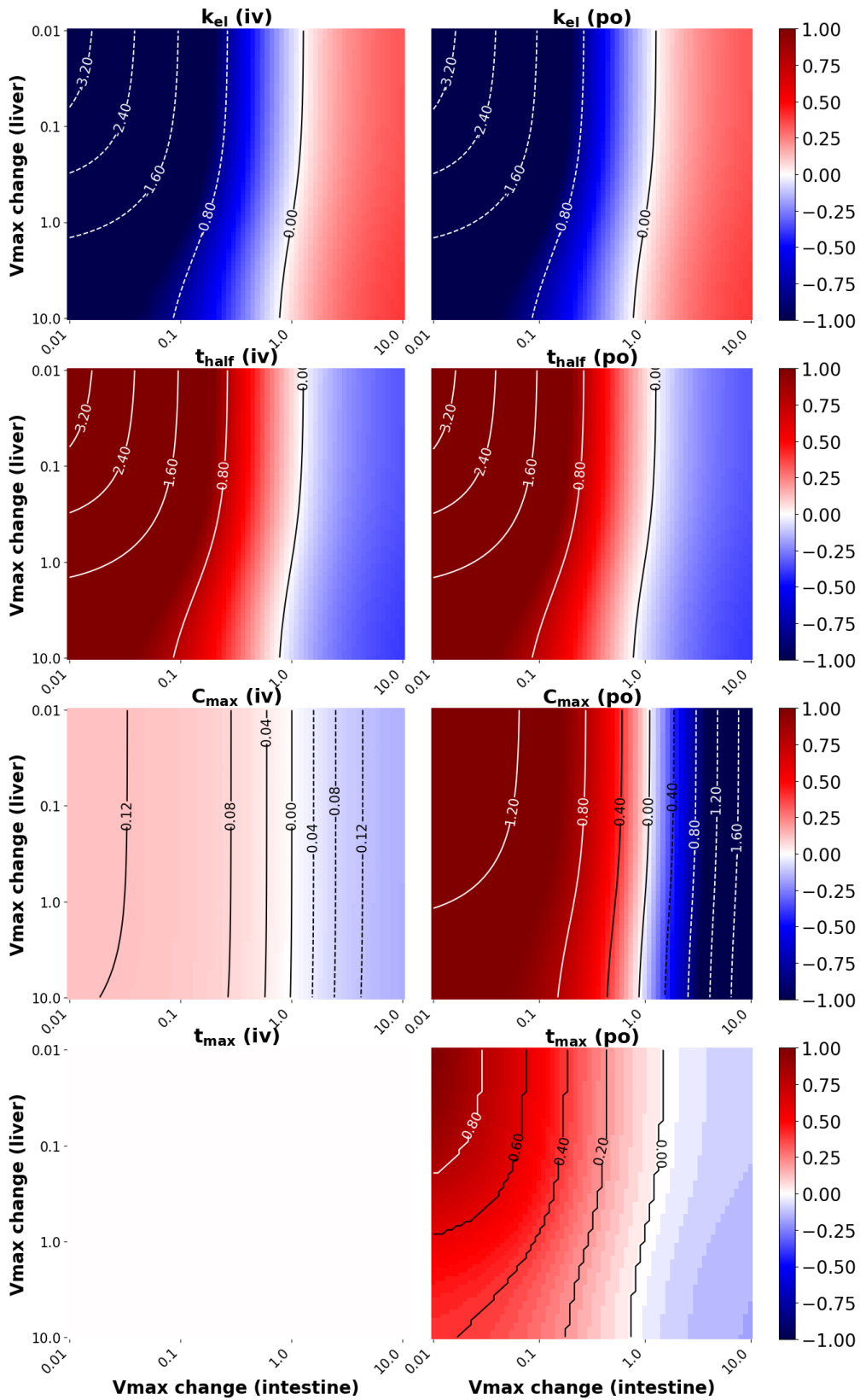


Figure 54: 2-D scan of CYP3A4 activity. Depicted is the log-change after changing v_{max} of the following pharmacokinetic parameters of midazolam: C_{max} , k_{el} , t_{half} and t_{max} .

2-D scan 1-hydroxymidazolam

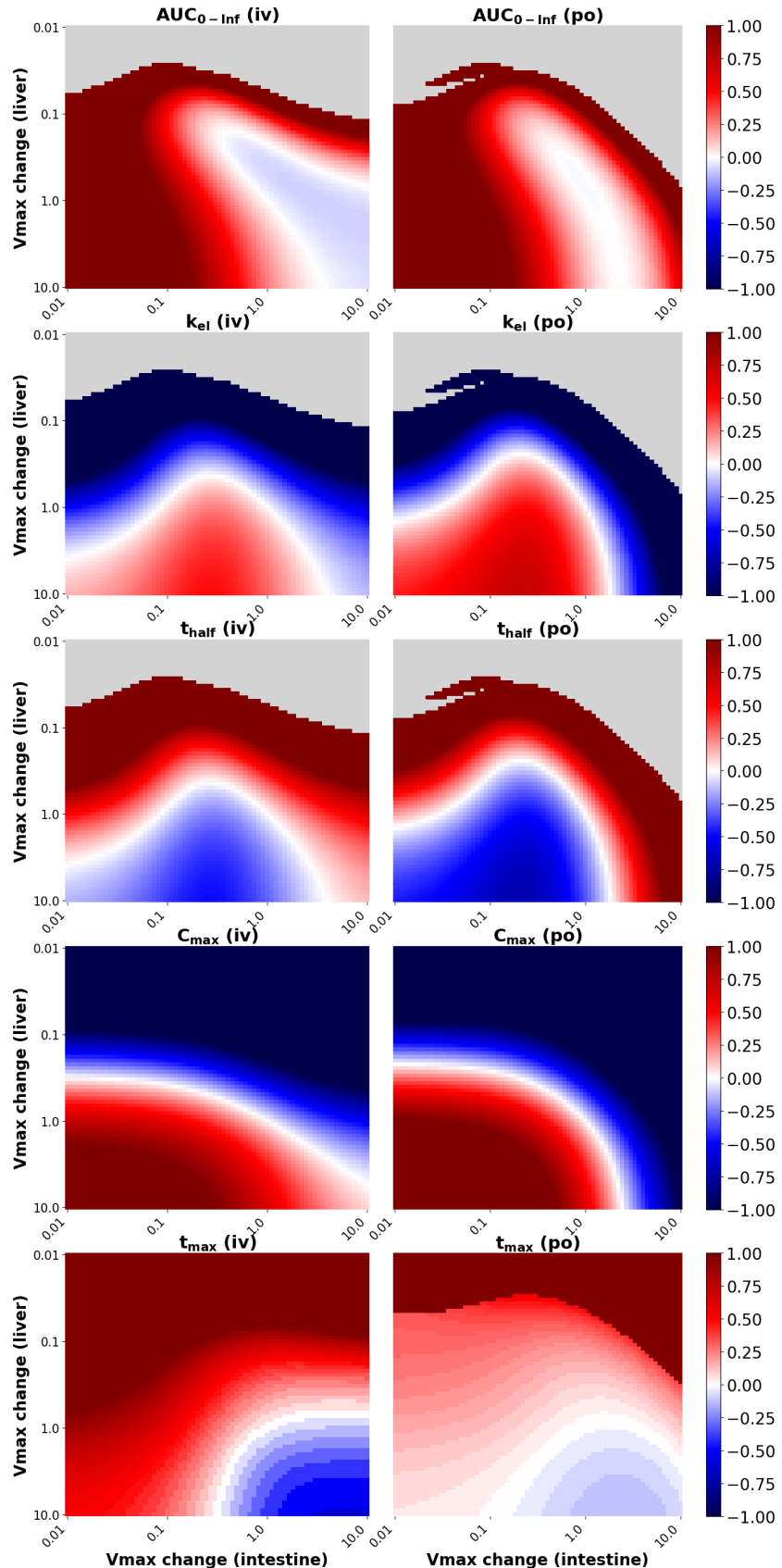


Figure 55: 2-D scan of CYP3A4 activity. Depicted is the log-change after changing v_{max} of the following pharmacokinetic parameters of 1-hydroxymidazolam: $AUC_{0-\infty}$, C_{max} , k_{el} , $t_{\frac{1}{2}}$ and t_{max} .